A GEOHYDROLOGIC ANALYSIS OF AN UPLAND-BEDROCK AQUIFER SYSTEM: APPLICATIONS TO INTERIOR ALASKA

A

THESIS

Presented to the Faculty
of the University of Alaska Fairbanks
in Partial Fulfillment of the Requirements
for the Degree of

MASTER OF SCIENCE

By

Emily K. Youcha, B.S.

Fairbanks, Alaska

May 2003

A GEOHYDROLOGIC ANALYSIS OF AN UPLAND-BEDROCK AQUIFER SYSTEM: APPLICATIONS TO INTERIOR ALASKA

By

Emily K. Youcha

RECOMMENDED: _____

_____

_____

_____
Advisory Committee Chair

_____
Chair, Department of Civil Engineering

APPROVED: _____
Dean, College of Science, Engineering, and Mathematics

_____
Dean of the Graduate School

_____
Date

ABSTRACT

Ester Dome, an upland-dome bedrock aquifer system, located nearby Fairbanks, Alaska, was studied to identify important geohydrologic processes occurring in Interior upland aquifer systems. The ground-water dynamics at Ester Dome are complex due to the fractured nature of the aquifer system. The geology at Ester Dome consists of metamorphic and igneous rocks. Valley bottom deposits include gravels and loess. The flow pattern of the dome aquifer system is radial. Ground-water flows from a central high elevation recharge area and discharges into lakes, streams, and wetlands in the valley bottoms. The primary form of recharge to the bedrock aquifer is from spring snowmelt. Snow water equivalent and snow depth increases with elevation. Ground-water levels were observed at fifty sites on Ester Dome for two years. Water levels in wells at high elevations or locations with no silt or permafrost coverage show seasonal fluctuations. However, ground-water levels in the valley bottoms show little seasonal fluctuations, except wells that penetrate gravel deposits and have no overburden. A ground-water flow model was developed to aid in the understanding of these geohydrologic processes. The ground-water flow model shows recharge and bedrock hydraulic conductivity as the most sensitive parameters.

TABLE OF CONTENTS

LIST OF FIGURES

LIST OF TABLES

LIST OF OTHER MATERIALS

LIST OF APPENDICES

ABBREVIATIONS

ADEC =	Alaska Department of Environmental Conservation
ADNR =	Alaska Department of Natural Resources
AMG =	Algebraic Multigrid Solver
ARSC=	Arctic Region Supercomputing Center
ASTM =	American Society for Testing and Materials
CORS =	continuously operating reference stations
CPCRW =	Caribou Poker Creek Research Watershed
DEM =	Digital Elevation Model
DLG =	Digital Line Graph
DRN =	drain
FGMI =	Fairbanks Gold Mining, Inc.
GPS =	global positioning system
GWS =	GW Scientific
GWSI =	USGS Groundwater Site Inventory database
LPF =	Layer Property Flow
RF =	radio frequency
SWE =	snow water equivalent
TOC =	Top of casing
UAF =	University of Alaska Fairbanks
UTM =	Universal Transverse Mercator
USCS =	Unified Soil Classification System
USGS =	United States Geological Survey
VANI =	vertical anisotropy
WELTS=	Well Log Tracking System
WERC =	Water and Environmental Research Center
WGS =	World Geodetic System

NOMENCLATURE

A = cross-sectional area perpendicular to fluid flow

b = estimated parameter

e = fracture aperture

C = conductance

css = composite scaled sensitivity

dss = one-percent scaled sensitivity

g = gravitational acceleration

h = hydraulic head

dh = head difference between two wells or piezometers

dl = length between two wells or piezometers

I = hydraulic gradient

k = permeability

K = hydraulic conductivity

L = length of stream reach

M = thickness of streambed

n = number of measurements

N = Source or sink term

ND = number of observations

NP = number of parameters

NPR = number of prior information

p = parameter

q = Darcy flux

Q = volumetric flow rate

ss = dimensionless scaled sensitivity

S = storativity

S_y = specific yield

t = time

n = porosity

w = width of fracture

W = width of stream

y' = simulated value

y = observed value

μ = dynamic viscosity

ρ = water density

ω = weight

UNITS

^{o}C =	degrees Celsius
cm =	centimeters
cfs =	cubic feet per second
d =	days
^{o}F =	degrees Fahrenheit
ft =	feet
gpm =	gallons per minute
h =	hours
in =	inches
km =	kilometers
L =	liters
MHz=	megahertz
m =	meters
min =	minutes
psi =	pounds per square inch
s =	seconds
yr =	year

ACKNOWLEDGEMENTS

Many individuals made this thesis effort possible, particularly the Ester Dome residents who permitted access to their private water-supply wells and land. I would like to acknowledge Alaska Science and Technology Foundation, GW Scientific, Fairbanks Gold Mining, Inc. (FGMI), University of Alaska Fairbanks Water and Environmental Research Center (WERC), Arctic Regions Supercomputing Center, Alaska Department of Natural Resources (ADNR), Alaska Department of Environmental Conservation, Tri-Con Mining, U.S. Geological Survey (USGS), and the Fairbanks North Star Borough for their financial support and participating. My advisory committee members, Larry Hinzman, Michael Lilly, Doug Kane, and David Barnes, provided guidance, knowledge, and scrutiny when needed. Bob Busey, Sally Swenson, John Anderson, and Johnny Mendez at GW Scientific, and Rob Gieck at WERC provided valuable technical assistance, which was greatly appreciated. The combined efforts of the WERC, Michelle Roller and Bill Jeffress of FGMI, and Jim Vohden of ADNR made it possible to collect the ground-water level data. Rainer Newberry, Florence Weber, Dan Hawkins, and Cheryl Cameron helped explain much of the geology of Ester Dome and the Fairbanks area. Richard Winston at the U.S. Geological Survey was very helpful with the ground-water modeling efforts. We acknowledge the German National Research Center for Information Technology for use of the Algebraic Multigrid Solver (AMG) for MODFLOW-2000. Intermap Technologies, Inc provided the Demo Star3i Digital Elevation Model. Thanks to Peter Prokein who helped with the Digital Elevation Model, along with the rest of the staff, students, and faculty at the WERC for their support. Lastly, thanks to Luke Boles for support, encouragement, and help in the field when needed.

INTRODUCTION

Mining development and increased urbanization in Alaska create potential conflicts for the most beneficial use of resources. Currently, there is a need for technical methods and protocols to achieve sustainable development. Ground water is a natural resource shared by private residents and industry. Outside of Fairbanks, much of residential rural water use comes from domestic ground-water wells. Most of these wells use upland-dome bedrock aquifer systems. This project investigates the Ester Dome upland-dome aquifer system in Ester, Alaska, which has mining and residential land use areas. This study will help develop geohydrologic investigation guidelines and methods for other Interior mining locations. Mining and other industrial projects often face water supply, dewatering, and environmental impact design and evaluation needs. The background work upon which to base methods and approaches for evaluating water resources often has not been conducted in Interior mining districts. At times, this has been problematic to both industry and regulatory agencies that are evaluating, designing, and operating facilities to minimize risk to water resources.

Upland areas generally have unconfined bedrock aquifers, which interface with fluvial aquifers in valley bottoms. Permafrost plays an important role in the ground-water dynamics. Valley bottoms and north facing slopes of many hills around Fairbanks, including Ester Dome, are underlain by discontinuous permafrost. Major regional geologic fault systems, fractures and joints in the bedrock, as well as changes in bedrock geology influence ground-water flow within bedrock aquifers. Long-term reductions in water levels may be associated with a decrease in the total annual recharge into the aquifer or due to increases in residential or industrial water usage. Summer precipitation provides little natural recharge to the main aquifer systems as potential evapotranspiration generally meets or exceeds summer rainfall (Gieck, 1986). An understanding of these geohydrologic processes and how they interact is needed to evaluate potential impacts to ground-water resources. Since most areas in the uplands have little current and historical geohydrologic data, the geohydrologic uncertainty is

high. We need to produce tools for reducing uncertainties in assessing water resources along with improving our understanding of the key processes important to water quantity and quality in Interior bedrock aquifers.

We test the hypothesis that upland-dome aquifer systems are 1) impacted by hillside and valley-bottom permafrost and geologic conditions and 2) the recharge distribution and bedrock fracturing are significant features controlling flow in these aquifer settings. The goals of this thesis are to characterize the important geohydrologic processes and parameters of the upland-dome bedrock aquifer systems of Interior Alaska. Ester Dome, Alaska is an excellent area to conduct this type of study because it has a history of development activities and available information. Additionally, Ester Dome has historical ground-water data available, and a number of monitoring and private water-supply wells to monitor. This thesis research has been an attempt to collect, distribute, and analyze hydrologic and geologic information that are important in characterization of the uplands aquifer systems. A ground-water flow model has been applied to examine geohydrologic processes. The model identifies the critical hydrologic parameters that are needed to perform accurate predictions in the Fairbanks uplands. We will identify criteria that are necessary for decision-making and provide recommendations for hydrologic investigations in the uplands.

LITERATURE REVIEW

GROUND-WATER FLOW THROUGH FRACTURED MEDIA

Ground-water flow in fractured rocks is a relatively new field of investigation. In many hydrogeologic studies, bedrock is ignored or treated as an impermeable unit. However, in the Fairbanks area, many residents obtain sufficient water from bedrock aquifers. Investigations of geohydrologic processes in fractured aquifers are limited. Recent investigations include the U.S. Geological Survey (USGS) Mirror Lake study in New Hampshire (Shapiro and Hsieh, 1993), the Turkey Creek watershed study in Colorado (Caine, 2000) and the inter-agency Yucca Mountain study in Nevada (Faunt, et al., 1999). Further research in the geohydrology of fractured-rock aquifers is necessary because much of rural western United States relies on these aquifers for public water supply.

The laws governing ground-water flow generally apply to porous media. Modifications and assumptions are made when applying these laws to fractured media. Accurate predictions are difficult to make when the aquifer in question is comprised of fractured rock. The number of uncertainties rises when examining fractured rock because most of the aquifer properties are unknown and vary on a variety of scales.

Darcy's Law is an empirical equation, which describes flow through porous media:

$$Q = -KIA \qquad \textbf{(1)}$$

where Q is the flow rate, K is the hydraulic conductivity, I is the hydraulic gradient and A is the cross-sectional flow area. Darcy's Law applies to saturated and unsaturated flow systems, steady state and transient state problems, homogenous, heterogeneous, isotropic, and anisotropic systems, and flow in consolidated and unconsolidated deposits (Freeze and Cherry, 1975). However, in fractured media, Darcy's Law may not always apply if flow is no longer laminar and the problem becomes nonlinear.

First, we must define some basic concepts of fractured media. Fracturing and jointing are typically a result of a stress applied to bedrock, such as the tectonic motion of

folding and faulting. Chemical dissolution can also create open channels or conduits in the rock. In fractured media, there are two types of porosity to consider. Primary, or matrix porosity, is the porosity of the pore spaces between the minerals or grains. Secondary, or fracture porosity, is a result of dissolution or fracturing of the rock, creating open conduits or channels for water to flow through. In fractured rock, the primary porosity is generally very low (or none), while the secondary porosity is several magnitudes of order larger. Fractures, joints, and foliation or bedding planes are examples of secondary porosity. Brittle rocks will fracture more easily than non-brittle rocks. Examples of brittle rocks include quartz-rich rocks such as quartzite. Limestone or rocks with low quartz content are likely to be more ductile and fracture less easily. Another important factor in the hydrogeology of fractured rocks is the permeability of the fracture rock. For water to actually flow through fractured rock with no primary porosity, the fractures present must be interconnected and have a high permeability. These rock features can lead to problems when making predictions of the flow paths because of the seemingly random nature of the fracture patterns. Three approaches are taken when investigating a fractured bedrock aquifer system; a continuum approach, a dual-porosity approach, or a discrete-fracture approach.

Freeze and Cherry (1975) and Domenico and Schwartz (1998) describe the continuum approach as treating the fractured-bedrock aquifer as a hydraulically equivalent porous medium. In this method, the individual fractures are not considered, but rather bulk or average aquifer properties. This means fractures must be numerous, the distance between fractures should be very small in comparison to the size of the study area, and fractures should be well connected (Bradbury, et al., 1991). This method allows us to use Darcy's Law to solve ground-water flow problems. In this situation, scale issues become important because we are typically examining a larger-scale problem, thus the smaller scale properties are excluded. Tiedman et al. (1997) and Hsieh et al. (1999) discuss how the continuum approach can be applied for fractured bedrock ground-water flow modeling.

The dual-porosity approach is described by Barenblatt et al. (1960), Streltsova-Adams (1978) and Gringarten (1982) and takes into account matrix and fracture porosity. This method is used if the primary porosity is still an important component in the ground-water flow dynamics. Water can be exchanged between the primary and secondary porosities. In general, most of the water is stored in the matrix and most of the flow occurs in the fractures.

The last approach is the discrete fracture approach and is described by Long et al. (1982). This method identifies each individual fracture and examines the flow through these fracture sets. It models the connectivity of the fractures and assumes the water moves only through these fractures. Each fracture or fracture network must be described. In this method, the matrix properties are not considered. Detailed knowledge of the fracture network is required, making it a difficult method to use for medium- to large-scale problems.

Flow through individual fractures, or two parallel and smooth plates, is described by the cubic law (Bear, 1993):

$$Q = -\frac{w\rho g e^3}{12\mu} I \qquad \textbf{(2)}$$

Where Q is the flow rate, w is the width of the fracture, ρ is the density of the fluid, g is the gravitational constant, e is the aperture, μ is the dynamic viscosity, and I is the hydraulic gradient.

The Ester Dome ground-water flow model uses the continuum approach to solve the governing ground-water flow equation for three-dimensional steady-state ground-water flow:

$$\frac{\partial}{\partial x}\left(K_X \frac{\partial h}{\partial x}\right) + \frac{\partial}{\partial y}\left(K_Y \frac{\partial h}{\partial y}\right) + \frac{\partial}{\partial z}\left(K_Z \frac{\partial h}{\partial z}\right) \pm N = 0 \qquad \textbf{(3)}$$

where h is the hydraulic head, N is the source or sink terms, x, y, z are the horizontal and vertical coordinates, and K_x, K_y, K_z, are the hydraulic conductivities in the x, y, and z direction. The modular three-dimensional finite-difference ground-water flow model,

MODFLOW-2000, is the code we used to simulate flow in the Ester Dome aquifer system. MODFLOW-2000 contains a new module, the "Observation, Sensitivity, and Parameter Estimation" package (Hill, et al., 2000). These packages use an approach also known as inverse modeling or parameter estimation. This package is used in the Ester Dome model to automate portions of the calibration procedure and estimate parameters such as recharge and hydraulic conductivity.

The Sensitivity package in MODFLOW-2000 uses the sensitivity equation method (Yeh, 1986). This method uses the derivative of the ground-water flow equation (3) with respect to each parameter, to look at the sensitivity of hydraulic head to changes in each defined parameter. The Parameter Estimation package in MODFLOW-2000 uses nonlinear regression to estimate optimal parameter values.

Poeter and Hill (1997) discuss the benefits of automated calibration techniques. Some of the benefits of automated calibration include: quickly determining optimal parameter values, statistics on the quality of calibration and parameter estimates, and identifying additional data needed for more accurate modeling (Poeter and Hill, 1997). Quantifying the calibration process is beneficial for describing the accuracy and usefulness of the model.

Little is known about the aquifer parameters in the Fairbanks uplands. The parameter-estimation method is a useful technique for learning more about the bulk geohydrology properties controlling ground-water flow in fractured bedrock aquifer systems.

GEOHYDROLOGY OF FAIRBANKS UPLANDS

The two main types of aquifer systems in the Fairbanks area are alluvial sand and gravel, and the upland-bedrock aquifer systems. Several hydrologic investigations of the Chena and Tanana alluvium aquifer systems exist (Cederstrom, 1963, Nelson, 1978, Farris, 1996, Glass et al., 1996, Wegner, 1997, Nakanishi and Lilly 1998, Hinzman et al., 2000). Anderson (1970) examined the vegetation, surface-water hydrology, water quality, and ground-water resources of the entire Tanana Basin. However, the upland-bedrock

aquifer systems have few detailed hydrogeologic investigations due to the complicated nature of the geologic system. Geologic investigations in the uplands exist due to the Fairbanks mining district being rich in gold deposits. Unfortunately, because of the complicated geologic history, limited large-scale subsurface maps and cross sections are available.

Hydrologic Investigations

Kane (1981a), investigated aufeis growth in Goldstream Creek, which is one of the boundaries of the project area. He showed winter discharge into Goldstream Creek comes from subpermafrost water. Smith and Casper (1974) reported on selected water-quality issues for Fairbanks and included Ester Dome. They found that the quality of well water improves with elevation above the Tanana-Chena flood plain. They also examined the costs of water supply systems for rural interior Alaskans. They found that well costs often exceed the land value during the time of the study (1974).

Wilson and Hawkins (1978) examined arsenic in streams, sediments and ground water in the Fairbanks area. Hawkins et al. (1982) studied the occurrence of arsenic in the Ester Dome area. This study shows concentrations of arsenic up to 200 times the safe drinking water limit occur in ground water sampled at Ester Dome (Hawkins et al., 1982).

McCrum (1985) reported chemical mass balances for the Ester Creek and Happy Creek watersheds. He showed arsenic and nitrate concentrations fluctuate during the study period. The increases in nitrate concentration in several wells during June occur when snowmelt recharges the aquifer. He also shows ground water from the bedrock aquifer and the valley bottom alluvial aquifer can be distinguished based on the water chemistry data. Gieck (1986) conducted a water balance on Ester and Happy Creek. He showed the primary form of ground-water recharge was from spring snowmelt. High rates of potential evapotranspiration occur in the summer-fall period while during the winter all precipitation is stored as ice or snow and no recharge occurs (Gieck, 1986).

Gieck (1986) also shows that precipitation increases and evapotranspiration decrease with increasing elevation at Ester Dome.

Weber (1986) looked for relationships between arsenic, well depth, and well yield in the Fairbanks area, which includes the uplands aquifer systems of Ester Dome, Murphy Dome, Gilmore Dome, Chena Ridge, and Farmers Loop. He found that the Ester Dome aquifer system had higher well yields, higher arsenic concentration, and shallower wells than the other upland-aquifer systems.

Hok (1986) examined lineament features for ground-water prospecting in the Fairbanks uplands. She found the relationship between well yield and lineament features found on aerial photographs was poorly correlated. She concluded that linear feature mapping is not a viable ground-water investigation technique in the upland metamorphic terrane at Fairbanks (Hok, 1986).

In 1985, a pump test was conducted at the Grant Mine on Ester Dome (Walther, 1987a, 1987b). The depth of the pumping well was 110 m deep and was pumped at 0.0189 m^3/s (300 gallons per minute) for 13 days during late fall. The test was conducted in a highly fractured and mineralized fault zone, resulting in high aquifer transmissivity (24.8-49.7 m^2/d or 2000-4000 gpd/ft). Additionally, Walther (1987b) concludes that the ground water exists under confined conditions with a storage coefficient of 0.0001-0.0002. However, upon review of the available information, there is no field evidence that the aquifer is under confined conditions at this location. One bedrock observation well is constructed through permafrost, but the water levels in the well are far below the base of the permafrost.

Farmer et al. (2000), Goldfarb et al. (1999), and Mueller (2002) have recently reported on arsenic and the chemical characteristics of ground water in the uplands surrounding Fairbanks. Mueller (2002) determined arsenic concentrations in sampled ground water are independent of the rock type through which the water has passed. He also showed that relationships existed between major, minor, and trace element data and the proximity to sulfide mineralization and that ground-water redox conditions play a role in the mobility and concentration of arsenic in ground water.

Many permafrost investigations related to hydrology, engineering, mapping, and vegetation have occurred in the Fairbanks area. Pewé et al. (1975a) constructed a permafrost distribution map in the Fairbanks area. Infiltration through frozen soils was examined by Kane (1980, 1981b) and Kane and Stein, (1983a, 1983b). They studied water movement through frozen soils and measured hydraulic conductivity of soils. They found the hydraulic conductivity of ice-rich silt is one or more orders of magnitude lower than unfrozen silt or silt with low moisture content. Kane and Slaughter (1973) examined subpermafrost recharge to a small lake in Interior Alaska. They reported even small sized lakes (0.02 km^2) can be hydraulically connected to the subpermafrost ground water.

Geologic Investigations

The Soil Conservation Service has reported various soil surveys for the area in 1957, 1963, and 1977. The surficial geology of the Fairbanks area was described by Pewé (1958) and Pewé et al. (1975b, 1976). Pewé described in detail the surficial deposits and their depositional history. The bedrock geology of the Fairbanks mining district has been described by Forbes (1982), Robinson et al. (1990), Foster et al. (1994), and Newberry et al. (1996). Newberry et al. (1996) applied geophysical, age-dating, and petrographic techniques to improve previous geologic investigations. We used the most recent geologic map (Newberry et al., 1996) and those of Pewé (1958) and Pewé et al. (1975b, 1976) to describe the bedrock and surficial geology in the Ester Dome area.

Hall (1985) described the mesoscopic metamorphic structures in the Fairbanks area. He identified four phases of folds and fabrics, which describe the deformation of the fractured bedrock in the Fairbanks area. The most recent geologic investigation at Ester Dome was by Cameron (2000), who examined fault hosted gold mineralization at Ester Dome. Cameron identified additional faults that are not included in the Newberry et al. (1996) geologic map. Multiple mining companies have conducted mineral and geological exploration over the years, with the most recent by American Copper and Nickel Company and Placer Dome Exploration during the 1990's (Cameron, 2000).

SITE DESCRIPTION

LOCATION OF THE STUDY AREA

The Ester Dome study area is approximately 181 square kilometers (70 square miles) and is located north of the George Parks Highway and approximately 11.3 km west of Fairbanks, Alaska (Figure 1). The city of Fairbanks is located on the north edge of the Tanana Valley approximately 160 km south of the Arctic Circle. The Tanana Valley consists of thick deposits of alluvium and loess bounded by the Yukon-Tanana Uplands to the north and the Alaska Range to the south (Anderson, 1970). The uplands surrounding Fairbanks are part of the Yukon-Tanana Terrane, which consists of domes and ridges reaching elevations of 900 m above sea level and valley bottoms at 135 m above sea level. Ester Dome is bounded to the north and west by Goldstream Creek and to the south by Chena and Parks Highway Ridges and to the east by Sheep Creek Road (Figure 2). Several small watersheds exist on Ester Dome and some include Ester Creek, Happy Creek, and Alder Creek.

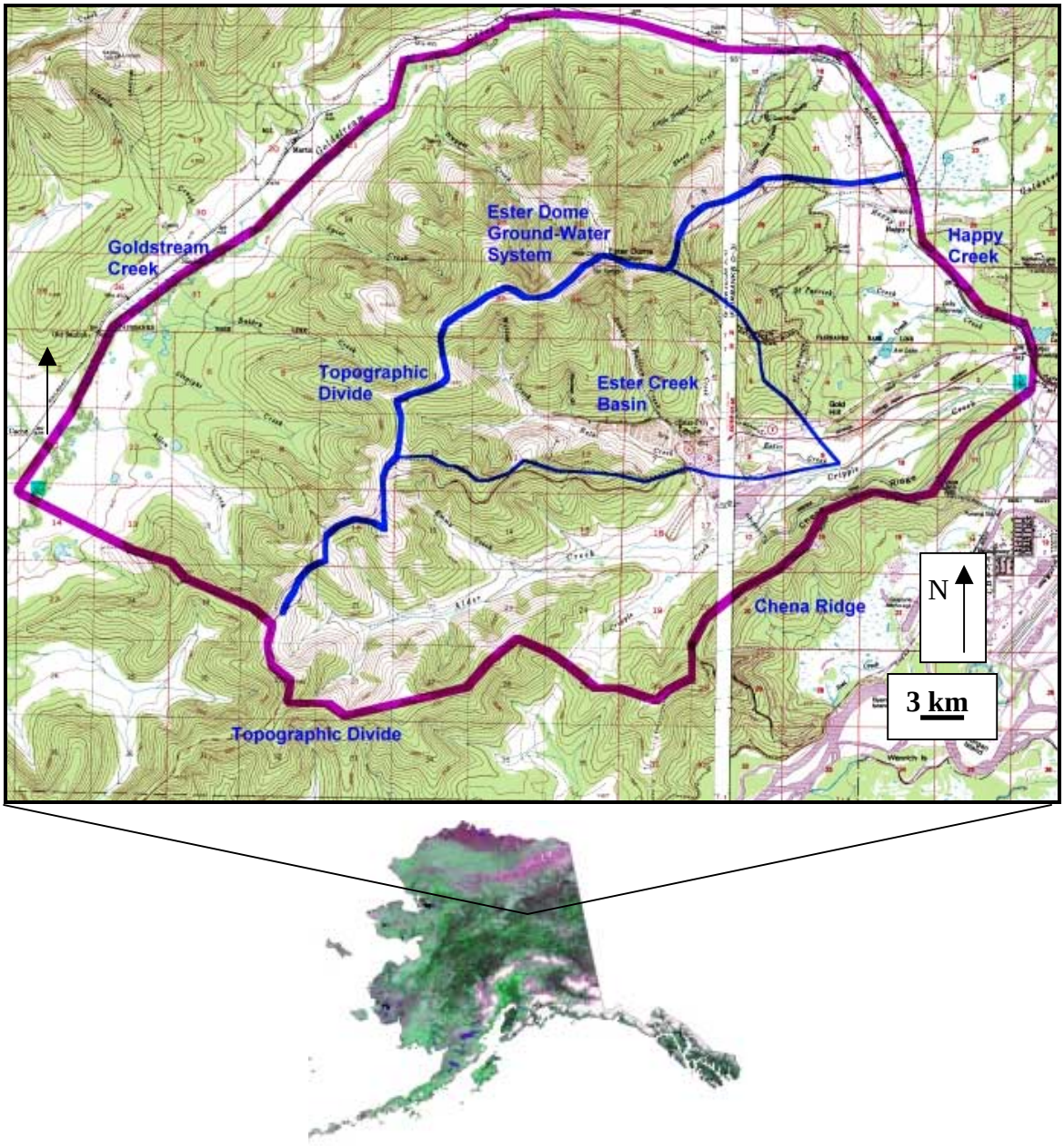

Figure 1. Topographic map showing the Ester Dome study area (topographic map by USGS, 1950 and Alaska image courtesy Bob Huebert, UAF-ARSC).

CLIMATE

The Fairbanks climate consists of large temperature variations, which include long cold winters and short warm summers. The spring and fall seasons are generally

very short, lasting only 2-4 weeks. The coldest month of the year is January and the warmest month is July. For the period 1904-2002, the average annual high temperature was 2.72˚C and low temperature was –8.72˚C (National Weather Service, 2002). Temperature differences also occur in the Fairbanks area. A temperature inversion during winter months occurs when cold air is overlain by warm air. Temperature differences between the valley bottoms and ridge tops can be as much as 15° C in the winter months. Fairbanks has an arid climate with an average winter snowfall depth of 179.8 cm (70.8 in) and an average annual snow water content of 9.83 cm (3.87 in) at the Fairbanks International Airport (National Weather Service, 2002). The average summer precipitation is 17.65 cm (6.95 in) at the Fairbanks International Airport (National Weather Service, 2002). During the study period, the total annual winter snowfall depth was 177 cm (70 in) for 1999-2000, 128 cm (50.5 in) for 2000-2001, 124 cm (48.7 in) for 2001-2002 (National Resources Conservation Service, 2002). For winter 2001-2002, of the 124 cm (48.7 in) of total snowfall, 43 cm (17.1 in) fell in April and May (National Resources Conservation Service, 2002). However, winter precipitation varies with elevation with the highest elevations in the uplands receiving more precipitation than the valley bottoms. Research at Caribou Poker Creek Research Watershed (CPCRW) shows this orographic affect (Haugen et al., 1982). At Ester Dome, there is a definite relationship between the elevation and temperature or precipitation, which was described by Gieck (1986).

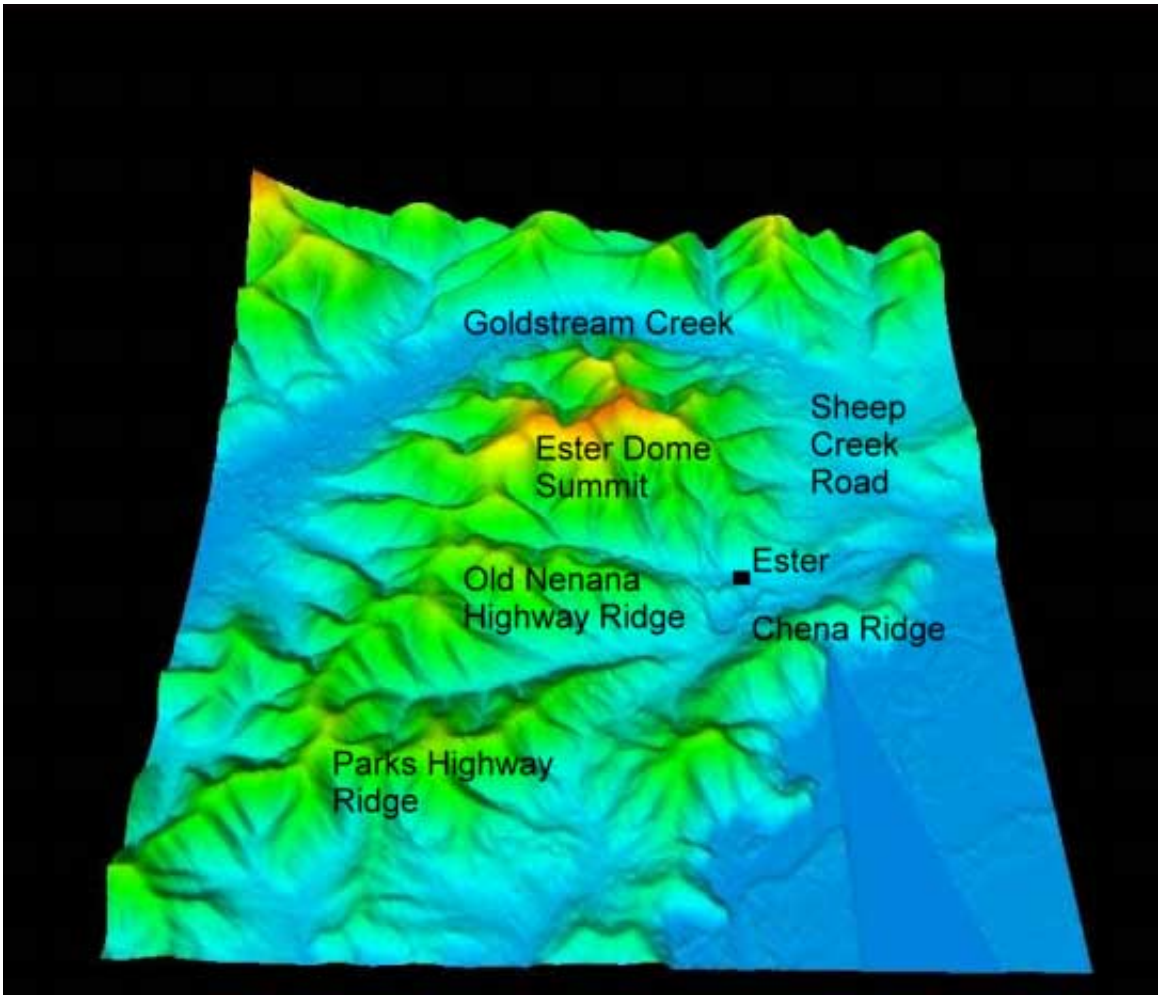

Figure 2. Digital elevation model of Ester Dome, Alaska (by Intermap Technologies, 2000).

ECOLOGY

Vegetation coverage provides useful information about the soil properties and infiltration processes. The boreal forest of Interior Alaska consists of forest, grassland, shrubs, bog, and tundra (Viereck et al., 1986). Upland forest vegetation includes aspen, birch, white spruce, and black spruce. Vegetation coverage can provide useful information for a geohydrologic investigation because it yields clues to subsurface geology and geohydrologic processes. Where permafrost is present, black spruce trees often dominate the landscape. Forest development is enhanced in areas where thick deposits of permafrost-free, nutrient-rich loess occur and the lowest along ridge tops

where there is little or no loess (Viereck et al., 1986). In general, permafrost is not present in south-facing forests where the prevailing vegetation is aspen and birch.

METHODS OF INVESTIGATION

There is a need to quantify the important geohydrologic processes of upland-dome aquifer systems. To solve the problem we collected and assessed several types of data. First, an extensive literature review was completed. Regional and local geologic information was collected. The hydrologic and geologic data was gathered and reviewed from state agency reports, university investigations, and mining investigations on Ester Dome or the Fairbanks uplands. Well-log information obtained from the USGS Ground water Site Inventory (GWSI) and the ADNR Well Log Tracking System (WELTS) was collected and analyzed. Information was reviewed on ground-water flow through fractured media. Next we examined what types of data should be collected in the field for the duration of the study. There was limited long-term ground-water level data for Ester Dome so water-level information was needed. In addition, ground-water temperature and climate data such as air temperature, summer precipitation, and winter snow-water equivalent (SWE) information was collected. During the data collection process, standards such as American Society for Testing and Materials (ASTM) were followed. The next step was the analysis of collected data. We examined the ground-water level data and looked for trends such as seasonal or pumping fluctuations. We examined the climate information to look for relationships between the climate data and recharge and water-level fluctuations. The next process of data analysis identified aquifer parameters and flow processes. A ground-water flow model was developed as a tool to aid in understanding the ground-water system. The inverse approach (also known as parameter-estimation techniques) was attempted to determine aquifer parameters based on field observations of hydraulic head and stream flow. However, the limited number of observations for several parameters did not allow use of this method. The parameter-estimation method did identify data shortcomings. Conclusions and recommendations were made based on the results of the data collection analysis and synthesis of related investigations.

OBSERVATION NETWORK

In cooperation with the Alaska Department of Natural Resources (ADNR) and Fairbanks Gold Mining, Inc. (FGMI), a network of approximately 50 ground-water-monitoring sites was established. Seven of these sites were continuous recording sites, where we monitored additional climate information. Campbell Scientific data loggers (CR10x, CR10, and CR500) were used to record sensor observations.

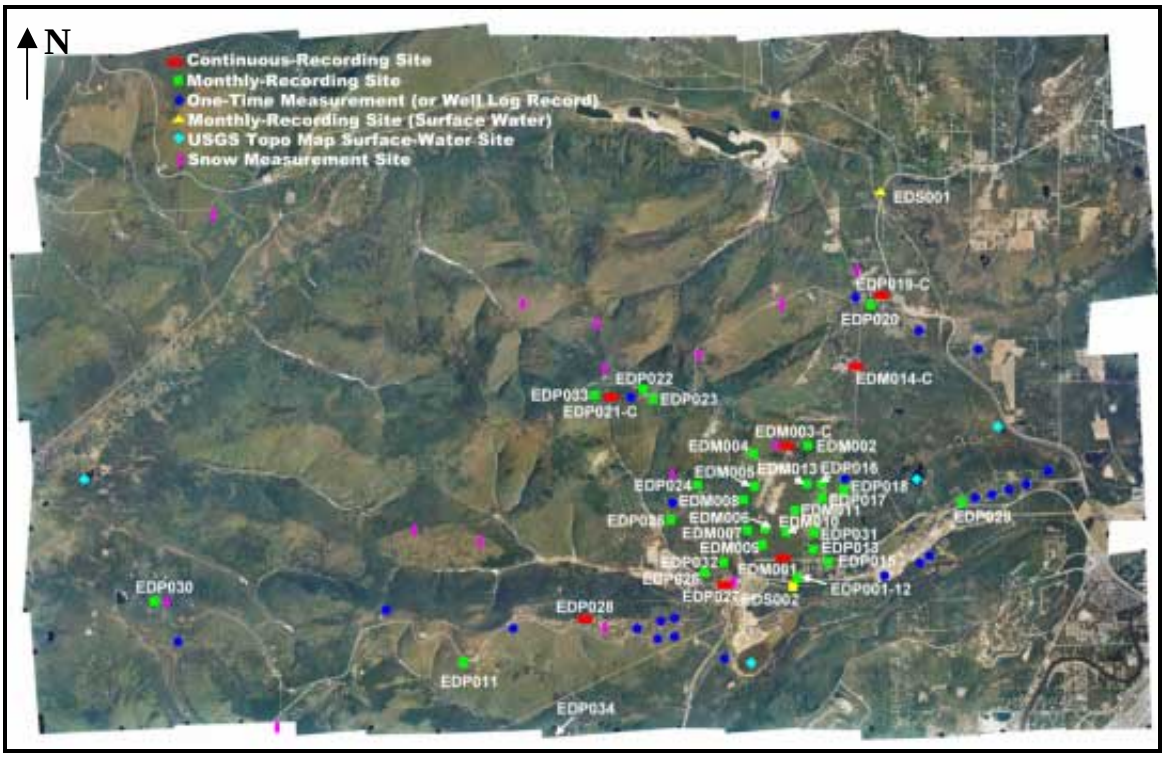

Figure 3. Aerial photograph showing Ester Dome site locations (photograph by Aeromap US, Inc., 1999) and aufeis in the stream channels.

Ground Water

The ground-water monitoring network consists of approximately fifty wells where manual water-level measurements were made monthly (Figure 3). Appendix A shows the site ID, location description, well information, for each site. Wells were chosen based on their spatial location, accessibility, well specifications, and the well or landowner participation. For this investigation, private water-supply wells and monitoring wells at

the Ryan Lode (FGMI) and Grant Mine (Tri-Con Mining) are used. Two-thirds of the 50 wells were private water-supply wells. We instrumented seven of the 50 wells with pressure transducers and thermistors to monitor the water levels and water temperature on an hourly schedule. The transducers used by the project are differential pressure gage sensors requiring a vent tube to the surface and give a measure of the height of water over the sensor. Campbell Scientific dataloggers record and store the data. Manual monthly measurements of the depth of water below the top of well casing (TOC) at the sites were also made to ensure accuracy of the pressure transducers and to permit calibration adjustments.

Climate

A climate-monitoring network exists at the sites equipped with dataloggers. Two shielded thermistors record hourly air temperature. The thermistors were calibrated in an ice bath before put to use. We installed precipitation gages at five of the seven continuous-recording locations on Ester Dome to obtain precipitation data and observe the variance in precipitation with elevation. Tipping-bucket precipitation gages recorded summer precipitation during 2001 and part of 2002. Two of the tipping buckets are Rainwise Raingages three are Texas Instruments TE525mm. The gage at site EDP021, located at the top of Ester Dome, is equipped with a windshield. Trickling a known volume of water through the gage and observing the number of times the bucket tips is the method of calibration for the precipitation gages. The Campbell Scientific data loggers record and store the precipitation data. SWE data was collected at Ester Dome using the double sampling method (Rovansek et al., 1993).

Survey Data

For any ground-water study, water-level elevations are typically examined instead of depth to water (from ground surface). Precise water-level elevations are necessary to calculate a water table, hydraulic gradients, and ground-water discharge. To convert a depth to water into a water-level elevation, the coordinates and elevation of the point at

which the measurement is made must be known. This point is typically either the ground surface or TOC. We used two surveying techniques to obtain the horizontal location of the measuring point. Surveys were also used for obtaining typical cross-sections of geomorphologic features within the study area and to establish the location of instruments or measurement sites.

Three groups (UAF/GWS, FGMI, and ADNR) conducted well surveys for the project. Appendix A notes which team surveyed each site. The purpose of this section is to explain the surveying techniques used by the project groups. Since our measuring point was the TOC, each well was surveyed to the TOC. The two surveying techniques used were traditional level surveying and Global Positioning Satellite (GPS) Surveying. Due to the large scale of the study area and limited benchmarks, the UAF survey team used GPS techniques to survey the vertical and horizontal coordinates. Fairbanks Gold Mining conducted their survey during the fall of 1999 and used total station surveying for the vertical and horizontal coordinates. The ADNR used a combination of GPS surveying and traditional level surveying. The GPS survey is used to obtain the horizontal coordinates and the level survey is used to obtain the vertical coordinate for the ADNR survey. Lastly, miscellaneous Ester Dome well log records were used to 1) construct a conceptual model of the hydrogeology 2) examine water levels for ground-water model calibration and 3) compare well yields.

Vertical coordinates obtained through GPS were differentially corrected using the National Geodetic Survey's permanent, continuously operating, reference stations (CORS) at Fairbanks and Central. Although the GPS accuracy is less in the vertical direction, GPS surveying for elevation will work for our purposes due to the large vertical scale of the dome. In areas with low vertical relief, and a high concentration of observation points, such as the Goldhill/Henderson Road area, more precision is needed. In this case, traditional level surveying was used for higher vertical accuracy.

The ground-water wells surveyed using a USGS topographic map have uncertainty according to USGS accuracy specifications, which reflects the error of the topographic map. Ground-water wells were surveyed with DGPS and have submeter

horizontal error and vertical error of approximately twice the horizontal error. Wells that were surveyed with traditional level surveying techniques for the vertical coordinate are located in the Goldhill Road area and had an assumed error of 1 m.

The vertical datum used for the project is the geodetic datum derived from a general adjustment of the first-order level nets of both the United States and Canada, formerly called Sea Level Datum of 1929 (NADV29). The horizontal datum used during all field surveying is the North American datum of 1927 (NAD27). The ellipsoid chosen for the GPS system is the GRS-80 ellipsoid. The datum incorporating this ellipsoid and used by GPS is called the World Geodetic System 1984 (WGS-84). All GPS coordinates obtained in this datum were converted to the horizontal datum NAD27 and the vertical datum NADV29.

We used the Universal Transverse Mercator (UTM) Coordinate System for the entire project. Zone six of the UTM grid encompasses the field area. Any coordinates obtained in a different system were converted to UTM coordinates.

NETWORK COMMUNICATIONS

Continuously recorded geohydrologic data, which is stored in data loggers, is retrieved and downloaded daily by means of a communications network. This network consists of field sites linked to a base station in Fairbanks by means of Radio Frequency (RF). This is achieved by connecting the data logger to an RF modem, which in turn is connected to an RF antenna. Packets of information are then modulated and transmitted from the field site to the base station near a 150 MHz frequency range. An RF antenna will receive the signal sent from the field and transport it down towards an RF modem, which de-modulates the information packets. The RF modem is connected to a computer through an Internet connection. The computer is used to gather and process all the data from all the field sites. During the summer, the geohydrologic data is downloaded on an hourly basis. In the winter, the data is downloaded on daily basis due to lower power received from the solar panels to run the radio. All collected geohydrologic data is

processed and uploaded to the Internet website http://www.uaf.edu/water/projects/ester for public use.

A GEOHYDROLOGIC ANALYSIS OF AN INTERIOR ALASKA UPLAND-DOME BEDROCK AQUIFER SYSTEM

ABSTRACT

We are investigating the Ester Dome upland-dome aquifer system located 11.3 km (7 miles) west of Fairbanks, Alaska. The bedrock of the Fairbanks area is composed primarily of pre-Cambrian to mid-Paleozoic metamorphic rocks of the Yukon-Tanana metamorphic terrain. Loess and alluvial deposits exist in the valley bottoms and drainages. The primary recharge is from snowmelt and occurs through weathered bedrock at the higher elevations of Ester Dome where there is the greatest snowpack and no overburden or permafrost. Ground water is flowing toward the valley bottoms and discharging into streams, lakes, wetlands and the regional ground-water system. Runoff occurs on the steeper slopes, particularly after snowmelt. Springs and seeps are common on Ester Dome. We also observe aufeis in the winter, which indicates ground-water surface outflow. The water-table surface, in general, mimics the topography of the dome. Water levels in water-supply wells fluctuate dramatically at the highest elevations, in response to snowmelt and pumping. Water levels in wells located at the lower slopes of the dome are more stable, with less daily and annual fluctuations. Water-level fluctuation will also be dependent on the volume of aquifer storage available to water-supply wells.

INTRODUCTION

Ground-water dynamics of fractured bedrock aquifers are not well understood and it is challenging to solve water-resources problems in bedrock settings. Increasing industrial and residential development in the Fairbanks area has led to increased water use from the upland-bedrock aquifer systems. Ester Dome has been mined for gold intermittently for the past 100 years. The geohydrologic processes of upland aquifer systems are poorly understood due to the lack of data and interpretive studies, leaving industry and regulators with difficult water-resources decisions. One of the goals of our study is to improve our understanding of ground-water systems in Interior upland

bedrock aquifers, and develop hydrologic guidelines and methods for evaluating hydrologic resources for other mining locations in Interior Alaska. Ester Dome is a good location to examine the hydrologic processes of Interior upland aquifer systems. Ester Dome has active surface mines of placer deposits and many areas of inactive surface and underground hardrock mining. Most of Ester Dome is undeveloped, but on the southern and eastern portions of the dome, residential neighborhoods with ground-water wells exist. It is estimated that half of the residences at Ester Dome obtain water from domestic wells, while the remainder use hauled water and water-holding tanks. This estimate is based on well logs from local drilling companies and the number of households in the study area. All wastewater at Ester Dome is disposed of through private septic systems. The majority of the domestic wells are completed in the upper saturated zones of the bedrock aquifer.

Withdrawal impacts to residential private water-supply systems are not well understood. The only known recent events of significant water withdrawal are associated with mining activities at Ester Dome. A pumping test at Grant Mine was conducted in 1985 (Walther, 1987a, 1987b) where approximately (741,280 ft^3) was pumped from the aquifer. The lowering of the water levels in the pond behind the Parks Highway weigh station at Ester occurred in the early 1990's and in 1998 (Vohden, 2003). In 1999, dewatering at Yellow Eagle Mine Pit99 (Vohden, 2000) occurred, resulting in a decline of nearby private water-supply wells.

METHODS

A ground-water monitoring network at Ester Dome includes approximately 50 wells, of which 7 are continuous-recording, data-collection stations. Water levels, summer precipitation, water temperature, and air temperature are recorded on an hourly basis at continuous recording sites. Approximately one-third of the ground-water wells are observation wells and the remaining are private water-supply wells. Ground-water levels are collected manually at all sites on a monthly basis. Pressure transducers are installed in the wells at the continuous-recording sites. Snow surveys are conducted at

the end of winter, just before snowmelt. Typically snow surveys take place around the end of March or early April and are conducted at multiple locations varying spatially and in elevation. Snow depth and density are measured to calculate the snow water equivalent (SWE). An Adirondack tube is used to measure five water densities and a measuring stick is used to measure fifty snow depths.

Well information and geologic well logs were obtained from local well drillers, ground-water well databases (GWSI, ADNR WELTS) and various other studies or surveys were examined and analyzed. Well depth and yield was examined to understand the aquifer storage properties. Geologic information was used to construct three-dimensional models of the subsurface for ground-water modeling.

GEOLOGIC FRAMEWORK

Regional Geology

The geologic history of the Fairbanks area is complicated due to metamorphic and tectonic events. Fairbanks area bedrock is comprised of rocks of the Yukon-Tanana Metamorphic Terrane. Newberry et al. (1996) mapped four metamorphic sequences in the Yukon-Tanana Terrane: 1) the Fairbanks Schist, 2) the Birch Hill Sequence, 3) the Muskox Sequence and 4) the Chatanika Terrane. All units are in structural contact with each other. The Proterozoic Fairbanks Schist is comprised primarily of quartz muscovite schist, quartzite of rare marble sedimentary origin, plus various mafic metaigneous rocks currently in greenschist facies but which have been retrograded from amphibolite facies (Forbes, 1982; Robinson et al., 1990; Newberry et al., 1996). The Ordovician to Upper Devonian low grade metamorphic rocks of the Birch Hill Sequence is made up of slate, metarhyolite tuff, quartzite, and phyllite (Pewé, 1976; Forbes, 1982; Robinson et al., 1990; Newberry et al., 1996). The Upper Devonian amphibolite facies retrograded to greenschist facies Muskox Sequence is composed of metarhyolite, amphibolite, and biotite schist (Newberry et al., 1996). The Chatanika terrane, a Devonian-Mississippian eclogite facies rock located in the northern part of the Fairbanks mining district, is comprised of schist, amphibolite, and quartzite (Newberry et al., 1996). Additionally,

Cretaceous igneous intrusives outcrop over much of the Fairbanks mining district.

Terranes are displaced fault-bounded regions, which exist across much of Alaska. The Yukon-Tanana Terrane, which is bounded roughly by the Denali Fault to the south and the Tintina Fault to the north. This terrane extends thousands of kilometers across Alaska and into parts of Canada (Forbes, 1982; Newberry et al., 1996). A series of northeast trending stress-relief faults cut across the entire Fairbanks mining district.

The valleys around Fairbanks are filled with alluvial and colluvial deposits and most of the hilltops and ridges are overlain with loess. Pewé et al. (1976) described the Tanana Valley floodplain deposits as well-stratified lenses and layers of unconsolidated sand and gravel. Alluvial deposits in the upland stream channels include valley-bottom accumulations of solifluction materials, designated the Cripple and Fox Gravels by Pewé (1975b). According to Pewé (1975b), the Cripple and Fox Gravels formed during a period of extreme climate fluctuations in the Pliocene and Pleistocene time.

Silt is an abundant fine-grained sediment in the Fairbanks area. Much of the silt was transported by wind into the Fairbanks area during the glacial episodes. The Fairbanks Loess is described by Pewé (1975b, 1976), Robinson et al. (1990), and Newberry et al. (1996) as a massive, homogenous, unconsolidated, and well-sorted silt. The Fairbanks Loess (or reworked silt) overlies the Cripple and Fox Gravels and bedrock and ranges in thickness of 1 m or less on ridge tops to 100 m thick in valley bottoms.

Much of the valley bottoms and north-facing slopes of many hills around Fairbanks, including Ester Dome, are underlain by discontinuous permafrost. Permafrost is defined as a surficial deposit or bedrock frozen continuously for two or more years at 0° C or less. Much of the valley bottom gravels and silt deposits are permafrost. Permafrost depth around Fairbanks ranges from 0.5 m below the surface to depths over 60 m (Pewé, 1958). However, permafrost may also occur in the bedrock, particularly on the north facing slopes of many of the domes and ridges around Fairbanks.

Ester Dome Geology

Bedrock

The bedrock units at Ester Dome include the Fairbanks Schist, Muskox Sequence, Birch Hill Sequence, and quartz monzonite plutonic rocks (Figure 4) (Newberry et al, 1996). The surficial deposits include the Fox and Cripple Gravels in the valley bottoms and the Fairbanks Loess, which blankets most of Ester Dome except at the higher elevations (Figure 4). Newberry et al. (1996) mapped four high angle northeast trending faults cutting across Ester Dome and two low-angle thrust faults (Figure 4). There are several additional smaller-scale faults at Ester Dome, which were mapped by Dashevsky et al. (1993), Rogers et al. (1998), and Cameron (2000).

The Fairbanks Schist (Figure 5) occurs over 75% of the Ester Dome study area of Ester Dome and occurs mainly as quartz-rich schist and quartzite. Newberry et al. (1996) identified two subunits of the Fairbanks Schist at Ester Dome: feldspathic quartzose schist (Zfw) and an amphibolite, magnetite-rich biotite schist (Zfa). After field inspection and geochemical analysis on these rocks, Cameron (2000) does not include the amphibolite, magnetite-rich biotite schist unit in the geology of the northwestern part Ester Dome. The Fairbanks Schist outcrops on many road cuts, and is seen at higher elevations of Ester Dome where there is no overburden. Where the unit is exposed, it appears very weathered and fractured.

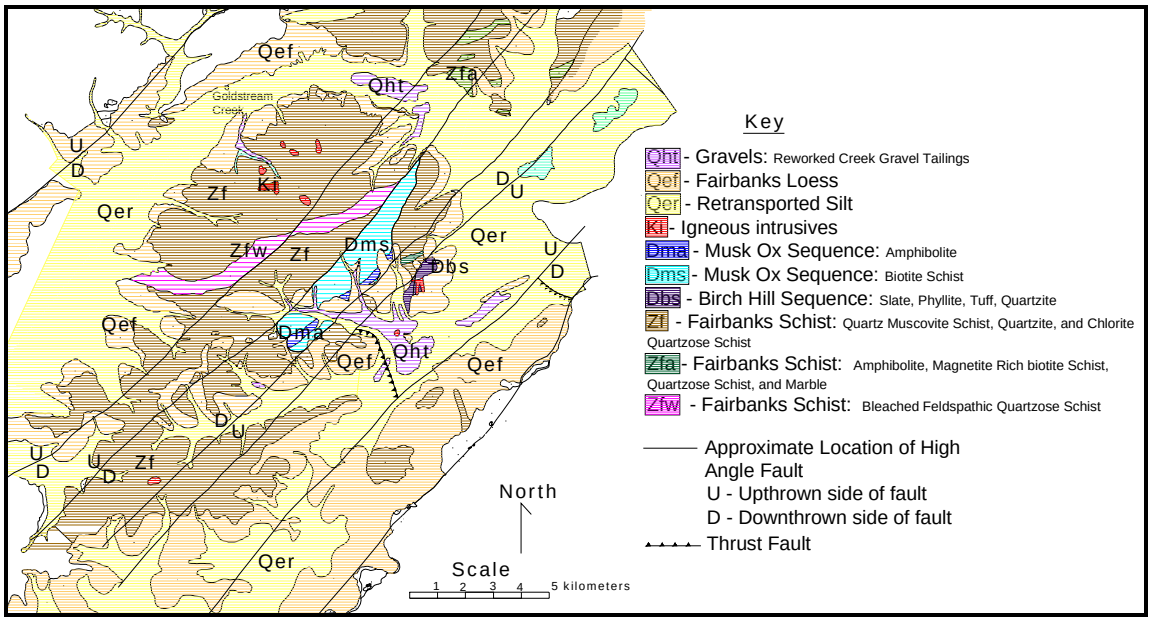

Figure 4. Geologic map of Ester Dome (Newberry et al., 1996).

The Birch Hill Sequence at Ester Dome is in fault contact with the Fairbanks Schist. It is bounded between two northeast trending high angle faults and a low angle thrust fault (Figure 4). This unit can be seen in the Ryan Lode shear zone where it is in fault contact with the Fairbanks Schist (Figure 4). Private water-supply wells completed in the weathered Birch Hill Sequence have discharged dark-colored water containing black sediments that are likely to be graphitic schist or slate, which are both characteristic of this unit. The Muskox Sequence occurs at Ester Dome in fault contact with the Fairbanks Schist. It is bounded by two northeast trending high angle faults. At Ester Dome, it occurs as a biotite schist and an amphibolite.

Figure 5. Photograph of the Fairbanks Schist at site EDP023 near the top of Ester Dome (photo by Philip Verplanck). The photograph shows the degree of weathering of the geologic unit.

Local geologists think that a large pluton exists at greater depths (1 km or more) under Ester Dome and is the source of the igneous rocks that are encountered in drill holes (Newberry, 2001). Two other domes in the Fairbanks mining district, Pedro Dome and Gilmore Dome, are igneous intrusives. At Ester Dome, the plutonic rocks are mostly quartz monzonites (Cameron, 2000). These units are non-resistant and are rarely exposed at the surface.

Quaternary Gravel Deposits

Most of the valleys and stream drainages at Ester Dome are filled with gravel or loess. The Ester Creek, Cripple Creek, Sheep Creek, and Nugget Creek drainages are

filled with mine tailings. In the valley bottom located on the eastern side of Ester Dome, large gravel deposits exist, ranging in thickness of 15-90 m (50-300 ft). This deposit is known as the Fox Gravel (Pewé, 1976) and is buried underneath the Fairbanks Loess. In the southern portion of the study area, along the Ester Creek and Cripple Creek drainages, the Cripple Creek Gravels are present. These gravels are similar to the Fox gravel in composition, consisting of pebble to cobble sized broken schist, quartzite, and slate (Figure 6) (Pewé, 1976).

Figure 6. Photograph of valley bottom gravels (photograph by Jim Vohden). Ruler shows units of inches on top.

Permafrost

Permafrost plays an important role in ground-water dynamics. Valley bottoms and north-facing slopes of many hills around Fairbanks, including Ester Dome, are underlain by discontinuous permafrost. Geologic data from wells drilled around the base of Ester Dome indicate the presence of frozen sediments and ice lenses. Ice wedges could be seen at the Yellow Eagle 99 pit near the southern boundary of the study area in the Cripple/Ester Creek area during the summer and fall of 2000 (Figure 7). The extent of permafrost varies vertically and horizontally resulting in complex ground-water flow patterns. In some instances, permafrost is considered a leaky confining unit. At Ester

Dome silt exists in all the valley bottoms and thins out as elevation increases. Kane and Stein (1983b) investigated the hydraulic properties of permafrost. They showed that ice-rich silt has very low hydraulic conductivity (10^{-8} m/s) and dry frozen silt can have hydraulic conductivities several orders of magnitude greater than ice-rich silt. It is important to identify zones of ice-rich silt because confined or artesian conditions may exist in these zones. However, due to the discontinuous nature of permafrost, delineating horizontal and vertical permafrost boundaries can be very expensive using drilling techniques. Using geologic maps, well and boring logs, and aerial images, we can roughly approximate the extent of the permafrost at Ester Dome.

Figure 7. Photograph of Fairbanks Silt and ice lens (outlined in white) at the Yellow Eagle 99Pit (by Jim Vohden).

The aerial photograph of Ester Dome (Figure 3) was examined to look for vegetation differences. Permafrost is common in valley bottoms and parts of the north-facing slopes. Permafrost may exist in areas where the dominant vegetation is black spruce (Viereck et al., 1986). Permafrost is likely to be less common on the south facing slopes of Ester Dome and where the dominant tree type is aspen or birch. However, the aerial photograph of Ester Dome also shows a significant portion of north-facing slopes to have large forests of aspen or birch, indicating either permafrost-free conditions or permafrost much deeper than plant root zones.

Little information is available on permafrost in frozen bedrock at Ester Dome, however, ground-temperature research at several CPCRW sites located in upland bedrock aids in determining the permafrost extent at Ester Dome. Six bedrock ground-temperature sites were established at CPCRW to better understand temperatures in the bedrock geologic unit (Collins et al., 1988). One site was located at a south-facing valley bottom in a mixed spruce, aspen, and alder forest and drilled to 10.8 m below ground surface. Three sites were located at mid-slope south-facing locations in three different vegetation types (aspen, black spruce, and alder). These sites were drilled between 12.8-16.2 m below ground surface. Two high elevation sites, one located near the summit of Caribou Peak (drilled 5.6 m below ground), in scattered black spruce (with trees no more than 3 meters in height) and one below the summit on a north-facing slope in a black spruce forest (drilled 4.6 m below ground). Average ground-temperature data was collected from June 1, 1986 through May 31, 1987. The three mid-elevation sites, and the valley bottom site all had average ground and surface temperatures above zero throughout the borehole. The summit site had a surface temperature near –1 ºC and at the deepest measurement (4 m) the temperature was 0 ºC (Collins et al., 1988). At the north-facing high-elevation site, the temperature averaged –1.3 ºC throughout the borehole (Collins et al., 1988). The results of this investigation can be transferred to Ester Dome. At Ester Dome it is likely that the south-facing slopes are permafrost free, while the north-facing slopes are frozen. Although the ground is frozen in the high elevation sites, it is not well understood how the permafrost affects recharge processes through the fractured bedrock.

The geologic maps by Pewé (1958) and Newberry et al. (1996) describe the surficial geology, which helps to estimate the permafrost distribution at Ester Dome. One can examine the areas of valley bottom sediments and compare to the vegetation in the aerial photograph and well log records. At Ester Dome, the north-facing slopes actually have little silt accumulation and forests of aspen, birch and alder. However, it is still likely permafrost exists on the north-facing slopes in the fractured bedrock, based on the results of the CPCRW investigation.

Yoshikawa and Hinzman (2002) created a mean annual ground-surface temperature map for the Fairbanks area. The map was constructed from an equivalent latitude/elevation model. The method looks at field air and soil temperatures, topography effects, and finally determines the site-specific freezing index and mean annual surface temperature. The information was also used to verify the delineation of the permafrost at Ester Dome.

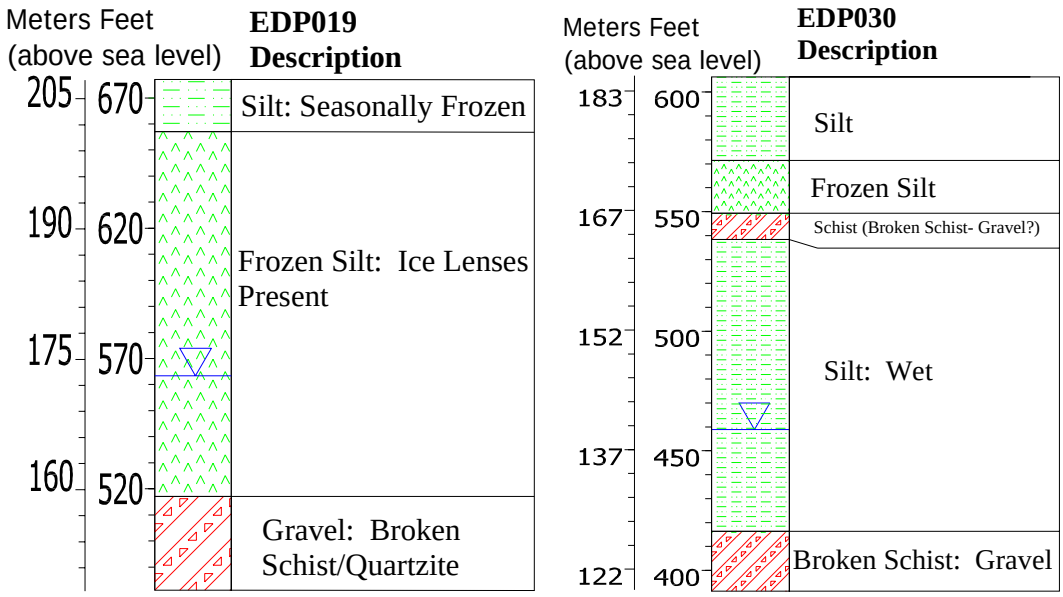

Figure 8. Well logs for EDP019 and EDP030

The methods mentioned above for determining the permafrost distribution can be verified by examining geologic well records. However, one complication is the limited amount of well log records spatially distributed across the study area. Most geologic well logs indicate permafrost along the valley bottoms. The northern part of Ester Dome is undeveloped and only mining company records exist from mineral exploration. Figure 8 shows the well log for well EDP019, located near the eastern boundary of the study area and site EDP030, located near the western boundary of the study area. These wells are located in valley bottoms and the geology in both areas consists of thick deposits of silt, which is often frozen. Both wells are screened in the fractured schist or gravel. Water levels in well EDP019 indicate confined conditions because the water level is located

above the base of the permafrost. Although geologic well log records are useful for identifying geologic units, interpretation of these records is usually difficult due to incomplete or vague descriptions of the geologic unit.

At Ester Dome, it is likely that frozen silt (dry and ice-rich) exists in the valley bottoms that are forested with black spruce. It is likely that the south-facing mid-slope locations are permafrost free. The north-facing slopes at Ester Dome have less silt accumulation, but the bedrock may be frozen, particularly in areas where black spruce is the dominant vegetation type. However, the presence of dry frozen fractured bedrock may not affect infiltration processes.

HYDROGEOLOGY

One of the main goals of this project is to identify important geohydrologic processes in Interior Alaska upland-bedrock aquifer systems. This information will be useful for land-use planners, residential development, industrial and mining operations, environmental assessments, and for future hydrologic studies. The conceptual model for Ester Dome will be the most important aspect of defining the geohydrologic processes for future ground-water flow models. Due to the limited knowledge of the geology and the aquifer properties, we must examine multiple conceptual models, which are developed and tested in the numerical modeling process. The conceptual models are based on previous scientific research, reports, and data in Interior Alaska uplands.

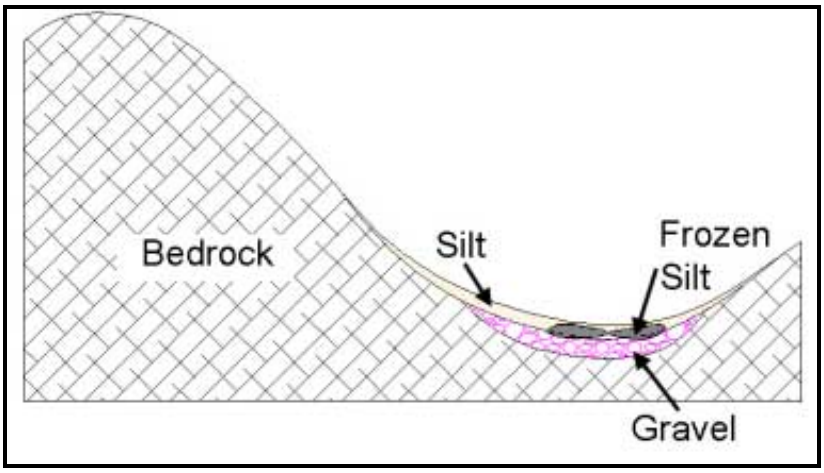

Figure 9. Generalized cross section showing hydrogeologic units.

The continuum approach is used for our conceptual and numerical models. Other main approaches include dual porosity and fracture network models. The project covers a relatively large scale, where bulk properties characterize the overall processes. Investigation of small-scale features and fracture networks is beyond the scope of this project. The continuum approach is a useful because there have been few general studies of these aquifer processes on Interior Alaska uplands and this project can act as a starting point for future smaller-scale projects.

Four hydrogeologic units are identified in the Ester Dome study area: bedrock, gravel, frozen silt (permafrost), and unfrozen silt (Figure 9). The bedrock unit consists of the igneous intrusives and the metamorphic units: Fairbanks Schist, Birch Hill Sequence, and Muskox Sequence. These geologic units were grouped together into one hydrogeologic unit for simplification. Additionally, hydraulic properties that would differentiate the individual geologic units are not known. The gravel unit is broken schist, quartzite, and shale. These units occur as valley bottom alluvial deposits and also as colluvial deposits, which are reworked hillslope erosion materials. Unfrozen silt exists in the valley bottoms and on the hillsides. The thickness of this unit decreases as elevation increases. At the higher elevations on Ester Dome, this unit does not appear. Frozen silt, dry and ice-rich, exists primarily at the low-lying elevations of Ester Dome.

Scale Issues

Study scale is important to address in any hydrogeologic investigation. This project is a medium-scale study of an aquifer system located within the Tanana Basin. Ground water in the Tanana Basin is flowing from the higher elevations toward the Tanana River. Part of the Ester Dome study area is in the Goldstream Creek watershed, but a topographic divide exists along Ester Dome, where we assume water south of the divide flows into Ester, Alder or Cripple Creeks. This water then discharges into the Chena and Tanana Rivers. Figure 10 shows the concepts of regional and local flow and scale in a hydrogeologic investigation.

Although the Ester Dome aquifer system may seem like a relatively small-scale investigation, typical industrial or residential projects are usually smaller scale than the Ester Dome study. Within Ester Dome, one has to examine multiple smaller watersheds. For example, the Ester Creek watershed is one of the sub-basins on the south side of Ester Dome. Within the Ester Creek watershed is the Ready Bullion watershed, which is an even smaller scale. An investigation at the smallest scale may include a well field type study, where wells are distributed on a one-acre (or less) plot. Depending on the scale one is working at, the aquifer properties can vary several orders of magnitude due to heterogeneities within the scale (Shapiro, 1993). Hydraulic conductivity is influenced by the fractures in the bedrock. On a scale of several kilometers, aquifer properties are influenced by small scale and large-scale fractures, while on a scale of several meters, water levels in boreholes may significantly vary depending on their intersection with fracture zones (Shapiro, 1993). The values of the bulk aquifer properties of the Tanana Basin will not be the same as the values for bulk aquifer properties of Ester Creek Basin due to scale effects. Therefore it is important to consider the aquifer properties presented in this study may vary by orders of magnitude depending on the scale of the problem.

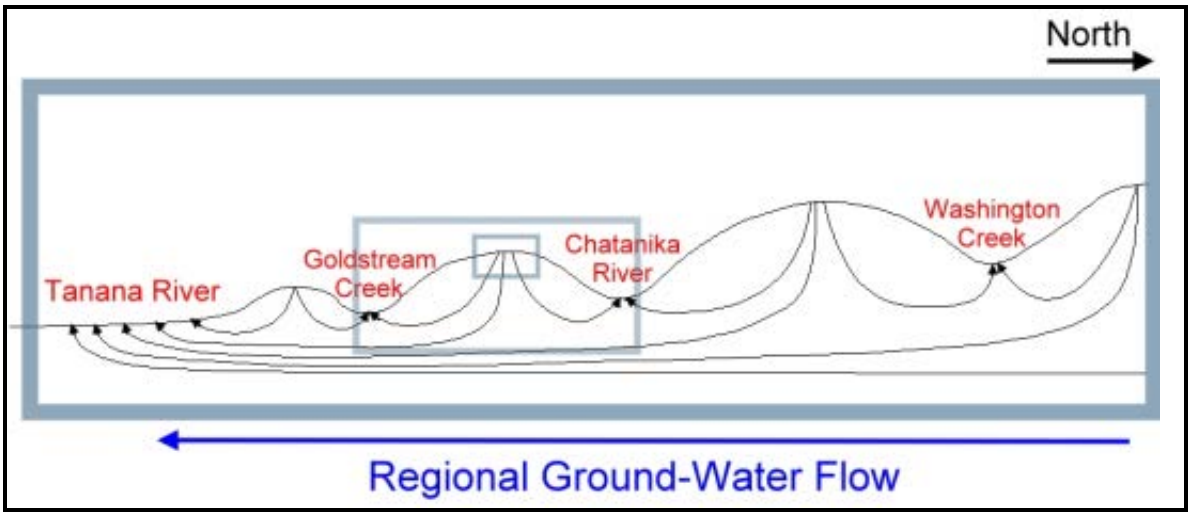

Figure 10. Schematic demonstrating the local and regional ground-water hydrology. Boxes indicate the concept of different hydrologic scales.

Conceptual Model

Of the four hydrogeologic units at Ester Dome, only the bedrock and gravel units are potential aquifer systems. The primary aquifer system is the fractured bedrock unit. The hydrogeology of fractured rock aquifers is poorly understood due to the complex flow behavior through fractures. The governing ground-water flow equations may not apply to these types of aquifers at a small scale. We are assuming the fracture density is high and the length and spacing of these fractures is much smaller than the scale of the entire dome. Because quartz-rich schist and quartzite are the primary rock type on Ester Dome, we are assuming that this rock is highly fractured due to the brittle nature of the rock type.

At Ester Dome, in the bedrock aquifer, storage and ground-water flow are mainly controlled by fractures, joints, and foliation planes. Additionally, geologic data shows parts of the northeast trending fault zones consist of gouge material and mineralized quartz veins (Newberry et al, 1996; Cameron, 2000). This may restrict or increase ground-water flow, however most of the faults at Ester Dome have not been entirely mapped in detail. The bedrock aquifer is almost entirely unconfined except in the valley

bottoms where there may be locally-confining permafrost layers. Confined conditions are known to occur in the valley bottoms in the Goldstream Creek, Sheep Creek Road, Cripple Creek, and Alder Creek areas due to the presence of permafrost. Water levels in several valley bottom wells that penetrate through the permafrost and into the bedrock typically are above the base of the permafrost. Well yields are relatively high and little drawdown from pumping is observed in these wells.

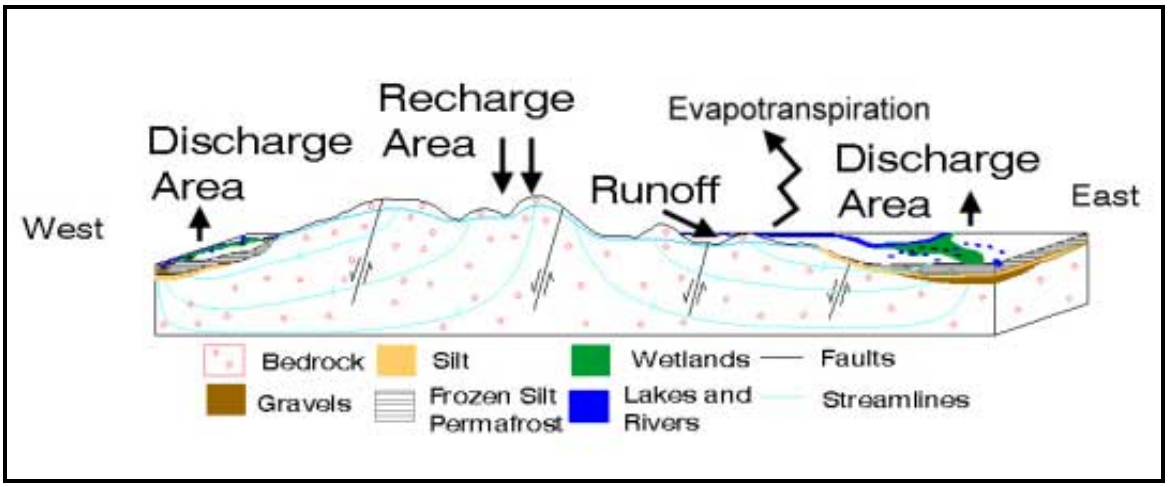

Figure 11. Conceptual model of Ester Dome.

The other significant water sources are the Quaternary gravel deposits, also described as the Cripple and Fox Gravels by Pewé et al. (1976), which exist in the valley bottoms. These deposits consist of broken schist and quartzite. Nearly all of this deposit is overlain by silt, much of it frozen. The valley bottom gravel aquifer is generally confined due to the permafrost and frozen silt overburden. However, in areas having an extensive placer mining history, the permafrost and silt is, in most cases, no longer present, indicating unconfined conditions. Because of the uncertainty in the geology, we developed several conceptual models of the permafrost distribution. There may be areas of suprapermafrost ground water above permafrost at Ester Dome, however, these are typically non-producing, and would not be suitable for water supply.

Ester Dome can be thought of as the inverse of a watershed. The general drainage and flow pattern at Ester Dome is radial, where surface and ground water originate from a central area. The center, or top, of the dome is the main recharge area

for the bedrock aquifer. Ground water is flowing from the recharge area, generally at a high elevation, downward toward the valley bottoms. The boundaries of the dome are discharging ground water to streams, lakes, or ponds. Surface-water features in the valley bottoms coincide with local or regional ground-water divides. Flow velocities through fractured bedrock are relatively high due to the steeper gradients and the increased hydraulic conductivity through fracture zones. In general, the water table follows the topography. In the Fairbanks area, most ground water for domestic use is within the upper 300 meters of the bedrock hydrogeologic unit. Figure 11 is a schematic of the conceptual model for Ester Dome.

Aquifer Characteristics

In a typical hydrogeologic investigation, aquifer properties and ground-water levels are determined to calculate flows, gradients, and make predictions of ground-water processes. Conducting aquifer tests to determine parameters such as hydraulic conductivity and storativity are not within the scope of this investigation. In fractured media, aquifer tests are done by isolating a known fracture zone and conducting a pump or slug test in that zone. This determines the hydraulic conductivity for that fracture set. Since our project is at a larger scale, obtaining point measurements of aquifer properties was not practical. It is felt that further field studies to better understand the aquifer parameters would be very useful, though small-scale tests will be less transferable to larger-scale studies.

The parameters of the Fairbanks upland aquifers are needed for understanding and interpreting the geohydrologic processes. Hydraulic conductivity is an important parameter, which needs to be defined for ground-water flow modeling and predictions on how ground-water aquifers will be impacted by long-term climate changes or development activities. In this study, aquifer properties are estimated from previous investigations of the particular hydrogeologic unit. We selected a range of values reasonable for each hydrogeologic unit. A ground-water flow model was developed to aid in the interpretation process and to better estimate these parameters and take into

account the complexity of the ground-water flow systems. During the model calibration process these ranges were refined to obtain a better approximation of the hydraulic conductivity.

Hydraulic Conductivity

The values shown in Table 1 for hydraulic conductivity of fractured bedrock, gravel, silt, and frozen silt were compiled from numerous previous investigations. Ranges are given for many of the hydrogeologic units because of changes in grain size, sorting, degree of fracturing, etc. The bedrock hydraulic conductivity is highly variable and varies several orders of magnitude. This is due to the variability of fractures, joints, foliation planes, or cementation of the grains.

Table 1. Literature values of hydraulic conductivity.

Hydrogeologic Unit	*Hydraulic Conductivity (m/d)*	*Hydraulic Conductivity (ft/d)*	*Reference*
Fairbanks Silt (dry)	8.64E-2	0.283	Kane and Stein, 1983a
Fairbanks Silt (frozen, low water content)	8.64E-2	0.283	Kane and Stein, 1983a
Fairbanks Silt (frozen, high water content)	8.64E-4	2.83E-3	Kane and Stein, 1983a
Silt (dry)	8.64E-5 to 0.864	2.83E-4 to 2.83	Freeze and Cherry, 1979
Silt (dry)	8.64E-4 to 8.64E-2	2.83E-3 to 0.283	Fetter, 1994
Silt (dry)	8.64E-5 to 1.73	2.83E-4 to 5.67	Domenico and Schwartz, 1998
Gravel	8.64 to 864	28.3 to 2.83E+3	Fetter, 1994
Gravel	0.864 to 864	2.83 to 2.83E+3	Freeze and Cherry, 1979
Gravel	25.9 to 2.59E3	84.9 to 8.50E+3	Domenico and Schwartz, 1998
Fractured Igneous and Metamorphic Rocks	8.64E-4 to 8.64	2.83E-3 to 28.3	Freeze and Cherry, 1979
Unfractured Igneous and Metamorphic Rocks	8.64E-9 to 8.64E-6	2.83E-8 to 2.83E-5	Freeze and Cherry, 1979
Fractured Igneous and Metamorphic Rocks	1E-8 to 8.00	3.28E-8 to 26.2	Heath, 1983
Schist	0.2	0.65	Morris and Johnson, 1967
Fractured Igneous and Metamorphic Rocks	6.91E-4 to 25.9	2.27E-3 to 84.9	Domenico and Schwartz, 1998
Unfractured Igneous and Metamorphic Rocks	2.59E-9 to 1.79E-5	8.49E-9 to 5.87E-5	Domenico and Schwartz, 1998
Weathered Granite	0.285 to 4.49	0.935 to 14.7	Domenico and Schwartz, 1998

Kane and Stein (1983a) reported the hydraulic conductivity for frozen and unfrozen silt through field investigations (Table 1). As shown, the values for unfrozen, and low water content frozen silt are similar. The hydraulic conductivity for ice-rich silt is several orders of magnitude lower. The hydraulic conductivity for unfrozen and dry frozen permafrost is significantly higher than other reported values. Further investigation into these values took place in the ground-water modeling portion.

In the eastern portion of Ester Dome, thick gravel deposits exist in the valley bottoms. The deposits are from hillside erosion of bedrock materials and later reworked by stream action (Pewé, 1976). The deposits are overlain by silt and only exposed at the surface where placer mining occurred in creek beds. The hydraulic conductivity of these deposits is much higher than the silt and bedrock. The range of hydraulic conductivity for the gravel deposits is listed in Table 1.

Well Yield and Well Depth

At Ester Dome, well yields vary based on the hydrogeologic properties of the aquifer, topography, fracturing, and where the well is located in relation to the recharge area. It is likely well yield also depends on the fracturing in the aquifer and the interconnectivity of these fractures. We examined the well yields of wells located in the bedrock aquifer and the gravel aquifer. Overall well yields at Ester Dome, during initial well tests upon installing a pump in a domestic well, range from 3.2E-5 to 1.9E-2 m^3/s (0.75 to 300 gpm). Table 2 shows the statistics on well yield for the wells examined at Ester Dome. Weber (1986) reported a mean yield of 6.3E-4 m^3/s (10 gpm). However, yields may be higher than the reported yield because the driller usually stops drilling when a reasonable yield is reached for a domestic well, or pumping equipment limits the rate of water pumped from the well. The highest well yields occur in the gravels or highly weathered or fractured bedrock in the valley bottoms. The valley bottom part of the aquifer generally yields higher flows because 1) local ground water at Ester Dome is flowing toward the valley bottoms, 2) there may be confining conditions, and 3) higher hydraulic conductivity. Weber (1986) reports a region of high well yield (5E-3 to 1.3E-2

m^3/s or 15 to 40 gpm) along the Sheep Creek Road area near Ester Dome. It is likely that the higher yield wells in this area are drilled into the high permeability gravels and are overlain by a confining layer of permafrost.

Table 2. Well yields and depths from well log records at Ester Dome, Alaska.

Well Yields and Well Depths at Ester Dome	***Overall Range***	***Bedrock Aquifer-Average***	***Bedrock Aquifer-Median***	***Gravel Aquifer-Average***	***Gravel Aquifer Median***
Well Yield	3.2E-5 to 1.9E-2 m^3/s (0.5 to 300 gpm)	1.7E-3 m^3/s (28 gpm) (N=39)	6.9E-4 m^3/s (11 gpm)	1.3E-3 m^3/s (20.3 gpm) (N=11)	1.1E-3 m^3/s (19 gpm)
Well Depth (m)	10.7-149	79.2 (N=62)	77.4	45.7 (N=13)	47.2

Figure 12a shows distribution of well yields at Ester Dome for the gravel (broken schist, quartzite, amphibolite, slate) and bedrock aquifers. Although the bedrock aquifer has a higher average well yield than the gravel aquifer, the median well yield is much lower than the average well yield. The high well yield average for the bedrock aquifer is due to three extremely high well yields. Two of these extremes are located near the high transmissivity Grant Mine area fault zone. This is a region of intense fracturing and faulting.

In general, the higher well yields tend to occur in the valley bottoms, where confining conditions and high permeability gravel deposits occur. Along ridge tops, well yields vary, based on the degree of fracturing and weathering of the aquifer. Due to the small contributing area of recharge and the seasonal pattern of recharge, there is limited water available on the ridge tops during most of the year. Well yields on Ester Dome summit, and ridges such as the Old Nenana and Parks Highway Ridge show very low yields. These wells are generally very deep with low water-level elevations. Although the yields of all ridgetop wells are very low, wells on Ester Dome Summit are shallower and have much higher water-level elevations than other ridge tops. Robinson et al. (1990) mapped Ester Dome as an antiform, which is an arch-shaped fold. Antiforms can develop severe fracturing at crests resulting in increased porosity and well yield (Singhal and Gupta, 1999), which could explain the higher water levels at the summit of Ester

Dome. Harsher climate environment at high elevations lead to increased bedrock erosion rates at the Ester Dome summit. Another explanation could be increased quartz content in this area, which leads to greater fracturing due to the more brittle nature of quartz-rich rocks.

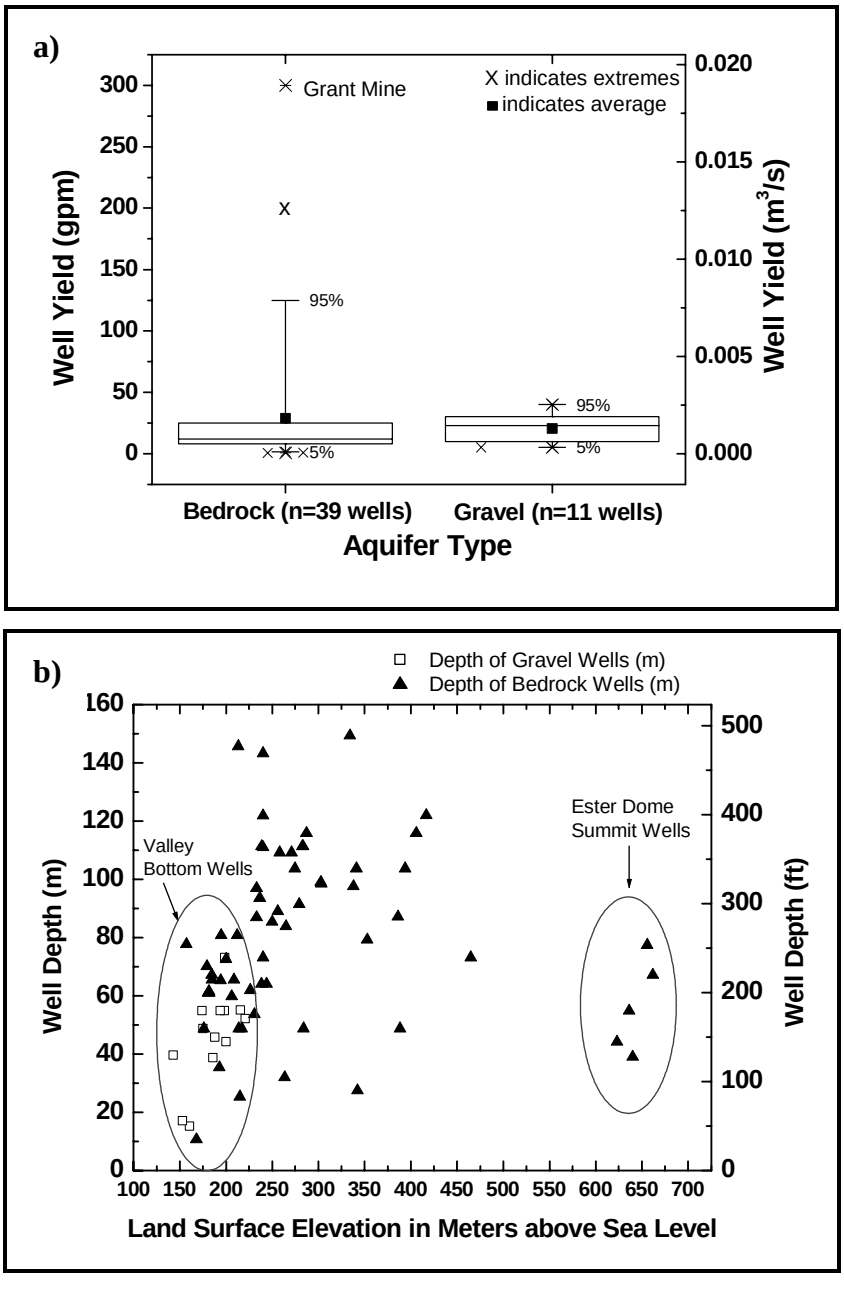

Figure 12. a) Boxplot showing the distribution of well yields and b) graph showing the well depth with elevation at Ester Dome.

Well depths in the Ester Dome study area range from 11-150 m (30-492 ft) deep. Weber (1986) reported an average well depth of 54.56 m (179 ft) for 42 wells on Ester Dome. Figure 12b shows a graph of well depth versus land surface elevation. Most private water-supply wells are drilled to a depth in the aquifer that yields a sufficient water supply. The data shows wells located in the valley bottoms are generally shallower than the higher elevations. The deepest wells in this study are located on the ridge tops of Old Nenana Highway Ridge and the Parks Highway Ridge, in the southern portion of the field area. Wells that are 91 m (300 ft) or deeper generally exist at elevations greater than 260 m (850 ft). Wells less than 91 m (300 ft) deep generally occur at lower elevations ranging from 137 to 260 m (450 to 850 ft). An exception is the Ester Dome summit wells. Four of the five summit wells are less than 61 m (200 ft) deep, with the fifth well 77 m (254 ft) deep. The construction of these relatively shallow wells, which is generally unlikely along a ridge top, is probably due to the intense weathering and fracturing of the rock in this area, creating a high secondary porosity and permeability.

Surface-Water Contributions

Surface-water features exist along the valley bottoms and also as runoff down the slopes of the dome (Figure 13). One relatively large stream, which flows around north side of Ester Dome, is Goldstream Creek, which is the northern boundary of the study area. Goldstream Creek originates in the uplands east of Fox, Alaska and flows west through Goldstream Valley toward the Chatanika and Tanana Rivers west of Ester Dome. Goldstream Creek coincides with a ground-water divide between Ester Dome and Murphy Dome/Moose Mountain. Ground water and surface-water runoff discharges into Goldstream Creek from Ester Dome. Stream flow measurements at Goldstream Creek in August 2000, measured a gain of 5.6E-2 m^3/s (2 cfs) over a distance of 6.3 km. Winter stream flow was not measured due to the thick ice coverage. Goldstream Creek is located in an area of continuous permafrost, apart from thawed areas beneath the creek. Many bedrock wells located near Goldstream Creek around Sheep Creek Road show confining conditions where water levels in wells can be less than 5 m below the ground surface.

Runoff occurs as intermittent or perennial streams on the steeper slopes of Ester Dome. These streams start flowing at higher rates as snow melts in April and May. The highest flow rates in these streams occur after snowmelt and during the rainy summer months (typically August). During the 2000-2002 study period, Happy Creek, Ester Creek, Eva Creek, Cripple Creek and Alder Creek flowed all summer long, even at the higher elevations, although the flow rates are generally lower than 0.028 m^3/s (1 cfs).

Data collection efforts at Caribou Poker Creek Research Watershed (CPCRW), located 48 km northwest of Fairbanks in the uplands, show that streams located in continuous permafrost areas have a "flashier" response to precipitation, compared with streams in non-permafrost areas (Slaughter and Kane, 1979; Haugen, 1982). Although this was not investigated in the Ester Dome study, it is likely that similar stream behavior occurs at the Ester Dome sub-basins.

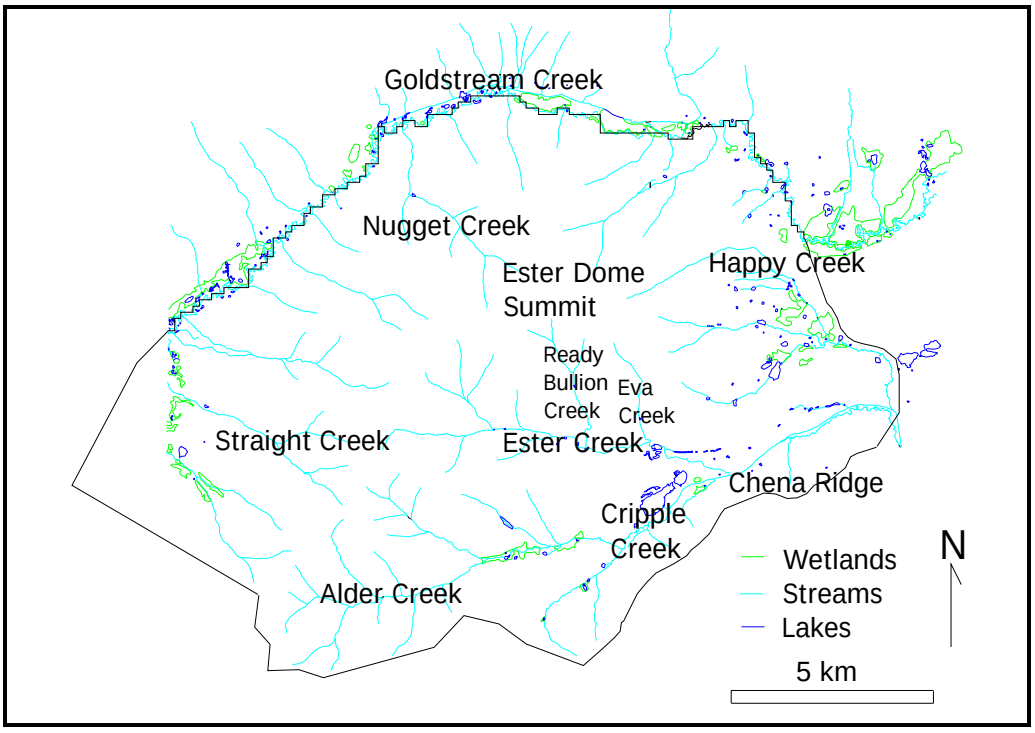

Figure 13. Surface-water features at Ester Dome.

We observed aufeis in the stream channels during winter. This is an indication that ground-water springs could be feeding the channels all winter long. After time, thick

deposits of aufeis occur and remain in the channel through spring breakup often into June. The aerial photograph (Figure 3) of Ester Dome taken on May 18, 1999 shows the presence of aufeis in many stream channels. The aufeis often exists over very long lengths of the stream channel and even occurring at elevations over 450 m. Figure 14 is a photograph of aufeis in the upper reaches of Ester Creek. The photograph shows that the aufeis may be up to one meter thick.

Figure 14. Aufeis up to one meter thick surrounds vehicle in Ester Creek channel, March 2001 (photograph by Paul Overduin).

Wetlands exist in most of the low-lying elevations around Ester Dome. They are most common in the Sheep Creek Road, Goldstream Creek, and Alder Creek, and Cripple Creek areas. Ground water makes its way through thawed zones in the permafrost and discharges into the low-lying wetlands. Most lakes are present at elevations less than 250 m (850 ft). Many oxbow lakes exist along Goldstream Creek. Many small lakes in the valley bottoms are areas of ground-water discharge (Kane and Slaughter, 1973). Ground water is likely to be discharging through thawed areas underneath Goldstream Creek and the ponds that are located immediately adjacent to Goldstream Creek. It is

likely that most valley-bottom lakes at Ester Dome are hydraulically connected to the subpermafrost aquifer. Little information is available because there are few wells close to the lakes. In the western edge of the study area, near the low-elevation site EDP030 (Figure 15), where well logs report permafrost thickness as 15 m (50 ft), subpermafrost ground water is flowing from the higher elevations in the east and discharges into Goldstream Creek. Several unnamed lakes around 155 m elevation located immediately west of site EDP030 (Figure 15), may be in hydraulic connection with the bedrock aquifer. Yoshikawa (2001, personal communication) noted the water levels declining in many of these smaller lakes. Measurements from a piezometer installed at one of the ponds indicate a very high vertical gradient downward. This indicates that water is leaking downward out of the pond and may indicate a thawed zone under the lake. Additionally, aerial images taken from 1950 and present indicate shrinking of several ponds in this area (Yoshikawa, 2001, personal communication), based on changes of the configuration of the lake area and examination of the shorelines.

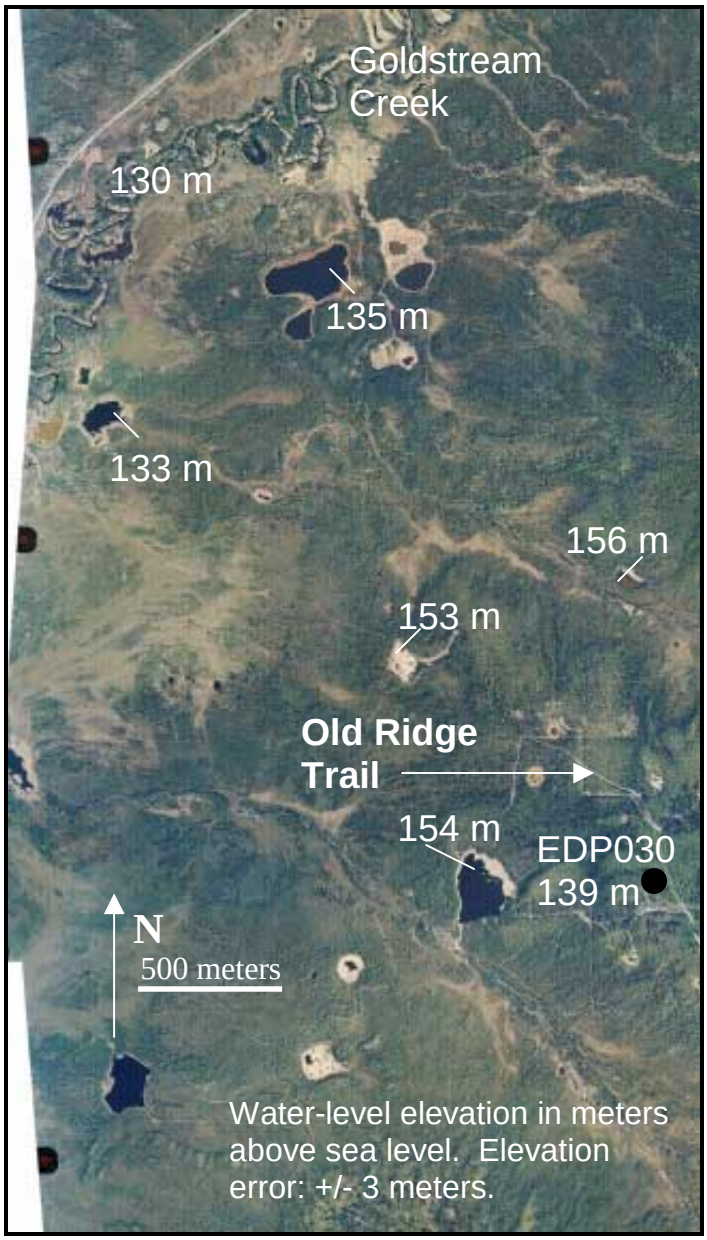

Figure 15. Surface-water and ground-water level elevations (in meters above sea level) near the western boundary of study area (photo from Aeromap, Inc., 1999).

Ponds located in the Ester and Cripple area along the Parks Highway also show hydraulic connection with the subpermafrost aquifer system (Figure 16). Ground-water elevations in wells upgradient of several ponds in the Yellow Eagle Mine area indicate ground-water flow from the gravel or fractured bedrock aquifers into these ponds.

Figure 16. Aerial photograph showing approximate pond and ground-water level elevations in the Ester area (photo courtesy Aeromap, Inc., 1999). The hydrographs for colored wells are shown in figure 17.

The 1999 dewatering incident at the Yellow Eagle Mine in Ester shows a relationship between ground water and surface water. Personnel working for Yellow Eagle Mine, Inc. had been excavating a pit (known as Pit99) 152.4 m by 121.9 m and a depth of 30.5 m below the initial ground surface during the summer and fall of 1999 (Vohden, 2000). They excavated through layers of unfrozen silt, ice-rich silt, frozen and unfrozen gravel. In late September, excavators in the pit intercepted the water table and ground water began discharging into the pit. Private water-supply wells in this area are drilled through frozen and unfrozen silt and screened in broken schist and quartzite

(Cripple gravels) or highly fractured Birch Hill Sequence. Natural water levels are above the base of the permafrost in most wells, indicating confining conditions. There are approximately five ponds in this area that are at elevations around 170 m (557 ft). The ground-water level elevations in the area immediately north of the pond are 169 to 177 m (554 to 580 ft). When dewatering of the subpermafrost ground water occurred in the pit, ground water began flowing at reported rate of 3.15E-2 m^3/s (500 gpm) (Vohden, 2000) into the pit and water levels in the wells upgradient dropped significantly as shown at well EDP006 and EDP015 in Figure 17. All wells show recovery after the dewatering. Additionally, water that discharged into the pit and the ground-water wells shows similar geochemical characteristics (Vohden, 2000). Vohden (2000) plots geochemistry data on a trilinear diagram and shows the water chemistry of Pit99 and all the wells in the gravel or fractured bedrock aquifer to be very similar.

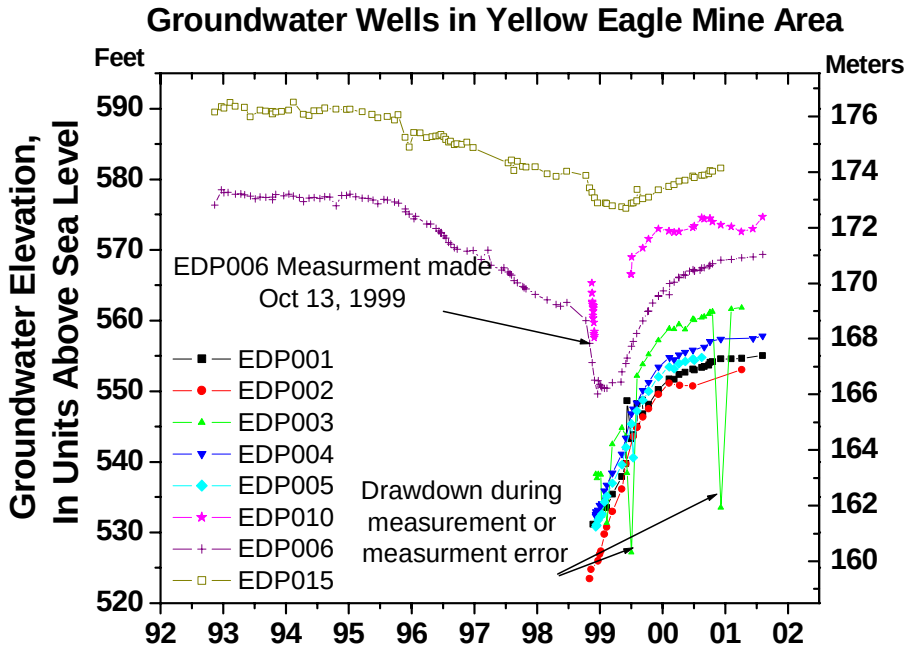

Figure 17. Hydrograph showing wells affected by Yellow Eagle Mine activities.

RECHARGE AND EVAPOTRANSPIRATION

Aquifer recharge is water that reaches the water table and replenishes an aquifer system. The forms of potential aquifer recharge at Ester Dome are 1) snowmelt infiltration, 2) summer precipitation, and 3) septic-system discharges. However, of the three, spring snowmelt infiltration is the only significant form of recharge. Recharge from discharging septic systems was not examined in this study, and is suspected to be an insignificant component of recharge due to high evapotranspiration during the summer. Additionally, septic system recharge to the aquifer is nearly equal to domestic water use by pumping ground water out of the aquifer. The exception is households that have water delivered to their homes from outside Ester Dome and store it in water-holding tanks.

Figure 18 is the conceptual model for seasonal hydrologic processes in Interior Alaska upland systems. Most of the ground-water recharge in upland-aquifer system occurs at the higher elevations on ridge tops. Less recharge occurs in the lower elevations and valley bottoms due to the increased presence of ice-rich permafrost and no exposed fractured bedrock. Evapotranspiration is an important component of the water cycle during the summer months. Gieck (1986) showed that potential evapotranspiration either met or exceeded precipitation in the months of June and July at all elevations during the study period 1982-83. The highest evapotranspiration levels occurred at the lowest elevations.

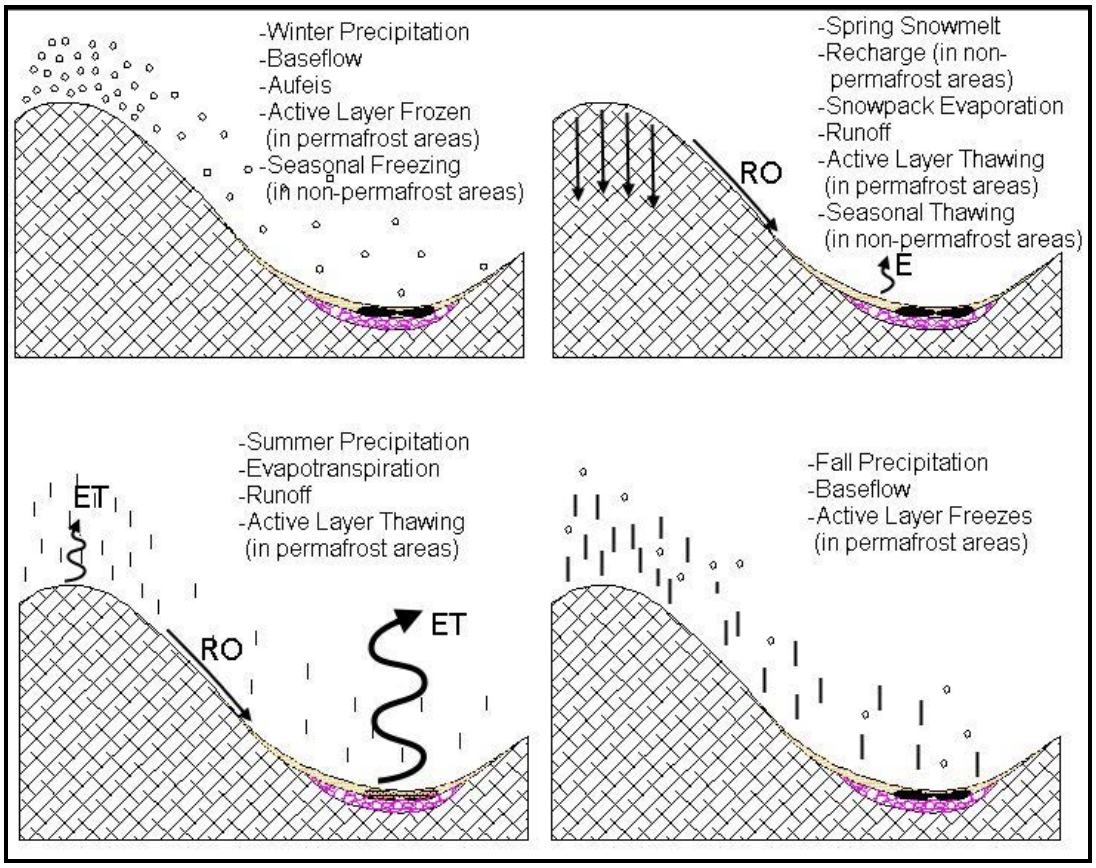

Figure 18. Conceptual model of seasonal hydrologic processes in the uplands.

Most of the recharge in the Fairbanks uplands takes place in non-permafrost areas during the spring months when the snowpack melts. This can be seen from many of the well hydrographs showing seasonal rises in water-level elevation in the proceeding weeks after snowmelt. During the winter months, no recharge to the aquifer can occur because freezing temperatures do not allow the snowpack to melt. Summer precipitation shows little or no impact on the subpermafrost aquifer system due to the high evapotranspiration rates and continuous permafrost coverage at the lower elevations. It is possible recharge could occur during the wetter fall months at the higher elevations, where there is no silt coverage and lower evapotranspiration. However, water-level records do not indicate this occurring during the period of study. More continuous observations of water levels in bedrock wells at higher elevations may show otherwise.

At Ester Dome, along with many of the ridges and domes in Interior Alaska, different recharge rates exist based on the maximum SWE, the geology of the area, and evapotranspiration variations. At the base of Ester Dome, where ice-rich permafrost is thickest and more continuous, direct vertical recharge to the bedrock aquifer is very low. Ground-water recharge can occur quickly and easily where silt coverage is thin or bedrock fractures are exposed at the surface, depending on the evapotranspiration rates. Additionally, in thawed zones under surface-water bodies and areas of discontinuous permafrost, ground-water recharge may occur. Although permafrost exists on the north-facing slopes of Ester Dome, it is possible recharge occurs through the fractured bedrock at the surface, despite the freezing ground temperatures. The infiltration processes through frozen (high and low ice content) bedrock are unknown due to limited data and information. Infiltration through frozen fractures could be slower or restricted, if there is a high ice content in the fracture.

Poorly drained soils, continuous permafrost, or ice-rich active layer conditions, and a high slope angle allow for surface runoff to occur. At site EDP019-C, located at the base of Ester Dome, which has thick ice-rich frozen silt deposits, standing water was seen on the ground surface into late May every spring during the study period. Primary recharge to these valley bottom bedrock wells is likely from up-gradient recharge areas. As the elevation increases, the silt and permafrost thickness decreases and fractures in the bedrock control the recharge processes. Significant amounts of recharge may enter the aquifer through the weathered bedrock. Once the recharge infiltrates into the weathered bedrock, it accumulates as storage in fractures and can flow through the fractures.

Most of the lakes and largest streams at Ester Dome are located around the base of the dome in discharge areas. These lakes may provide aquifer recharge. Ground-water recharge may occur from a few “flow through” lakes around the dome. Most lakes are hydraulically connected to the aquifer system through thawed zones under the lake. Large lakes such as Ace Lake and several lakes near the western boundary of the study area may be hydraulically connected to the subpermafrost aquifer because they often do not freeze to the bottom during winter. As previously mentioned, Yoshikawa (2001)

indicates lakes in the western portion of the field area losing water to the aquifer. Unfortunately, little data is available around these lakes for further investigation of these recharge sources.

Another area that could have potential increased recharge to the aquifer is in the mined areas of Ester Dome. Several trenches and pits exist on Ester Dome where vegetation and overburden is cleared and bedrock is exposed at the surface. Many of these areas could see increased recharge if water from snowmelt and summer rainfall can accumulate in these pits and directly infiltrate through the exposed fractures, joints, and bedding planes. The Ryan Shear at Ryan Lode mine has previously been excavated, resulting in open-pits into the bedrock with no vegetative cover. It was originally thought that the open pit at Ryan Lode is a mechanism for recharge to the aquifer. It was also hypothesized that these open-pits are also getting recharge from summer/fall precipitation. However, during field investigations of the geology in the Ryan Shear, significant amounts of gouge material is present in the shear zone. The clay-like material exists in the fractures, not allowing water to infiltrate easily through open fractures. During the snowmelt period of 2002, the Ryan Shear pit stored a large pool of water for a period of at least one to two weeks. Due to the blockage of open fractures with gouge material, evaporation of the pooled water may be an important process. However, if gouge material is not present, significant amounts of water may infiltrate easily through these highly fractured fault zones and excavated or cleared mining areas.

In the Ester Creek/Yellow Eagle Mine area, several placer mining operations exist in the valley bottom. The geology in this area consists of gravels and mine tailings, which allows water to infiltrate quickly. Well EDP027 (Figure 19) at Ester Fire Department penetrates the bedrock aquifer, which is overlain by 26 m of gravel/tailings. Ground water is pumped into a storage tank on a weekly basis and this is seen on the graph as drawdown spikes. It is unknown how far the water level drops from pumping because it falls below the pressure transducer in the well. This well exhibits a response to snowmelt and summer precipitation events indicating infiltrating water reaches the water table in this area. The timing of the increase in water levels suggests the recharge to this

site is local rather than from higher elevation recharge areas. Most wells penetrating bedrock in the valley bottoms overlain by silt and permafrost and exhibit little or no response to snowmelt or summer precipitation.

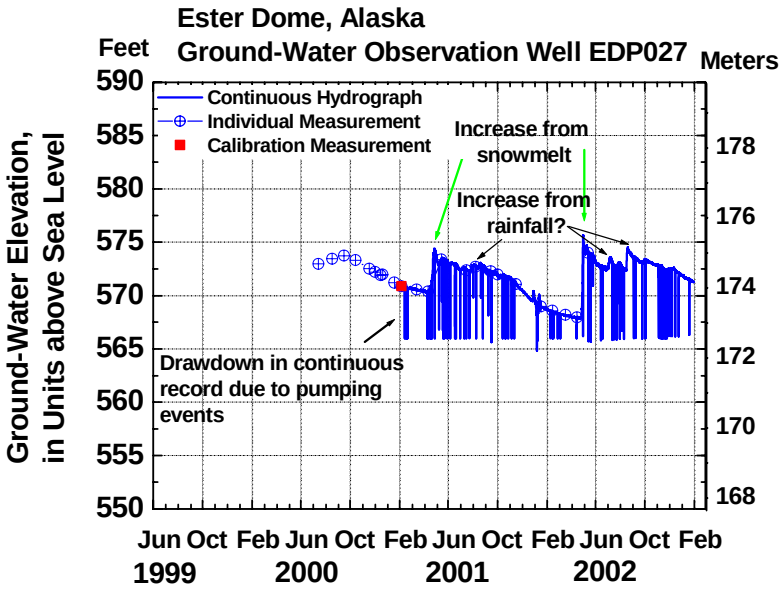

Figure 19. Hydrograph for Ester Fire Department well EDP027 located in the Ester Creek area.

Previous studies indicate infiltration rates and hydraulic conductivities decrease in ice-rich permafrost areas. Monitoring of ground-water elevations in many of the wells may indicate whether water is infiltrating to the water table after snowmelt. From the water-level observations, little vertical recharge to subpermafrost ground water occurs in areas of continuous ice-rich permafrost in the valley bottoms at Ester Dome. Water levels in wells penetrating known areas of continuous permafrost do not increase after snowmelt. Some permafrost areas in the valley bottoms, particularly in zones of thin permafrost, may allow some recharge to enter the bedrock aquifer on the edges of the permafrost, however seasonal ground-water level fluctuations indicating recharge are not seen in any of the wells monitored in permafrost zones. Water levels taken on a monthly

basis may not be adequate to measure seasonal fluctuations due to snowmelt or summer precipitation recharge.

Precipitation during the preceding fall months can affect spring snowmelt recharge. If there is a dry fall, the soil water content will be low and the ground will have lower ice content for greater snowmelt infiltration and less runoff the next spring. If there is a wet fall, the soil water content will be higher, resulting in ice-rich frozen soils during spring. This can decrease snowmelt infiltrations and increase surface runoff.

Snow surveys were conducted in late March and early April of 2001 and 2002 to measure the amount of snow available for recharge. The snow depth and density were measured at approximately 18 sites on Ester Dome. The sites were chosen based on their spatial distribution and type of vegetation to better understand the variability in SWE and potential aquifer recharge. Sites were also chosen that were in close proximity to the continuous-recording ground-water sites. Appendix B shows the characteristics and snow-water equivalent (SWE) at each site. The snow survey information was used to help identify areas of high potential recharge. SWE was calculated to estimate the amount of water available for infiltration. Snow surveys conducted during the 2001-2002 and the 1983-84 study period (Gieck, 1986) show an increase in SWE with elevation. Figure 20 shows this trend for the 2001 data. The trend is less pronounced because winter 2001 was a low snow year. The SWE values for the 200-300 m elevation range were slightly higher than expected due to one high value.

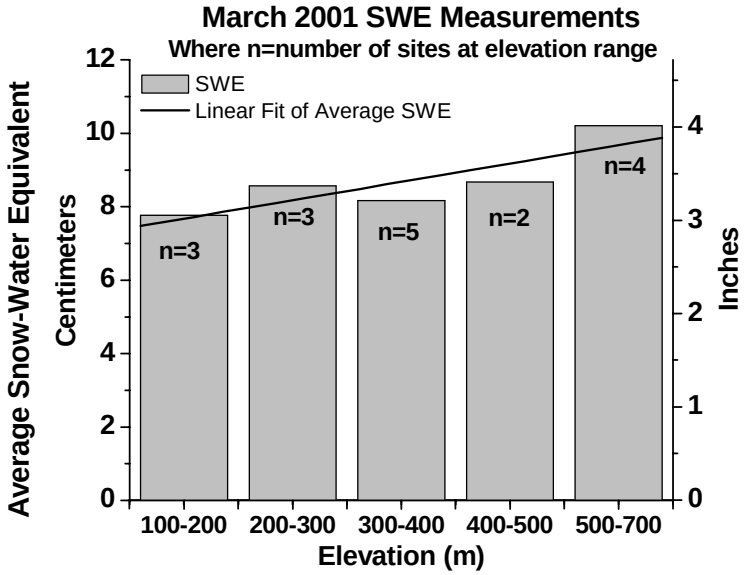

Figure 20. Snow-water equivalent for the Ester Dome area, 2001.

Recharge zones were established for ground-water modeling. Four zones were identified based on the geology, elevation, and SWE. Four zones of recharge were identified (Figure 21). The first zone is located in the valley bottoms where ice-rich permafrost is likely to exist and be more continuous. This zone gets the least amount of recharge due to the high silt thickness and permafrost. The second zone of recharge is located at low to mid elevations where there are permafrost-free silt deposits. The third and fourth zones occur where there is little (less than 5 m) or no silt coverage, and water can easily infiltrate into open fractures in the bedrock. These zones have a higher SWE than the first and second zones. The third zone generally occurs at the mid to higher elevations where bedrock or gravel deposits are exposed at the land surface. The fourth zone is at the highest elevations where the bedrock is very weathered and the SWE is the highest. Table 3 shows the average SWE during the March/April 2001 measurement for each recharge zone. Multipliers are applied to the average SWE for each zone to estimate the amount of recharge into the aquifer. The multipliers were based on work done by Kane et al. (1978), Gieck (1986), and Gieck and Kane (1986) and were further adjusted in the ground-water modeling calibration process. Gieck (1986) shows that 50%

of the snowpack at the Ester Creek watershed became recharge, while less than 22% at Happy Creek became recharge during the study period. The Ester Creek watershed consists of bedrock overlain by silt and gravel deposits. The Happy Creek drainage consists of bedrock overlain by gravel, silt and ice-rich permafrost deposits. Kane et al. (1978) show that approximately 35% of the SWE in a snow pack represents potential ground-water recharge in well-drained soils found on non-permafrost sites. We suspect that an even lower percentage of this water actually reaches the water table.

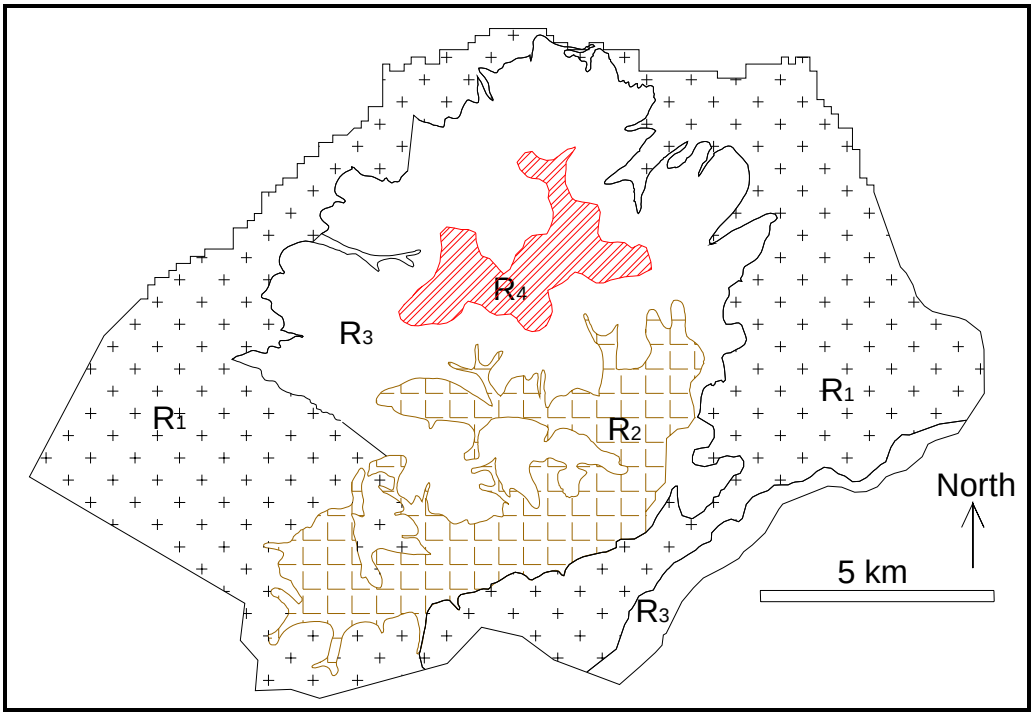

Figure 21. Recharge zones at Ester Dome.

Table 3. Estimated recharge rates in Ester Dome study area.

Recharge Zone	*Average 2001 SWE (cm)*	*Geology*	*Geology Multiplier*	*Estimated Recharge (cm/yr)*	*Estimated Recharge (in/yr)*
R_1	7.35	Permafrost	0.05	0.37	0.14
R_2	8.16	Silt	0.25	1.63	0.64
R_3	7.99	Bedrock	0.50	3.99	1.57
R_4	9.70	Bedrock	0.75	7.27	2.86

Geochemical investigations conducted by the USGS on several Ester Dome wells indicate a relationship between specific conductance and well screen elevation (Verplanck et al., 2003). Ground water was sampled from monitoring and private-water supply wells at various elevations on Ester Dome during the period of 2000-2001. Figure 22 shows the specific conductance increases with decreasing well screen elevation (above mean sea level) for July 2001. Water recharging the aquifer at the higher elevations has a lower specific conductance because it has only been in contact with subsurface for a short time. The wells at Ester Dome summit have a low conductance during July and two additional summit wells sampled during a different time period have very low conductance also. Ground water sampled from the lower elevations at Ester Dome have a higher specific conductance, indicating the water has been in contact with the rocks for a longer period of time. However, since recharge can enter the aquifer at some lower elevations, there may be younger, low conductivity water at some low elevation locations. Surface water that was sampled from Eva Creek and Happy Creek has a low conductance.

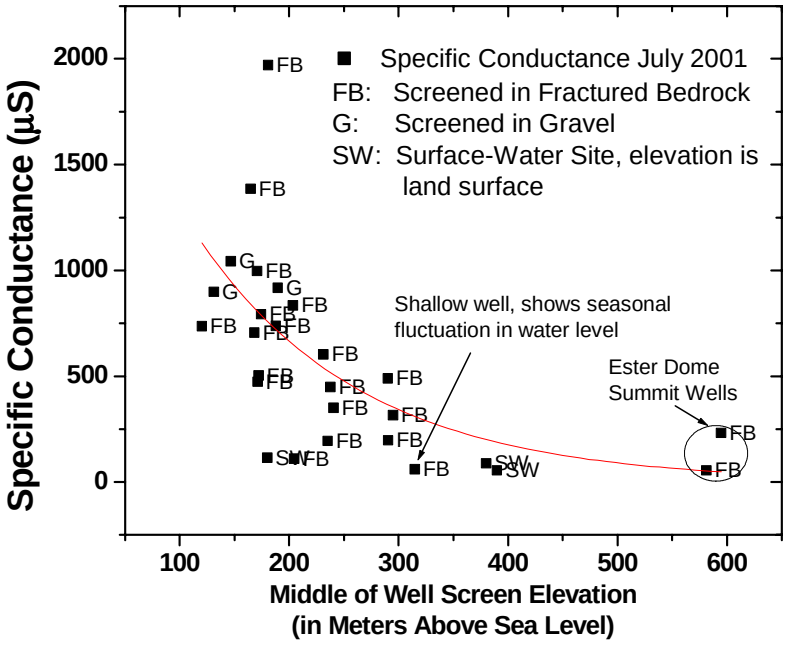

Figure 22. Relationship between specific conductance and elevation at Ester Dome (data from Verplanck et al., 2001).

WATER-LEVEL FLUCTUATIONS

Few studies related to ground-water hydrology in the Fairbanks area have addressed ground-water level variations in the uplands. Different aquifer systems in the Fairbanks area have distinct geohydrologic processes and exhibit different responses to hydrologic stresses. Characterization of aquifer systems around Fairbanks is important for understanding ground-water processes, development impacts, and aquifer responses to climate conditions. Examination of historical trends in ground-water levels is important for many reasons. Industry, land-use planners, and regulators need baseline ground-water data to manage water resources. Unfortunately, little data is available in the upland-aquifer systems. There is no continuous historic record of water levels at Ester Dome. The objectives of this section are to present historic and current ground-water data collected in the Fairbanks and Ester Dome areas, and discuss the variations and trends in the hydrologic conditions. Wells labeled with an "ED" indicate the well is at Ester Dome. If a "P" follows the "ED", the well is a private water-supply well. If an "M" follows the "ED" the well is a monitoring or sampling well. Wells located designated "Ryan Lode" are located in the bedrock aquifer at or near the Ryan Lode Mine. Wells not labeled "Ryan Lode" but labeled MW are private water-supply wells in the Ester area.

Water Table

Figure 23 shows the water-table map for the month of March 2001, based on data collected in the field. Several ridges at Ester Dome had little or no data to map the head contours, particularly on the north and west sides of the dome. In this case, we applied what we learned on ridges where we did have data to these unknown areas. Most of the Ester Dome bedrock aquifer is unconfined, but parts of the valley bottoms are locally confining due to ice-rich permafrost.

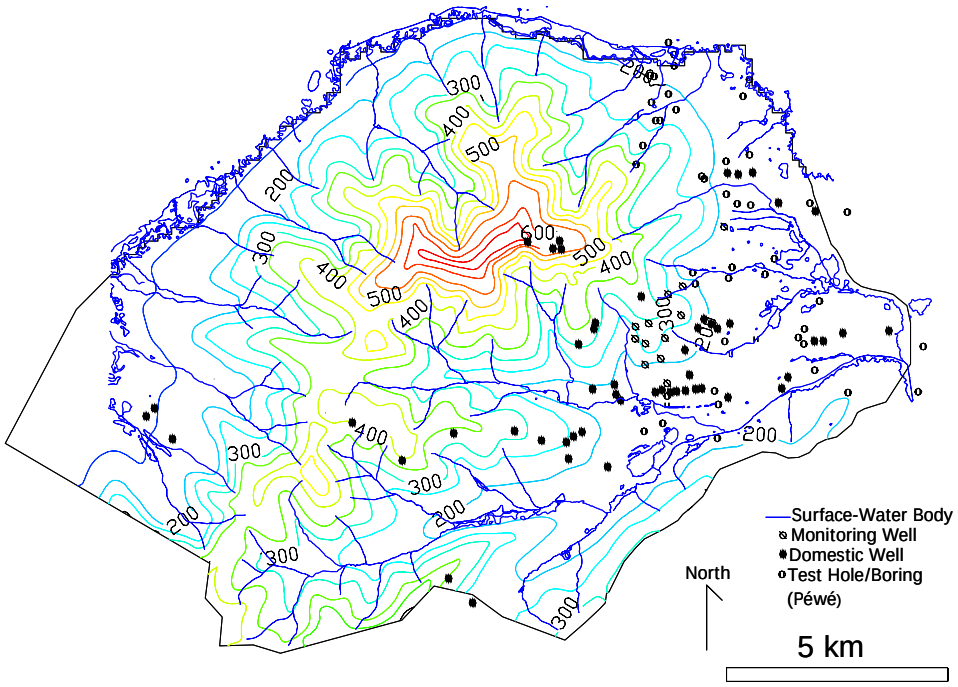

Figure 23. Water-table map at Ester Dome.

Historical Fairbanks Water-Level Fluctuations

Historical water-level records for uplands aquifer systems were examined (Figure 24). There are only seven wells in the uplands with a period of record longer than 5 years (USGS, 2001, Trabant, 2001, Fathauer, 2001). Other water-level data collected in the uplands includes required baseline environmental monitoring by the larger mining companies (Design Science and Engineering, 2000). All wells are located in the bedrock aquifer with the exception of well EDP006, which is screened in a gravel aquifer of the Cripple Creek gravel deposits. Although many of the historical records are incomplete, trends can still be observed. One significant observation is that many of the water levels in upland-bedrock aquifer systems show seasonal fluctuations in water levels in response to changes in annual snowfall.

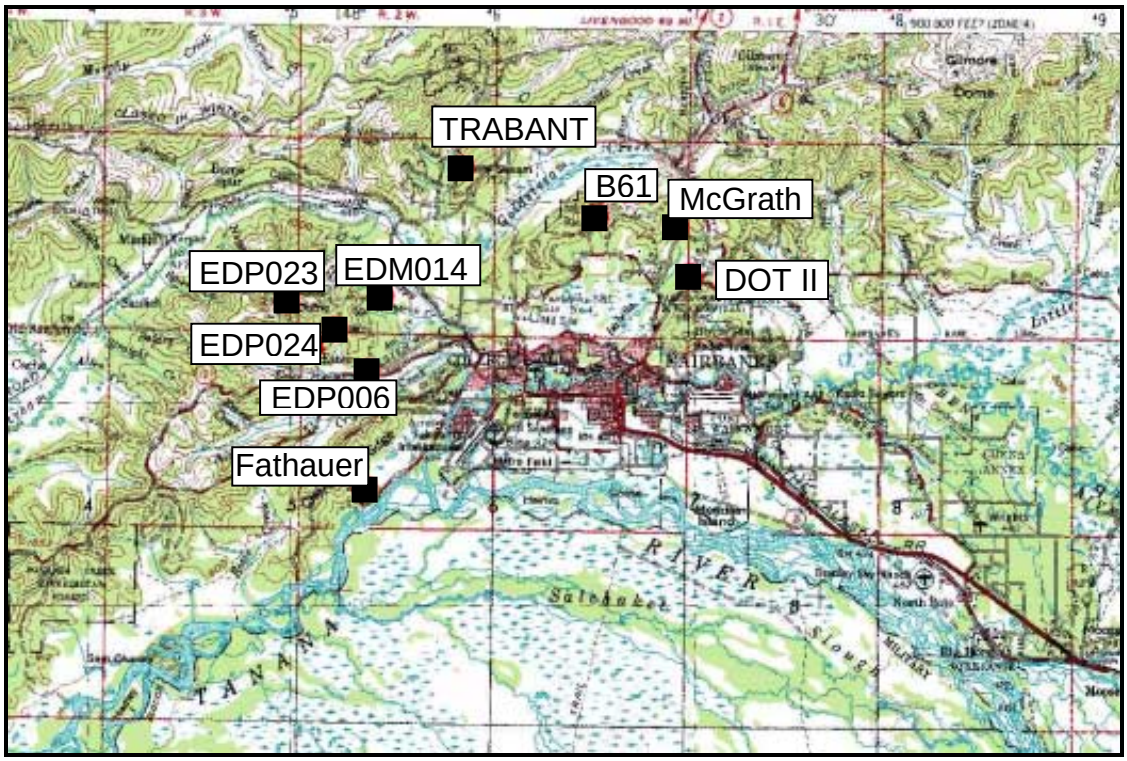

Figure 24. Map showing historical record observation well locations.

Figure 25 shows hydrographs of long-term snowfall and ground-water level data at these upland wells from 1979 to present. Because the only significant recharge to the bedrock aquifer comes from snowmelt infiltration, we also examine ground-water level changes to total annual snowfall. From 1986 to 1991 there was an increasing trend in snowfall. After 1993, the total annual snowfall began to decrease. Several of the wells show water-level responses to changes in the total annual snowfall. Water levels at wells EDM014 and Trabant rise in response to the large total annual snowfall and increased recharge during 1986 to 1993. Well B61 shows a large increase in water level after the 1991 high snowfall year. The water levels in the McGrath Road and DOT II wells also appear to rise to the increased snowfall, but with a delayed response. However, missing data for DOT II and B61 makes it difficult to make more accurate conclusions.

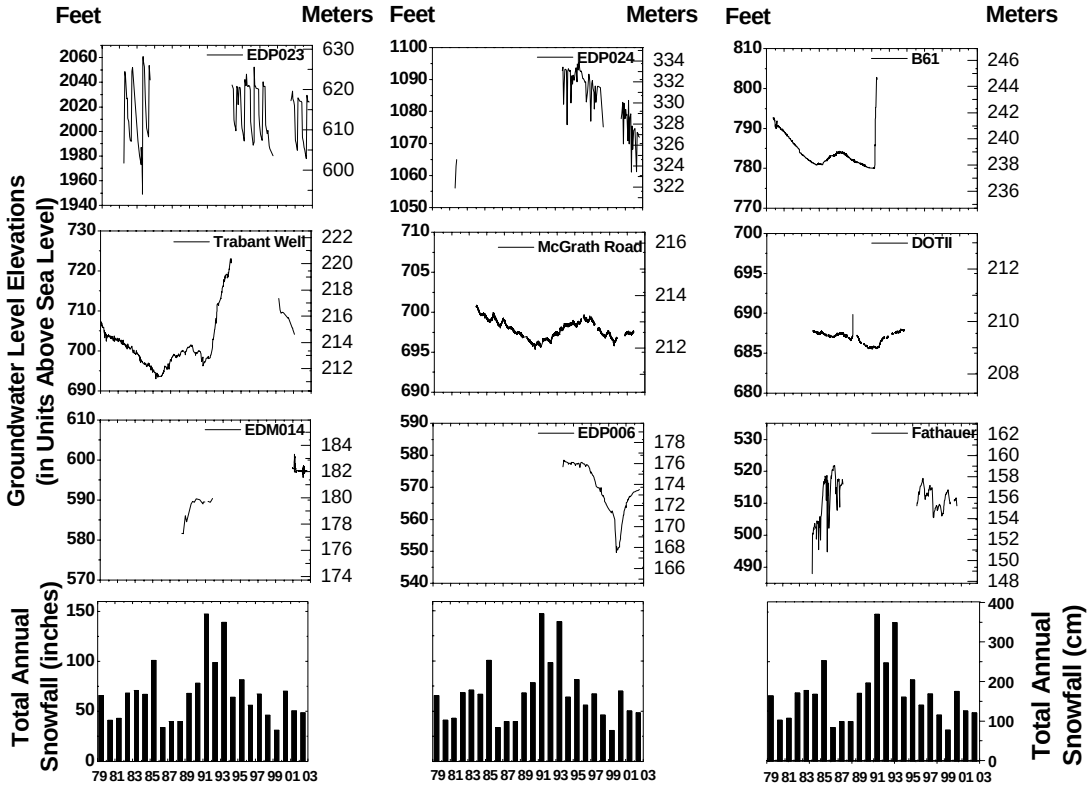

Figure 25. Hydrographs of long-term data from the Fairbanks uplands and winter snowfall at the Fairbanks International Airport. Note change in y-axis scales.

The overall trend from 1993 to present is a decrease in snowfall. Water levels in EDP006, EDP024, and McGrath Road wells show declines with recent low snowfall years. Well EDP023, located at the top of Ester Dome, exhibits extreme seasonal fluctuations in the water level (Figure 25). Levels in this well range from 15-30 m (50-100 ft) of change seasonally. Increased precipitation, increased permeability, and decreased silt thickness at the top of Ester Dome would allow for such responses. Well EDP024 is a domestic water-supply well that shows drawdown from pumping of the well, but also shown is the overall decline in water levels after 1993.

Well EDP006 had been declining since 1997, but in late September 1999, water levels abruptly dropped approximately 3.6 m (12 ft) in response to the aquifer dewatering at Yellow Eagle mine (Vohden, 2000) as shown previously in Figure 17. Recovery of

this rapid drop in water levels began in January 2000 and as of July 2002, the water levels have nearly reached a stable level. The relatively short time between the drop in water levels and the recovery indicates the hydrogeologic unit has a higher permeability and water can flow through the unit quickly.

The long-term water-level fluctuations in the Fathauer well, located on the south side of Chena Ridge, seems to show an increase in water levels after the 1985 snowfall, however, due to incomplete records conclusions are difficult. This well is located in the Chena Ridge bedrock aquifer (Fairbanks Schist). The Fathauer well also shows a different pattern of seasonal fluctuations (Figure 26). The water level begins to rise in mid to late July (after snowmelt) and continues to rise through the summer, fall, and winter. The water level drops quickly in early April. Most ground-water levels in upland wells do not continue to rise through the entire winter. It is possible the hydrogeologic units on Chena Ridge may have a lower permeability, lengthening the time it takes for ground water to reach the well from the up-gradient recharge area.

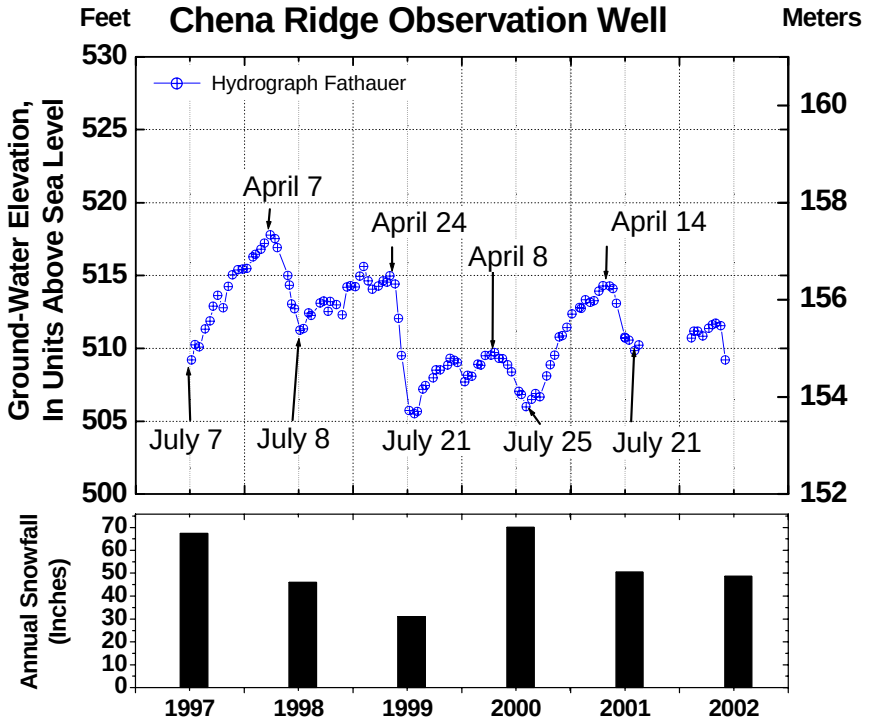

Figure 26. Ground-water level and total annual snowfall at an observation well on Chena Ridge.

During the early to late 1990's water-level data were collected on a monthly basis at Ester Dome monitoring wells in the Ryan Lode area and several private water-supply wells adjacent to Ryan Lode. Personnel from Ryan Lode Mines, Inc. and Design Science and Engineering for Silverado Inc. monitored the wells for the Ryan Lode baseline environmental monitoring requirements (Design Science and Engineering, 2000). The data were analyzed for long-term and seasonal water-level variations during the period of record. Several hydrographs show spikes in the data. Downward spikes (lower water levels) are considered to be either measurement error or drawdown from pumping of the well during the measurement. Upward spikes (higher water levels) are likely to be measurement errors. During a manual measurement with an electric or steel measuring tape, condensation on the sides of the well casing can cause error in the measurement, yielding a water level that is higher than the actual water level.

The bedrock aquifer observation wells MW36_H59_Ryan Lode and MW08_C35_Ryan Lode and the private water-supply well MW27 in the Ester area show seasonal fluctuations in water level (Figure 27 and 28). The Ryan Lode wells are located at a higher elevation on Ester Dome. The bedrock at the higher elevations may be more weathered without the silt coverage, allowing snowmelt infiltration to reach the bedrock aquifer quickly. Well MW27 is located in the town of Ester near the Eva Creek drainage. This well is located in a zone of fractured or broken schist. Additionally, the well is on a south-facing slope, with no ice-rich permafrost, and gravel deposits exposed at the surface, allowing for easy infiltration.

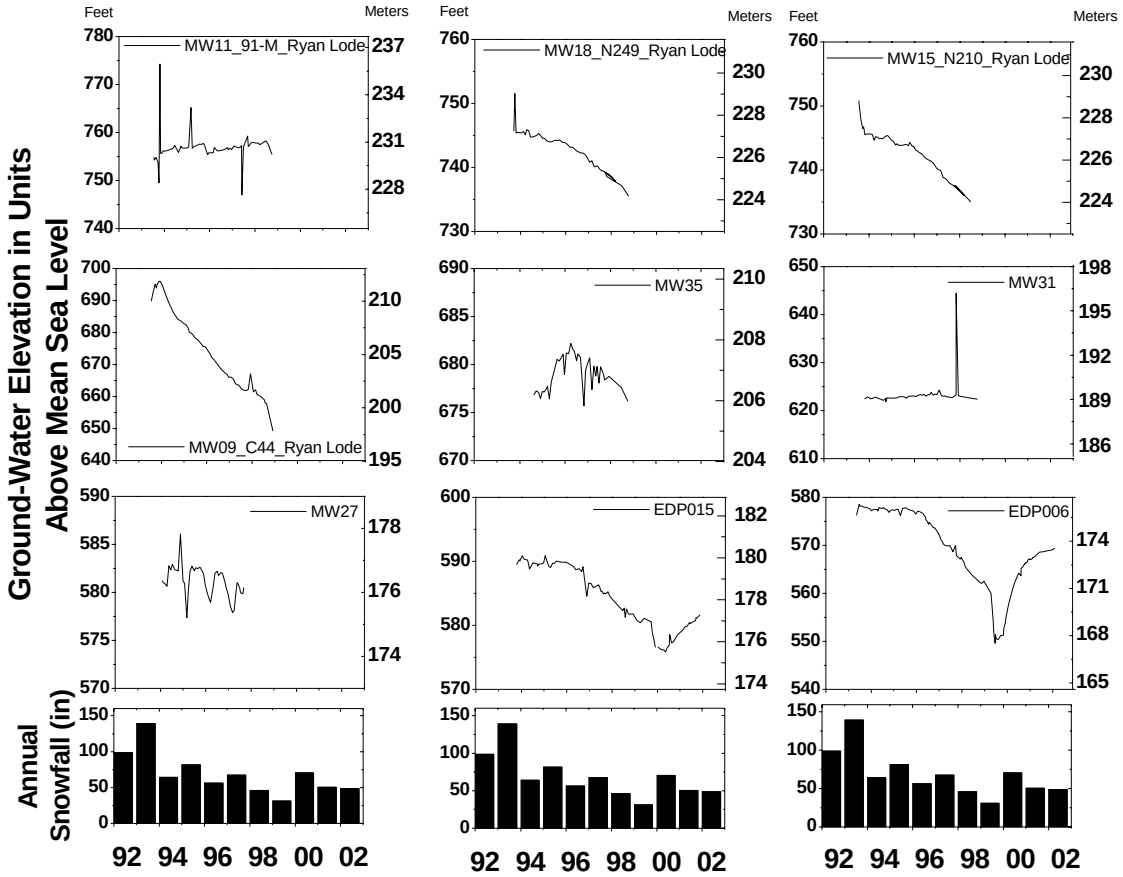

Figure 27. Winter Precipitation and hydrographs of lower elevation Ryan Lode/Ester Dome wells. Note the change in y-axis scales.

In regards to longer-term trends, Ryan Lode bedrock aquifer wells MW36_H59, MW17_N225, MW08-C35, MW16_S60, MW09_C44, MW18_N249, and MW15_N10 responded to the overall declining trend in total annual snowfall during 1993-1999 with a decrease in water level. Yellow Eagle Mine area wells EDP006 and EDP015 also showed a decline in water levels.

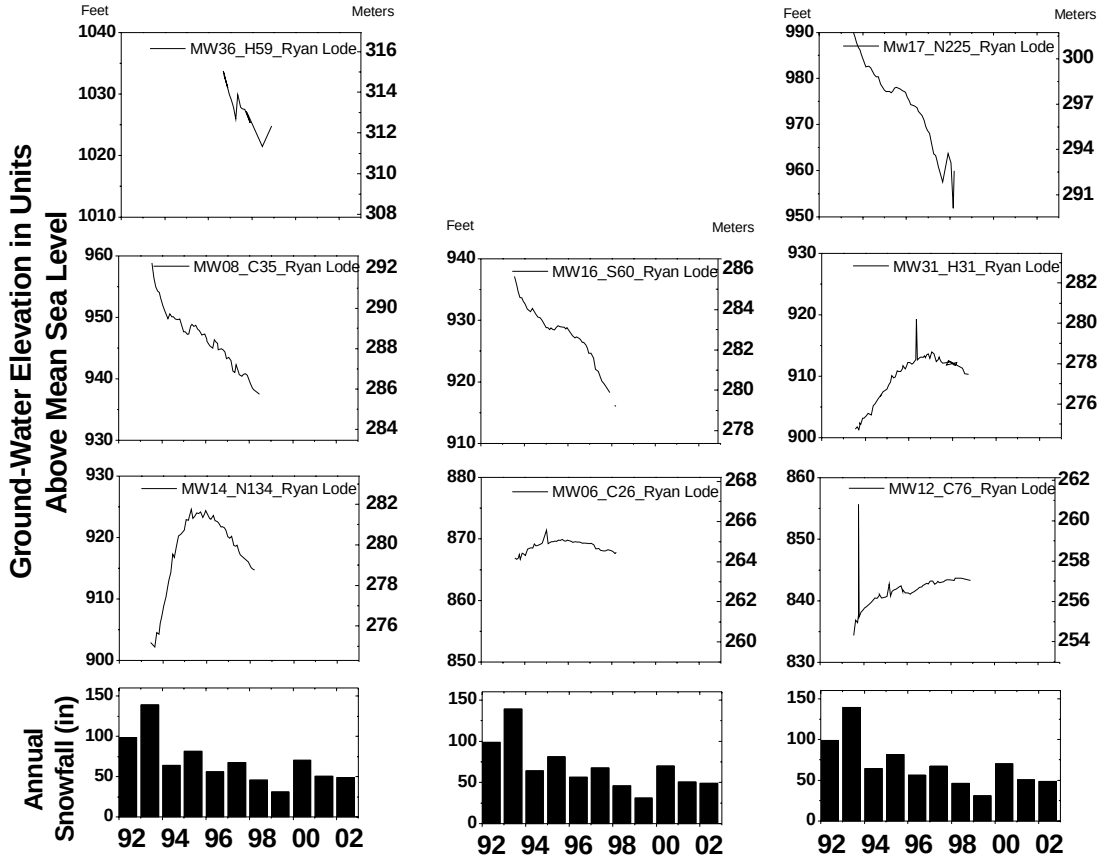

Figure 28. Winter Precipitation and hydrographs of higher elevation Ryan Lode/Ester Dome wells. Note the change in y-axis scales.

Several of the mid-elevation wells show a "delayed response" to the decrease in total annual snowfall. Wells MW31 and MW11_91M showed no change during the period of record. Ryan Lode wells MW31_H31, MW14_N134, and MW06_C26 showed a "delayed response" to the higher snowfall years of 1991 and 1993 and the overall declining trend in snowfall from 1993-1999. Although the water levels rise in response

to the higher snowfall years and decline in response to lower snowfall years, there is a delay in the response time to these events of one or more years. Bedrock aquifer well MW35 in the Henderson Road area may show a "delayed response" but with the drawdown from pumping of the well it is difficult to make an accurate conclusion. This "delayed response" could be due to the lower permeability of the hydrogeologic unit, resulting in slower travel times. Ryan Lode well MW12_C76 actually showed an increase in water levels during the 1991-1999 overall decline in snowfall. It is possible that this is a delayed response to the high snowfall years of 1991 and 1993, but with the incomplete record it is unknown if the water levels will begin to drop, responding to the relatively lower snowfall years.

Current Ester Dome Water-Level Fluctuations

Water levels in Ester Dome wells vary based on precipitation infiltration, aquifer characteristics, and well pumping. Figures 29-31 show the ground-water elevations for the observed wells during the 2000-2002 study period. Seven wells had continuous recording pressure transducers in the well and are designated with a "C" behind the site name. As previously stated, upland-dome ground-water levels are impacted by the amount of winter snowfall. At Ester Dome, ground-water levels are examined in wells located in different geologic conditions and elevations. Most wells in the Ester Dome area penetrate the bedrock aquifer, with a few wells located in the gravel deposits (Cripple and Fox) near the Ester Creek drainage and along eastern portion of the field area.

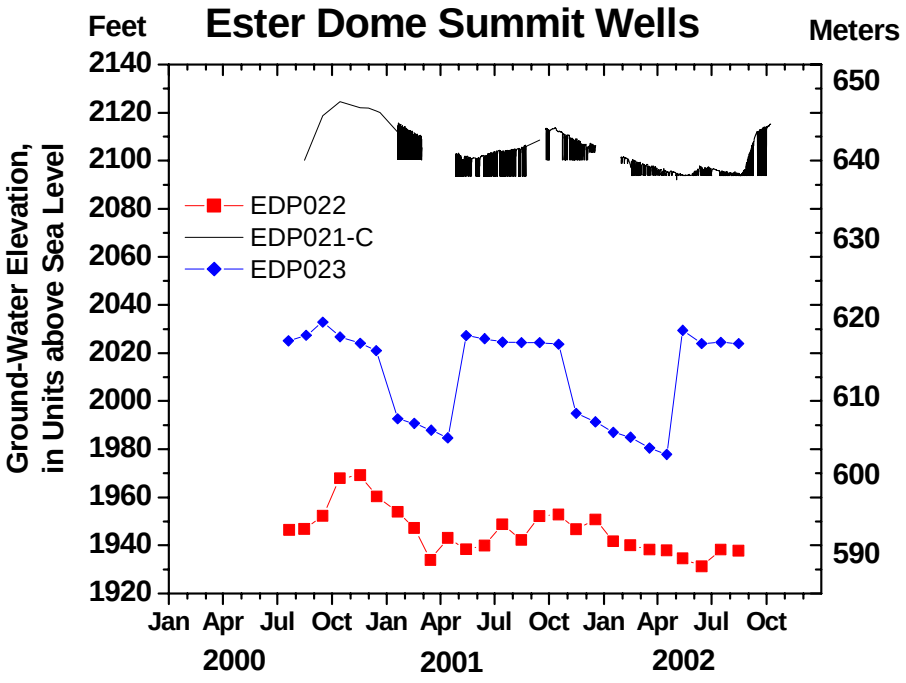

Figure 29. Hydrograph showing water-level fluctuations at high-elevation wells on Ester Dome.

Wells located at the top of the dome have extreme fluctuations in water levels and show dramatic response to each spring snowmelt event. At the top of the dome, no known confining layers of ice-rich permafrost or silt exist to block recharge into the bedrock aquifer. Additionally, increased weathering and fractures in the bedrock allow snowmelt water to more easily infiltrate. Figure 29 shows the water levels at the Ester Dome summit wells. Rising water levels in response to summer or fall precipitation is not evident in the data collected during this study at the upper elevation wells. However, only one out of the three monitored wells on Ester Dome Summit is continuously monitored. When the wells at the top of Ester Dome are pumped, significant drawdown occurs. Well EDP021-C is a private water-supply well, which is continuously monitored. At well EDP021-C, water levels drop at least 10 m from the static water level during pumping. It is not known exactly how far the water level drops because it decreases below the pressure transducer. However, during manual measurements at this site when

the well is being pumped, water levels were at least 20 meters below the static water level. The large drawdown affect is either due to the limited contributing area of recharge to the well or the hydrogeologic properties of the bedrock aquifer.

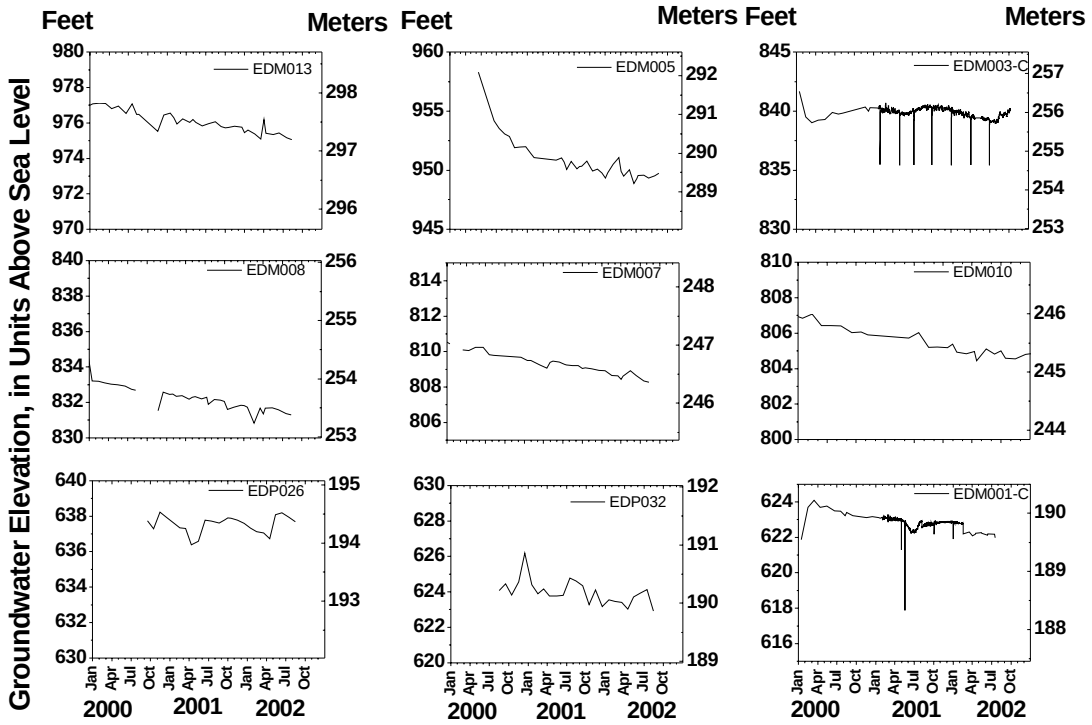

Figure 30. Hydrographs showing water-level fluctuations at mid-elevation wells on Ester Dome. Note the change in y-axis scales.

Figure 30 shows the water levels at several mid-elevation wells. Wells located at mid-elevations on Ester Dome typically penetrate a thin silt layer (5-10 m) and fractured schist, quartzite, or igneous intrusives. One mid-elevation continuously-monitored well, EDM003-C, showed slight seasonal water-level fluctuations in response to spring snowmelt. Well EDM001-C, which was continuously-monitored during February 2001 to March 2002, shows an increase in water levels beginning mid-June 2001 in response to snowmelt infiltration. Both wells EDM001-C and EDM003-C are pumped several times

a year for water chemistry sampling. The drawdown spikes in these two wells are due to these pumping events. Well EDP026, located in the town of Ester, shows seasonal fluctuations. This well is screened in fractured bedrock. Most wells at mid-elevation monitored on a monthly basis did not show any response to snowmelt. Wells EDM013, EDM005, EDM008, EDM007, EDP032, and EDM001-C all show a declining trend during the period of record. During the winters of 2001 and 2002, snowfall was below average, which could result in the decreased water levels.

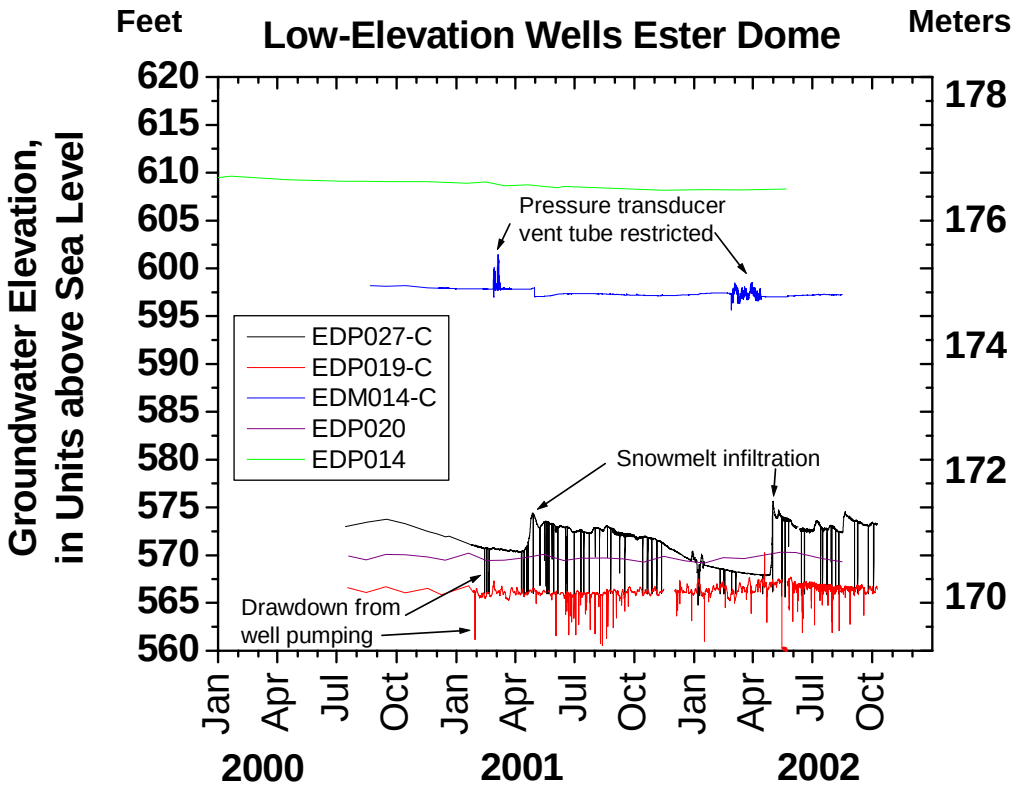

Figure 31. Hydrographs showing water-level fluctuations at low-elevation wells on Ester Dome.

Water levels in most wells at the base of Ester Dome are very steady with little seasonal, pumping, or long-term fluctuation (Figure 31). Geologic logs indicate the wells located at the base of Ester Dome penetrate though thick layers of silt with the exception of wells in parts of the Ester Creek/Cripple Creek area, where higher permeability sandy-gravel

deposits exist at the land surface. Ice-rich permafrost in the silt deposits at the base of the dome may act as a confining unit, resulting in little infiltration into the aquifer and high quantities of water for domestic water use. Geologic logs show confining conditions due to ice-rich permafrost occurring along the valley bottoms in the Sheep Creek Road/Ester Dome Road area, Goldstream Valley area, Cripple Creek and Alder Creek areas. These regions have deposits of permafrost ranging from 10-70 m. Well EDP019-C, located on Ester Dome Road near the base of Ester Dome penetrates the gravel aquifer system that is overlain by a thick deposit of ice-rich frozen silt. Water levels in this well are fairly constant for the entire year; drawdown of water levels occurs because the well is pumped frequently during the summer months to water produce in greenhouses. EDM014-C, EDP014, and EDP020 do not show any seasonal variations. None of these wells show any significant long-term declines (with the available period of record). As previously discussed, well EDP027-C, located at Ester Fire Department, shows seasonal fluctuations in water levels. The high permeability deposits allow water to infiltrate and recharge this well during spring snowmelt and possibly during extreme summer precipitation events. It is important to recognize measurements made on a monthly basis may not be sufficient to see most minor fluctuations in water levels in unconfined aquifers.

CONCLUSIONS

The Ester Dome upland-bedrock aquifer system is very complex due to the nature of fractured media, complicated geology and geohydrologic processes. However, from this investigation we have made several observations of the aquifer processes that were previously poorly understood. The four main hydrogeologic units at Ester Dome are the fractured bedrock, gravel (or broken rock), silt, and frozen silt (permafrost). However, only the fractured bedrock and the gravel unit have developable aquifer systems. The primary form of aquifer recharge is from spring snowmelt. Recharge varies spatially based on SWE, geology and permafrost, and evapotranspiration variations. Wells that are located in highly fractured bedrock or gravel deposits show seasonal water-level fluctuation responding to snowmelt if there is no permafrost or thick silt layer to retard or block recharge.

Several valley bottom wells show no changes in water levels. A decline in ground-water levels occurs for many wells in the historical records during the period of 1993 to 1999 during the overall declining trend in total annual snowfall. Many records also show increases to an increasing trend in total annual snowfall during 1986 to 1991. The data collection effort at Ester Dome provides useful information for environmental and mining regulators, land-use planners, developers, homeowners, and the scientific community. The collection of ground-water levels on a continuous basis indicates fluctuations that occur seasonally, depending on the available recharge and hydrogeologic conditions of the aquifer.

ACKNOWLEDGEMENTS

This project was supported by Alaska Science and Technology Foundation Grant #00-1-049. The project was co-funded by University of Alaska Fairbanks, GW Scientific, Alaska Department of Natural Resources, Fairbanks Gold Mining, Inc., Alaska Department of Fish and Game, Alaska Department of Environmental Resources, Alaska Department of Transportation and Public Facilities, Fairbanks North Star Borough, and Arctic Region Supercomputing Center. The residents and mining companies of Ester Dome who participated in this study were critically important to the success of this project. Through their cooperation we were able to extend the number and geographic distribution of our measurements far beyond what would have been possible without their support.

A NUMERICAL ANALYSIS OF AN INTERIOR ALASKA UPLAND-DOME BEDROCK AQUIFER SYSTEM

ABSTRACT

A three-dimensional finite-difference ground-water flow model is used to aid in the characterization of the geohydrology at Ester Dome. The ground-water flow model helps to identify critical parameters that influence the geohydrologic processes of upland-bedrock aquifer systems. The geohydrology of an upland dome is characterized by open boundaries. A typical watershed approach is to define a drainage system and define no-flow boundaries. Characterizing Alaska Interior dome aquifer systems require the inverse to this approach. MODFLOW-2000 is the numerical ground-water flow model used to simulate the Ester Dome aquifer systems. Types of boundary conditions for the model include specified heads along the discharge areas (streams, lakes, wetlands) bounding the north, east and west sides of the modeled area. The southern boundary of the modeled area extends to an adjacent ground-water divide (Chena Ridge). Initial aquifer parameters for bedrock and surficial deposits are obtained from the reported values in the literature. Initial recharge values are estimated from snow survey field data from Ester Dome and our current understanding of the recharge processes. The Observation and Sensitivity packages in MODFLOW-2000 indicate the most sensitive parameters are the bedrock hydraulic conductivity and certain recharge zones. MODPATH results show particles flowing from high elevation recharge areas to low-elevation constant head boundaries.

INTRODUCTION

Ester Dome, an upland-dome aquifer system, is located 11.3 km (7 miles) west of Fairbanks, Alaska. In Interior Alaska, the mining industry plays an important role in Alaska's economy. Ester Dome has been mined for gold intermittently for the past 100 years. Due to the lack of information about upland geohydrologic processes, water-resources management decisions are difficult. One of the initial goals of the overall study

is to develop guidelines and methods for evaluating hydrologic resources in Interior mining locations. We will apply our conceptual model to a numerical ground-water flow model. The purposes of a ground-water flow model are 1) interpret aquifer systems, 2) make predictions, or 3) create a generic modeling exercise (Anderson and Woessner, 1992). We developed a ground-water flow model for Ester Dome to aid in the interpretation of the geohydrology of the system. Some of the main goals of the Ester Dome ground-water flow model are to quantify the hydrogeologic properties, improve the understanding of dominant hydrologic processes, and simulate the ground-water flow system. We chose to develop a ground-water flow model because it requires one to study the hydrologic system thoroughly, identify aquifer parameters, locate recharge and discharge areas, and examine boundary conditions and important ground-water flow processes. It allows one to further investigate processes such as ground water and surface-water interactions, ground-water flow around permafrost regions and the simulation of stresses (such as pumping or recharge) to predict potential changes in ground-water flow patterns. A ground-water flow model additionally helps to identify what types of data are needed when examining an aquifer system. It can be useful for many applications common in Interior Alaska such as environmental assessments, land-use planning, and designing mine dewatering programs.

Simulating ground-water flow is very involved and initial steps entail developing a conceptual model, and turning it into a numerical representation of the hydrogeology. The main constraint in developing this ground-water model lies in the lack of information about the subsurface geohydrologic features. A sensitivity analysis was conducted to better understand the potential range of aquifer properties. This report documents the development and results of the ground-water flow model for Ester Dome.

BACKGROUND

Ester Dome is part of the Tanana Basin and Goldstream Creek Sub-basin. Water in the Goldstream Creek sub-basin is flowing toward the Tanana River to the southwest of the Ester Dome area, and is separated by a series of connected domes and ridges

extending to Nenana. Domes are a topographic feature common to Interior uplands where multiple watersheds exist within a single dome system. Tectonic forces or large igneous intrusions form the domes and ridges in the Fairbanks area (Forbes, 1982). The general drainage and flow pattern at Ester Dome is radial, where significant recharge originates from a central area and water discharges from the boundaries into valley bottom lakes, streams, and wetlands. A ground-water monitoring network of approximately 50 observation wells on Ester Dome (Figure 3) allows us to obtain field data to help interpret upland-dome geohydrologic processes. Seasonal and pumping water-level fluctuations occur in several wells, but many wells show no seasonal or short-term variation in water levels. Geologic variation on Ester Dome helps explain these differences. Ester Dome consists of five major geologic units: quaternary alluvial and eolian deposits, Fairbanks Schist, Birch Hill Sequence, Muskox Sequence, and cretaceous plutonic rocks. Additionally, permafrost is present in much of the low-lying valleys and some parts of the north-facing slopes of the dome. In general the aquifer is unconfined, except in valley bottoms where ice-rich permafrost may be locally confining. Snow surveys and precipitation recorders were established at varying elevations on Ester Dome to examine the changes in precipitation spatially and to evaluate recharge processes. The only significant form of recharge to the bedrock aquifer is spring snowmelt. Winter precipitation on the dome increases with elevation. Figure 11 shows a general conceptual model for Ester Dome.

APPROACH

The first step is to create a conceptual hydrogeologic model of the area to be simulated. This step is critical in constructing an accurate ground-water model. The conceptual model is a representation of the aquifer systems, boundary conditions, and hydrologic inputs, and any hydrologic stresses. Multiple conceptual models are made to test different configurations of the hydrogeology, aquifer properties, boundary conditions, and model discretization.

The USGS modular three-dimensional finite-difference ground-water flow model, MODFLOW-2000 (Harbaugh et al., 2000), is the numerical code selected to simulate flow in the Ester Dome aquifer system. MODFLOW-2000 contains several new modules, the Observation, Sensitivity, and Parameter Estimation packages (Hill et al., 2000), which are used for automated calibration. First we begin with a running forward model using estimated parameters from related literature. A forward simulation solves the ground-water flow equation for hydraulic head using certain input parameters and boundary conditions. Next, we use the automated calibration packages in MODFLOW-2000 to quantify the calibration process and examine model validity. Hill's (1998) effective-calibration guidelines are followed to ensure model convergence and better accuracy. MODPATH is used to examine ground-water flow paths and travel times through the aquifer.

ASSUMPTIONS

The assumptions used in developing the numerical model are listed below.

1. A continuum approach is used.
2. Steady-state hydrologic conditions.
3. Water-level conditions from data collected during March 2001 and geologic well log records are used for model calibration.
4. Zones of bulk or average uniform values represent hydraulic conductivity and recharge.
5. Ground water leaves the system through the constant head cells and spring-fed streams (drains).
6. A no flow boundary occurs along the top three layers of the southern vertical boundary.
7. Evapotranspiration is included in the net recharge value.
8. The withdrawal of water from the aquifer system by private water-supply wells is insignificant since it is offset by recharge through septic systems in the area.

9. No vertical flow can occur across the base of the model (except in constant head cells along boundaries).

It is not possible to accurately describe small-scale features such as individual fracture sets, or recharge into the subpermafrost aquifer from small ponds. We assume bedrock fractures are numerous and the distance between fractures is small compared to the size of the modeled area. Additionally, the model is a relatively large-scale system, where we use bulk properties to characterize the overall geohydrologic processes. Therefore we assume the continuum approach is valid and Darcy's Law applies.

The Ester Dome ground-water flow model is used in steady-state simulations even though seasonal processes are very important in upland bedrock aquifer systems. Significant changes in hydraulic heads and surface-water flow occur in some areas due to snowmelt. Seasonal changes in water levels in wells near the top of Ester Dome vary up to 20 m. It is a common approach to first develop a ground-water flow model using steady-state simulations, and later develop transient simulations given model-simulation objectives. Project objectives included improving the basic understanding of ground-water processes and providing improved understanding of upland-aquifer systems in the regional area. These goals were achievable with a steady-state version of the ground-water flow model. Further benefits will be gained in future projects, which develop and refine transient ground-water flow models. Data sets used to verify and calibrate the model were taken from late-winter conditions (March 2001). Additionally, water levels from geologic well log records were used. Appropriate weights to the calibration data were applied based on uncertainty in the measurement and quality of measurements.

Zones of hydraulic conductivity were defined based on the hydrogeologic units at Ester Dome. The zone boundaries were based on previous geologic maps by Pewé (1958) and Newberry et al. (1996). Each zone is given a bulk hydraulic conductivity value. Zones of recharge were also established based on the geology, permafrost distribution, snow water equivalent (SWE), and elevation because the recharge is not areally uniform.

The lower extent of the Ester Dome flow system is unknown, so we constructed the base of the model with a flat horizontal plane in which it is assumed no flow can occur across this boundary. However, some water is leaving the modeled area at many of the boundaries due to the inverse nature of the dome system and also because Ester Dome is part of a larger-scale ground-water flow process, where ground water is flowing toward the Tanana River. Ground water also leaves the system by discharging into many of the creeks and springs. Ground water is leaving the dome system along the western boundary, heading to the southwest toward the Tanana River. Ground water also leaves along the eastern boundary and either flows north into Goldstream Creek or south toward the Chena and Tanana Rivers. Additionally, it is possible that water is leaving the dome system at very deep locations along the southern topographic boundaries and flowing with the regional ground-water flow system toward the Tanana River. Constant-head cells and drains are designed to allow ground water to leave the dome system and simulate the above boundary conditions.

Evapotranspiration is an important process at Ester Dome. Evapotranspiration increases with decreasing elevation at Ester Dome (Gieck, 1986) and is the highest during the months of June and July. During these months evapotranspiration usually meets or exceeds precipitation at all elevations of Ester Dome (Gieck, 1986). Snowmelt is the only significant form of recharge to the bedrock aquifer in areas above lower drainage bottoms. This recharge event occurs during mid-May to early June when transpiration is still low. Recharge is spatially variable, depending on the geology and permafrost, transpiration, ground-surface slope, and SWE. For modeling simplification, we have included any evaporation of the snowpack and evapotranspiration terms into the recharge value of each zone. Figure 18 shows these hydrologic processes.

There are an estimated 200 private water-supply wells on Ester Dome based on well log records and surveying local residents. However, these small-scale withdrawals are not included in the model because they are not known to significantly influence the ground-water flow system.

GENERAL FEATURES

The Ester Dome model was constructed with the pre- and post-processor Argus-One MODFLOW GUI (Winston, 2000). The Ester Dome ground-water flow model input includes:

- Horizontal grid spacing
- Top and bottom elevation of each layer
- Hydrologic boundary conditions
- Initial hydraulic head conditions
- Vertical and horizontal hydraulic conductivity
- Recharge rates
- Solver information and convergence criteria
- Drain conductance and elevation
- Output options

The Observation and Sensitivity package in MODFLOW-2000 allows us to statistically compare observed versus simulated water levels and examine the sensitivity of the observed water levels to input parameters. Input for this package includes:

- Weighted observations of water levels in wells, water-level observations in surface-water features
- Starting value and upper and lower "reasonable" values for the aquifer parameters hydraulic conductivity and recharge for sensitivity analysis
- Convergence criteria

Weighting factors are based on the accuracy of the actual measurement and the accuracy of the well survey technique. Additional data required for MODPATH simulations include 1) effective porosity and 2) the location and number of the particles released.

Model Discretization

The Ester Dome model is a three dimensional finite-difference model that has four layers, 139 columns, and 117 rows. Each layer has a variable thickness (Figure 32a) ranging from 5 m to 200 m. Layer 1 is the uppermost layer and layer 4 is the lowest

layer. The horizontal grid contains cells 152.4 m by 152.4 m (500 ft by 500 ft) (Figure 32b). The top of layer one was constructed with a 5 m resolution digital elevation model (DEM) by Intermap Technologies (2000). The original DEM was resampled from 5 m resolution to 25 m resolution. Model layers were constructed based on the hydrogeologic units (Figure 32a). Layer one is constructed to contain bedrock, gravel, and frozen silt. Layer two consists of gravel and bedrock. Layers three and four consist only of bedrock. The base of the model is at constant 182 meters below sea level.

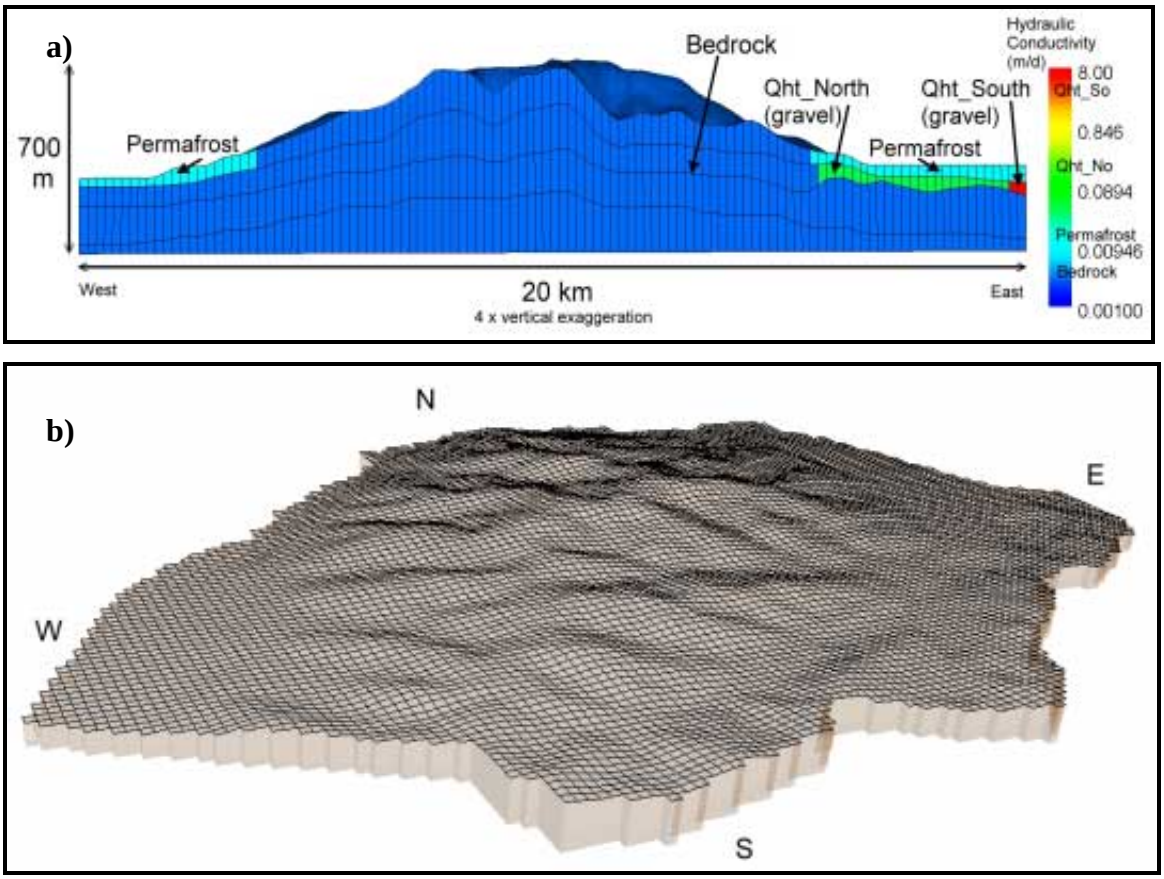

Figure 32. a) Cross section through row 64 and b) map view of the 3-D finite difference model grid.

Boundary Conditions

Ground-water flow model input includes hydrologic boundary conditions necessary to numerically solve the governing ground-water flow equation. The boundary

conditions in this model are made to represent the conceptual hydrologic system at Ester Dome as much as possible. Figure 33 shows the four boundary regions: Goldstream Creek, East Boundary, Chena Ridge Divide, and Southwest Topographic Divide. Three types of conditions are used in the Ester Dome model; specified head, specified flux, and head dependent flux.

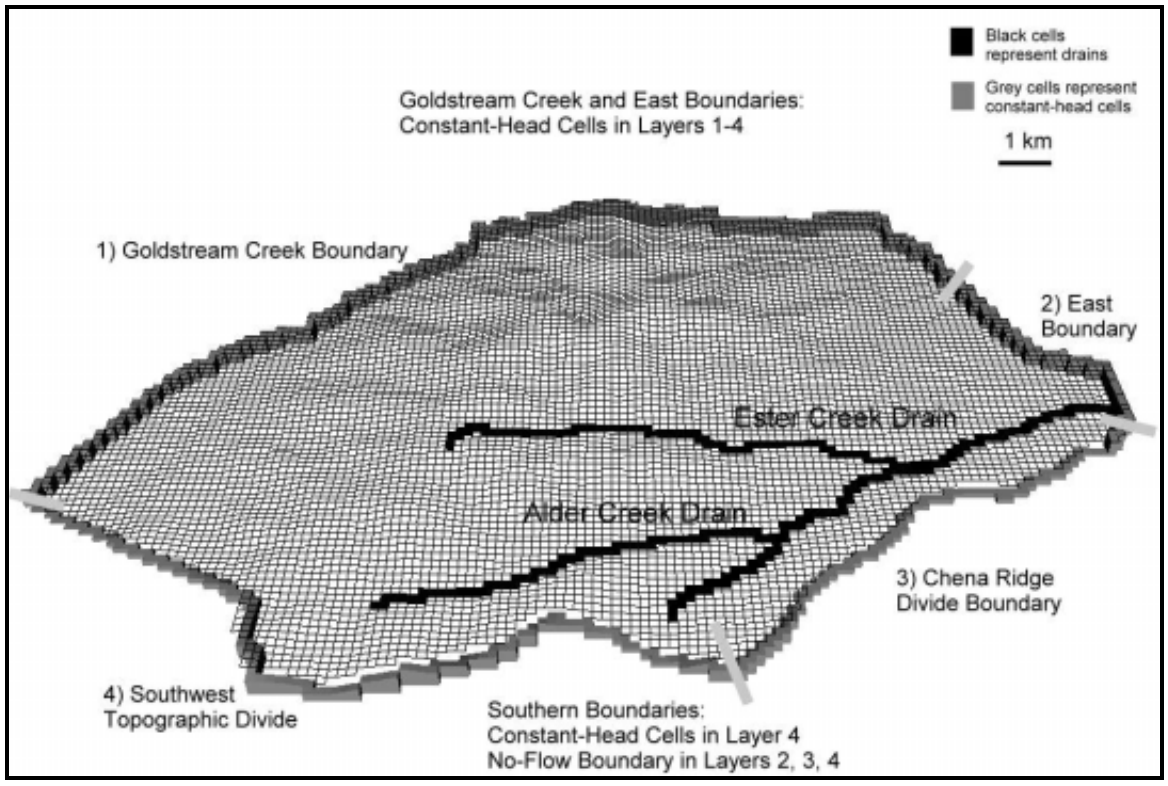

Figure 33. Ground-water flow model area showing boundary conditions, internal boundaries, and finite difference grid.

The Goldstream Creek boundary that occurs along Goldstream Creek in the north and west edges of the study area is a specified-head (water level) boundary in all four layers along the vertical boundary of the model area. The specified head in Goldstream Creek was calculated with a known river stage value obtained at surface-water observation site EDS001 and then a slope of 9.09×10^{-4} (m/m) was applied to the river to show the gradient toward the west. The cells in layers two, three, and four below

Goldstream Creek have a specified head which allows upward vertical flow by assigning an upward gradient of 0.001.

A similar specified head boundary occurs along the East Boundary, near the Sheep Creek area. The specified heads on this boundary occur in all four layers along the vertical boundary of the modeled area. A gradient of .001 was imposed to allow water to flow upward toward layer one.

A third specified head boundary occurs on layer four of the two southern boundaries, Chena Ridge Divide and Southwest Topographic Divide. Little is known about the deep Tanana Basin regional flow system and nothing is known about what depths below Ester Dome this regional flow occurs. The layer four cells along the two southern boundaries have a specified head of the topographic surface minus 50 meters because nothing is known about the head at that depth. This specified head boundary allows the deeper ground water to leave the ground-water model domain, simulating flow out with the regional flow system.

A specified flux of no-flow boundary condition occurs at the along the vertical surface in the top three layers of both southern boundaries (Southwest Topographic and Chena Ridge Divides) along the vertical surface in the top three layers. For initial ground-water model simulations, cells in all four layers along the entire southern boundary were no-flow cells. In this initial simulation, ground water tended to mound up along Chena Ridge and the Parks Highway ridge, probably because water could not leave the Ester Dome system in this area due to the ground-water model configuration. To fix this problem, we established constant head cells in layer four, and drains in nearby Ester and Alder Creek.

A specified flux of no-flow boundary condition also occurs along the horizontal bottom surface of the model at 182 m below sea level. We chose this depth because we did not know the lower extent of the Ester Dome system, but at such great depths it is likely that the flow is parallel with the regional system.

Sources and sinks include internal drains and recharge. Drains are a head dependent condition. When the aquifer head is above the drain elevation, ground water

discharges through the drain. When the aquifer head becomes lower than the drain elevation, the drain stops flowing. The discharging flow is calculated from the conductance of the drain and the head difference between the drain elevation and aquifer head (McDonald and Harbaugh, 1988). The purpose of the drain is to simulate spring-fed streams and allow water to leave the system and not re-enter. A specified flux occurs on the uppermost active cells, specified by areal recharge rates, and is further discussed later.

Initial Conditions

The model is a steady-state model, however, initial hydraulic heads are required for the simulation. Initial heads in all simulated cells are set to the land surface elevation. At specified head cells, the initial head is set to the specified heads because water levels are not calculated in these cells.

SYSTEM PARAMETERS

The required input parameters for the steady state ground-water model include horizontal hydraulic conductivity and vertical anisotropy of each geologic unit, recharge to multiple zones in the uppermost active cell, and drain conductance. Table 4 shows the 13 parameters that were specified in the Layer Property Flow (LPF) package of MODFLOW-2000.

Hydraulic Conductivity and Recharge

Hydrogeologic zones, or zones of bulk hydraulic conductivity, are established based on the geology described by Newberry et al. (1996) in Figure 1. The hydrogeologic units include:

- *bedrock*, which includes the Fairbanks Schist (Zf and Zfw), Muskox Sequence (Dma, Dms), igneous intrusives (Ki), and Birch Hill Sequence (Dbs)
- quaternary *gravels* (Qht)
- *frozen silt* (Qer, Qef)

Since flow in the unsaturated zone is not modeled, hydrogeologic units above the permafrost were not included. In the uplands, ground water above the permafrost layer typically does not produce enough water to be considered an aquifer. In forward simulations, the horizontal conductivity is set equal to the vertical conductivity because there is no available information about isotropy. Five bedrock zones are defined, however for simplification, all bedrock units are given the same starting hydraulic conductivity values, designated 'bedrock'. Ranges of starting values of the bedrock hydraulic conductivity are obtained from the literature because little is known about the hydraulic properties of the bedrock aquifer.

The gravel units are divided into two zones after initial simulations indicated there should be a division due to the discrepancy in simulated heads between the two regions. The unit is divided into two subunits partly based on the location of Pewé's (1958) Cripple and Fox gravels. Hydraulic conductivity ranges are taken from published literature and 'Qht_north' or 'Qht_south' designates the hydraulic conductivity of the gravels.

Kane (1980, 1981b), Kane et al. (1978), and Kane and Stein, (1983a, 1983b) examined hydraulic conductivity of the seasonally frozen Fairbanks Silt and ranges of hydraulic conductivity (designated 'Permafrost') are used from their work. The hydraulic conductivity of each zone is assumed to be isotropic. Figure 34 show the distribution of these zones of hydraulic conductivity in each layer and figure 32a shows the zones in cross section. Table 4 shows the starting values and ranges of hydraulic conductivity used for the calibration and sensitivity analysis.

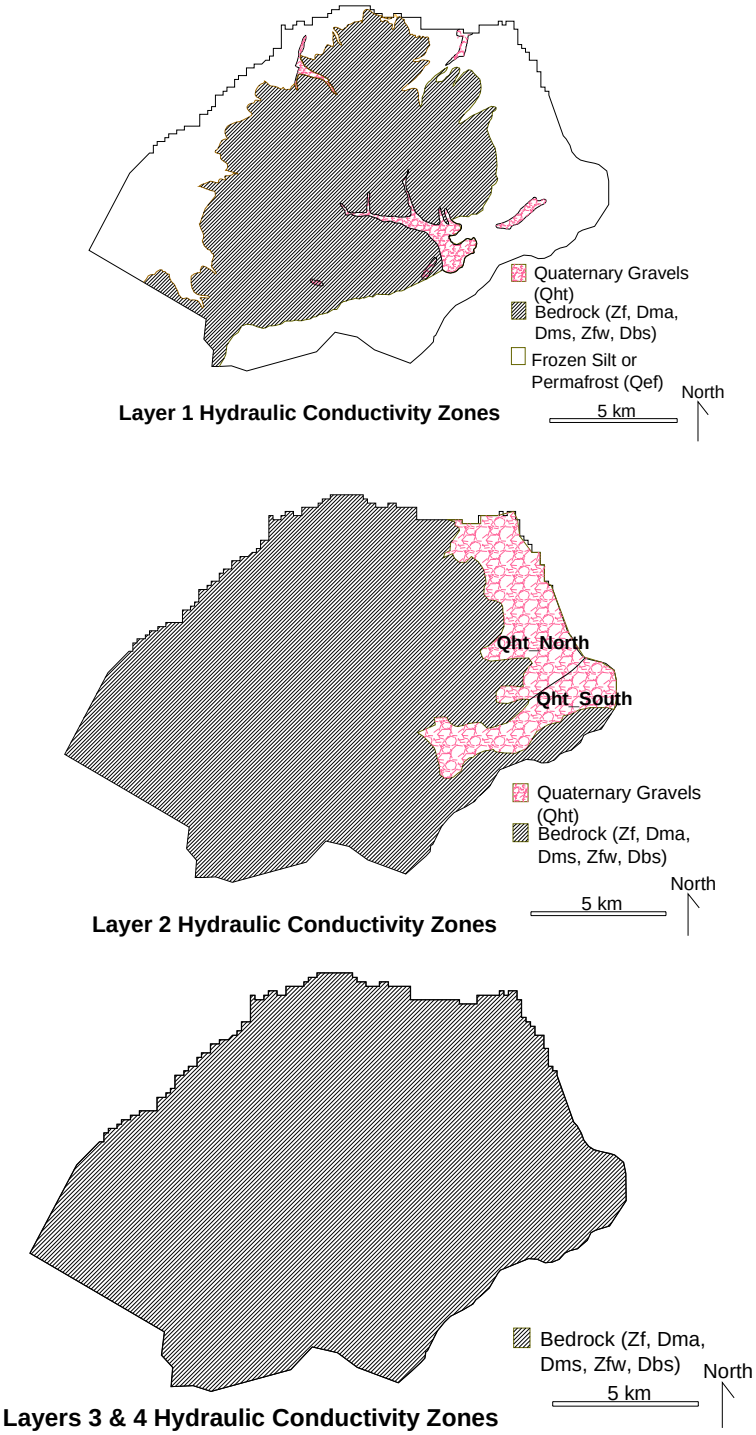

Figure 34. Hydraulic conductivity zones in Ester Dome ground-water flow model for layers 1 through 4, with layer 4 being the deepest.

Table 4. Parameters and values used for sensitivity analysis.

Features	*Description*	*Initial Value (Forward Run Value)*	*Low*	*High*
$K_{Permafrost\ or\ Frozen\ Silt}$ (m/d)	Low hydraulic conductivity	0.009	8.64E-5	.0864
$K_{Qht\_North\ –\ Gravel}$ (m/d)	Moderate hydraulic conductivity	0.0411	0.01	100
$K_{Qht\_South\ –\ Gravel}$ (m/d)	High hydraulic conductivity	8.0	0.01	864
$K_{Bedrock}$ (m/d)	Low hydraulic conductivity	0.0035	3.0E-5	0.3
VANI	Vertical anisotropy	1.0	0.8	1.2
R_1 (m/d)	Area of very low recharge	0	0	1E-8
R_2 (m/d)	Area of very low recharge	4.0E-6	1.0E-10	0.00006
R_3 (m/d)	Area of low recharge	4.45E-5	1.0E-10	0.00006
R_4 (m/d)	Area of high recharge	0.0001	0.00005	0.00015
R_5 (m/d)	Area of very high recharge	0.00019	0.0001	0.00022
DRN_Ald (m^2/d)	Drain- Low Conductance	0.00432*L	4.32E-5	4.32
DRN_Est (m^2/d)	Drain- Moderate Conductance	0.00864*L	4.32E-5	4.32

Recharge zones were defined based on geology and permafrost, SWE, and elevation. SWE data collected during March 2001 was used to quantify the amount of potential recharge. The amount of snow during 2001 was comparable to 2000 and 2002. In the Ester Dome ground-water model, five zones of recharge were established (Figure 35). SWE information was collected before snowmelt and averages were calculated for each zone. The first zone, R_1, was located in the valley bottoms, where thick deposits of silt and areas of ice-rich permafrost exist. This zone was given little recharge because we are assuming low permeability silt or ice-rich permafrost acts as a confining layer and blocks significant recharge from entering the confined aquifer.

The second zone of recharge, R_2, is located on the southernmost edge of the modeled area next to the no-flow boundary. This zone generally has low silt thickness, but since it is a north-facing slope it is likely that permafrost exists. In initial model simulations, this area was given higher recharge values and the result was unrealistically high heads along the no-flow boundary. This new zone of recharge was established and given a lower recharge rate to help bring the heads down.

The third zone of recharge, R_3, is located on the south-facing slopes of the Ester Creek and Alder Creek drainages where permafrost-free silt deposits, gravel deposits, or mine tailings occur at the surface. The silt deposits range in thickness from 5-20 m thick. The recharge rate at this zone was higher than the permafrost zones because more water can enter the aquifer with the absence of permafrost. Gieck (1986) showed that 50% of the snowpack at Ester Creek drainage, which is included in this zone, could become recharge during the 1982-83 study period. However, it is suspected that a significant portion does not reach the water table due to slow infiltration rates and high plant transpiration.

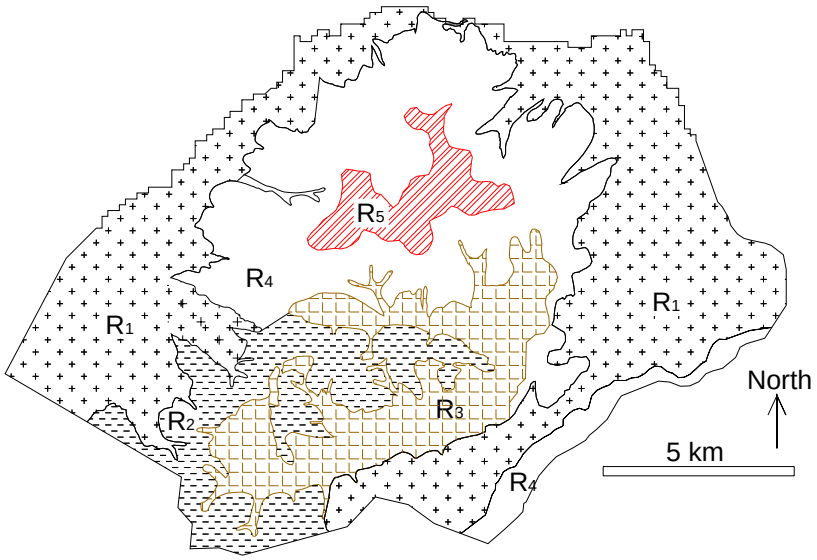

Figure 35. Recharge zones in Ester Dome ground-water flow model.

The fourth and fifth zones of recharge, designated R_4 and R_5, are located where bedrock is exposed at the ground surface, or only a thin layer of silt (less than 5 m) exists over the bedrock. These two zones have the highest recharge rates because of the exposed intensely weathered bedrock at the surface and the increased SWE in these zones. These zones generally occur at the higher elevations. In these zones, it is assumed that snowmelt water can infiltrate into fractured bedrock. The fourth zone is located at a lower elevation than the fifth zone. The fifth zone encompasses the highest elevations of Ester Dome at approximately 550-700 m.

Drain Conductance

Drains were used to simulate the spring-fed streams Ester Creek and Alder Creek/Cripple Creek. The drains allow water to leave the Ester Dome system as ground-water discharge to streams and flow out of the model. MODFLOW-2000 requires a conductance to be specified to rivers, general head boundaries, and drains. The conductance is defined as:

$$C = \frac{KLW}{M} \quad \textbf{(4)}$$

where C is conductance, K is hydraulic conductivity of the streambed material, L is the length of the reach, W is the width of the stream, M is the thickness of the streambed material. Table 4 shows the conductance values for each creek.

MODEL CALIBRATION

Calibration is the process of re-examining and changing the ground-water model parameters, based on results of previous simulations to minimize the difference between observations and simulated results. The forward model was initially calibrated manually by trial-and-error. This process involves using March 2001 field water-level measurements, well-log water-level records, and estimates of stream flow rates to match simulated values of hydraulic head and flow. The calibration process is also used to refine parameter estimates of hydraulic conductivity, isotropy, drain conductance, and recharge. After trial and error calibration procedures are completed, MODFLOW-2000's Observation and Sensitivity package (Hill et al., 2000) is utilized to quantify ground-water model calibration process. In this automated calibration process, sensitivity and model fit statistics are reported. Parameter-estimation techniques are attempted to further understand aquifer properties and ground-water flow processes.

Calibration Data

The ground-water flow model was calibrated to observed water levels. Little was known about stream flows, but the flow in Goldstream Creek constant-head cells was checked and compared to the estimated range of discharge reported for Goldstream Creeek. Flows out of the drain cells were checked and compared to estimated flows in Ester Creek, Cripple Creek, and Alder Creek.

Less accurate or less reliable measurements were given a weighting factor to reflect the measurement error for the residual analysis. Table 5 shows the weighting factors assigned to the various observation types. The water-level values used were from the March 2001 measurements in approximately 50 observation wells. An additional 25 water levels from well log records were also used in the calibration.

Table 5. Table of observation weighting factors.

Observation Type	***Measurement Error (m)***	***STATISTIC Standard Deviation (m)***	***WEIGHT= 1/STATISTIC^2 (1/m^2)***
Well Log Record	10 m (95% confidence level)	5.102	0.0384
Ground-water well or surface water site surveyed with USGS Topographic Map	90% confidence level plus or minus the contour interval	3.03	0.109
Ground-water well or surface water site surveyed with GPS	3 m (95% confidence level)	1.53	0.427
Ground-water well or surface water site surveyed with GPS Traditional Level	1 m (95% confidence level)	0.51	3.84

Data were entered into the Observation package in MODFLOW-2000 to compare simulated and observed values. The Observation package does the following: 1) calculates simulated equivalents of the observations using the hydraulic heads for the entire model grid, 2) compares observed values with simulated equivalent values, and 3) calculates observation sensitivities (Hill et al., 2000). Since most of the observations do not fall in the center of the finite-difference cell, interpolation methods are used to

calculate the head value at the observation location (given the observation location coordinates), which is known as a simulated equivalent.

SENSITIVITY ANALYSIS

The Sensitivity package uses the sensitivity equation method to examine the sensitivity of each model parameter. Sensitivities are used to identify where hydraulic heads or flows are the most sensitive to changes in a parameter. This involves taking the derivative of simulated hydraulic head with respect to the parameter of interest. Dimensionless scaled sensitivities (*ss*) and composite scaled sensitivities (*css*) are used to compare the different types of observations to the estimation of parameter value (Hill, 1998). Dimensionless scaled sensitivities indicate the importance of an observation to the estimation of a parameter or the sensitivity of the simulated equivalent of the observation to the parameter (Hill, 1998). This type of sensitivity analysis allows one to compare the sensitivities of different parameters to each other. Dimensionless scaled sensitivities (ss_{ij}) are defined by Hill (1998) as:

$$ss_{ij} = \left(\frac{\partial y_i'}{\partial b_j} \right) b_j \omega_{ii}^{1/2} \qquad \textbf{(5)}$$

where i defines one of the observations, j defines one of the parameters, y_i' is the simulated value, b_j is the jth estimated parameter, $\frac{\partial y_i'}{\partial b_j}$ is the sensitivity of the simulated value with the jth parameter and is evaluated at $\boldsymbol{b}$. Composite scaled sensitivities indicate the information content of all the observations for the estimation of the parameter (Hill, 1998). They are used to evaluate whether the available observations provide enough information for parameter estimation (Hill et al., 2000). Composite scaled sensitivity (css_j) for the jth parameter is defined as:

$$css_j = \left[\sum_{i=1}^{ND} (ss_{ij})^2 \Big|_b / ND \right]^{\frac{1}{2}} \qquad \textbf{(6)}$$

where *ND* is the number of observations and ***b*** is the vector which contains the values of each of the parameters being estimated. A one-percent scaled sensitivity (*dss*) is defined (Sun, 1994 and Hill, 1998) as the amount of change in the simulated head with a 1% increase in the parameter of interest and is calculated throughout the model with the equation:

$$dss_{ij} = \frac{\partial y_i'}{\partial b_j} * \frac{b_j}{100} \quad \textbf{(7)}$$

where *dss* is scaled sensitivity, y_i' is the simulated value associated with the ith observation, and b_j is the parameter of interest. Areas within the model, which have high one-percent scaled sensitivity indicate a greater sensitivity when the parameter is changed and that it would be useful to have more observations.

PARAMETER ESTIMATION

Because little is known about the aquifer properties of Interior Alaska upland systems, it would be useful to constrain the estimated ranges of hydraulic conductivity and recharge using parameter-estimation techniques. One can obtain the best model fit of an equation to our field observations by minimizing the difference between the observations and the simulated values (residuals). MODFLOW-2000 uses nonlinear regression to estimate the optimal parameter values by minimizing the objective function, a measure of the difference between the simulated and observed observations (Hill, 1998). The weighted least squares objective function used in MODFLOW-2000 is defined by Hill (1998) as:

$$S(b) = \sum_{i=1}^{ND} \omega_i \left[y_i - y'_i(b) \right]^2 + \sum_{p=1}^{NPR} \omega_p \left[p_p - p'_p(b) \right]^2 \quad \textbf{(8)}$$

where ***b*** is the vector which contains the values of each of the parameters being estimated, *ND* is the number of observations, *NPR* is the number of prior information values, *NP* is the number of estimated parameters, y_i is the ith observation, $y_i'(b)$ is the simulated value which corresponds to the ith observation, p_p is the pth prior estimate

included in the regression, p'_p is the pth simulated value, w_i is the weighting factor for the ith observation, ω_p is the weight for the pth prior estimate. The minimization of this objective function produces a solution that is a best fit to the observed data.

Although parameter-estimation simulations were not conducted successfully on the Ester Dome model, future simulations should include this method when additional observations are collected. Parameter-estimation techniques require a well-posed problem, where geohydrologic components and represented in the model as much as possible (Hill, 1998). Parameter-estimation techniques require observation information to estimate a parameter. In particular, flow observations are necessary in addition to hydraulic head data. For the Ester Dome model, few water-level observations were available in many of the parameter zones. Additionally, little information about flows was known. Difficulties reaching convergence (the solution) during parameter-estimation simulations lead us to believe we have an ill-posed parameter-estimation problem or not enough observation information. Also, parameter zones may not be described accurately. Further efforts will try to resolve these issues.

RESULTS OF CALIBRATION AND SENSITIVITY ANALYSIS

The calibration and sensitivity analysis give quantitative and qualitative information about the simulation accuracy. Figure 36a shows the simulated head distribution for layer one (simulated head distribution for layers two, three, and four are in Appendix C). We observe several differences when visually comparing the head distribution to the estimated water-table map (Figure 36b). In the estimated water-table map, which is based on data collected from March 2001, the water table, in general, follows the land surface topography. The simulated results do not show the topographic features. Additionally, ground water and surface-water relationships are not seen in drainages because most creeks are not simulated.

The following MODFLOW-2000 output statistics and characteristics are considered to examine the accuracy of our model and identify sensitivities for future parameter-estimation simulations:

1. Water budget
2. Maximum, minimum, and average weighted residuals
3. Positive and negative residuals
4. Number of runs
5. Least squares objective function
6. Correlation between ordered weighted residuals and normal order statistics
7. Composite scaled sensitivities
8. Dimensionless scaled sensitivities
9. One-percent scaled sensitivities
10. MODPATH flowpaths and travel times

In the Ester Dome ground-water model, we examined the sensitivity of each observation and the following parameters: recharge zones, anisotropy (VANI), hydraulic conductivity for each unit, and drain conductance. Each parameter is given a starting value and a high and low reasonable value for the sensitivity calculations (shown in Table 4).

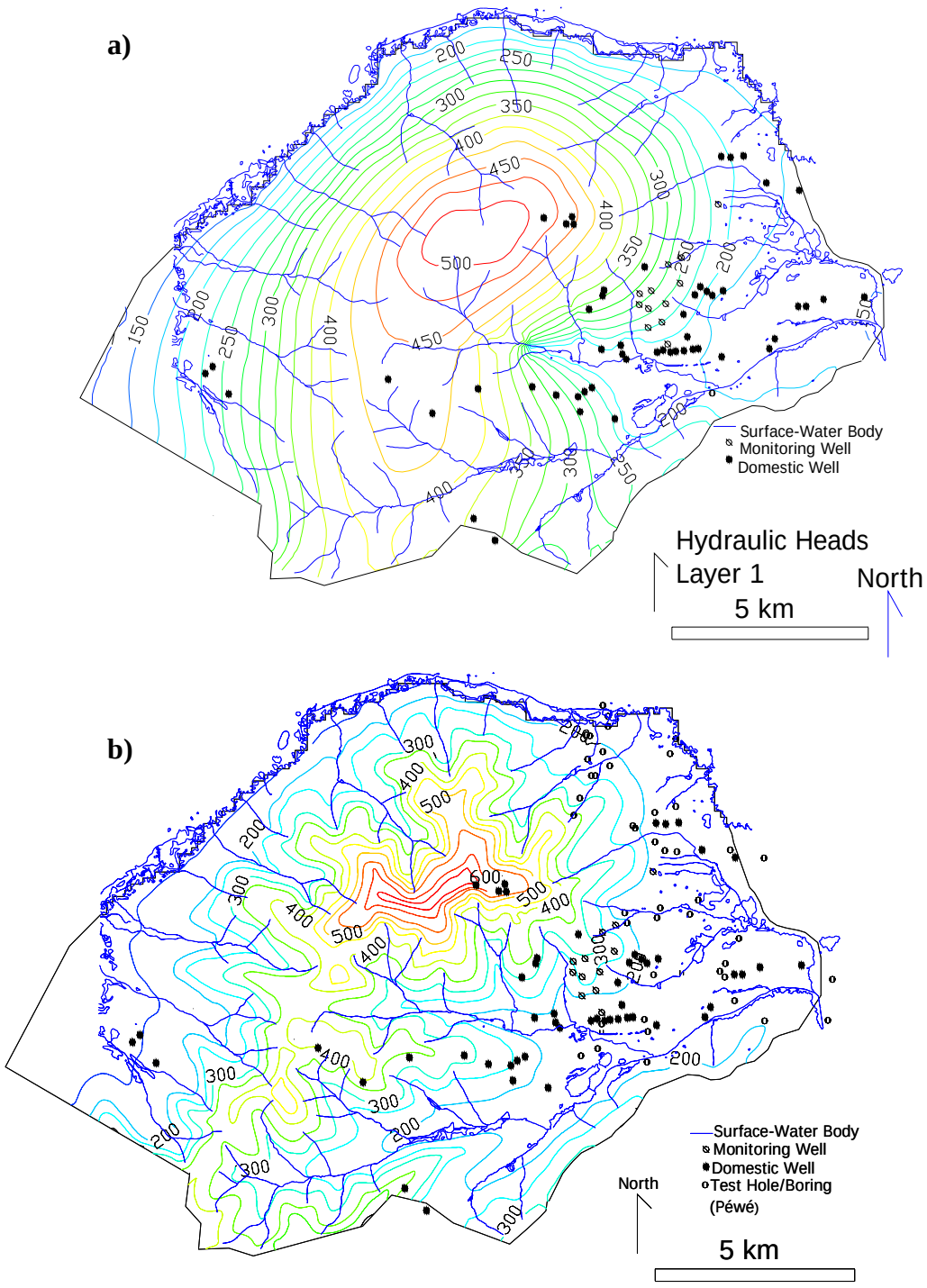

Figure 36. Simulated heads for layer one and water-table map (based on observations) for Ester Dome (in meters above sea level).

Water Budget

The volumetric water budget for the model is shown in Table 5. The source of water entering the Ester Dome aquifer system is recharge and water through constant head cells. Of the 6,127 m^3/d entering the model through the constant head boundary, approximately 4500 m^3/d enters the aquifer through the constant-head cells in layer two of the East Boundary. These cells are high conductivity gravel deposits. Water leaves the model through the drains (Ester and Alder Creeks) and the constant head boundaries. The actual streamflow in these creeks is estimated to be less than 240 m^3/d (0.1 cfs) during winter conditions. Water budget mass balances, indicating an acceptable solution. High water balance errors occurred due to the drain conductance, so the conductance was decreased until the water balance error was below 1%. This error occurs due to the way input information is stored and processed in the computer (Anderson and Woessner, 1992).

Table 6. Water Budget from MODFLOW output.

Budget Terms	*Cumulative Volumetric Flow Rates (m^3/d)*
IN	
Storage	0
Constant Head	6124.1
Drains	0
Recharge	7436.1
TOTAL IN	13563.7
OUT	
Storage	0
Constant Head	13365.2
Drains	199.2
Recharge	0
TOTAL OUT	13564.4
IN-OUT	-0.65
Percent Discrepancy	0

Residual Analysis

The residual analysis indicates the error between the simulated and observed water levels. It also yields clues to the success of future parameter-estimation simulations. Table 6 shows the residual statistics for the simulation. Both unweighted and weighted residuals were examined to evaluate the model fit. Residuals that are positive indicate the simulated water levels are lower than the observed water levels. Negative residuals indicate the simulated water levels are higher than the observed water levels. Weighted residuals (dimensionless) are examined because they reflect the uncertainty in the observation and model fit. The maximum residual occurred for a well located at the top of Ester Dome. The simulated heads at the top of Ester Dome were lower than the observed heads. The minimum residual occurred in well EDP030, which is located in a valley bottom in the far western region of the study area. All the head observations were lower than the simulated heads in this region. Ideally, the number of positive residuals should equal the number of negative residuals and should appear random. But in this simulation, most of the residuals were negative, indicating most simulated heads are higher than the observed heads. This problem occurred for most of the valley-bottom wells. The "number of runs" statistic checks for the randomness of the weighted residuals. The critical value of –1.96 indicates if the statistic is less than –1.96, there is less than a 2.5% chance that the values are random.

Table 7. Residual Statistics

Maximum Unweighted Residual (m)	*Minimum Unweighted Residual (m)*	*Maximum Weighted Residual*	*Minimum Weighted Residual*	*Average Weighted Residual*	*Total Sum of Squared, Weighted Residuals*
67.9	-106	44.4	-69.2	-16.0	0.497E+5

Number of Positive Residuals	*Number of Negative Residuals*	*Runs Statistic*	*Number of Runs*
10	61	-0.670	15 in 71 observations

Figure 37 shows the graph of unweighted observations versus unweighted simulated equivalent. Points should preferably lie along the line with a slope of 1.0. A significant number of points fall below the line with a slope of 1.0, showing the unweighted simulated values are higher than the unweighted observations. A cluster of

points falls above the line at the higher elevations where the simulated water levels were less than the observed water levels. However, since the values are unweighted, the uneven spread of the data points does not necessarily indicate problems with the solution (Hill et al., 2000). Figure 38 shows the graph of weighted observation versus weighted simulated equivalent. This graph shows that after the observations are weighted based on the error of the measurement, many fall on the line with a slope of 1.0. The model performed better in areas where the water-level observations had a higher error associated with the measurement. However, at water-level observations with lower uncertainty associated with the measurement, such as the observations at the Gold Hill Road area surveyed with traditional leveling, model results were not as accurate. For example, for certain observations there is a high range of error associated with the measurement. Therefore, the model-simulated water levels may be within that large error range. However, for observations where there is little uncertainty associated with the measurement, the model-simulated values might not fall within that smaller error range. Additionally, because we are conducting a steady-state simulation, we do not take into account transient variations, which are significant (up to 30 m of water-level change seasonally) in some regions of the model.

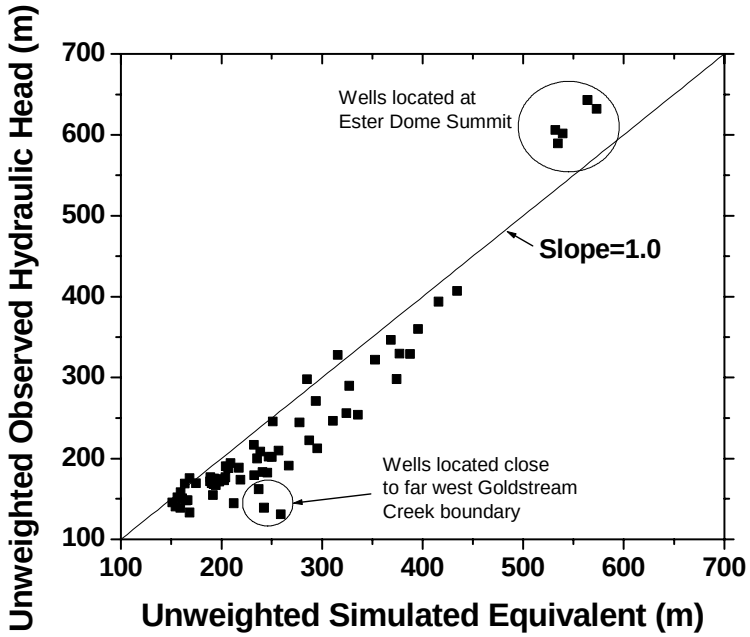

Figure 37. Unweighted hydraulic head versus unweighted simulated equivalent.

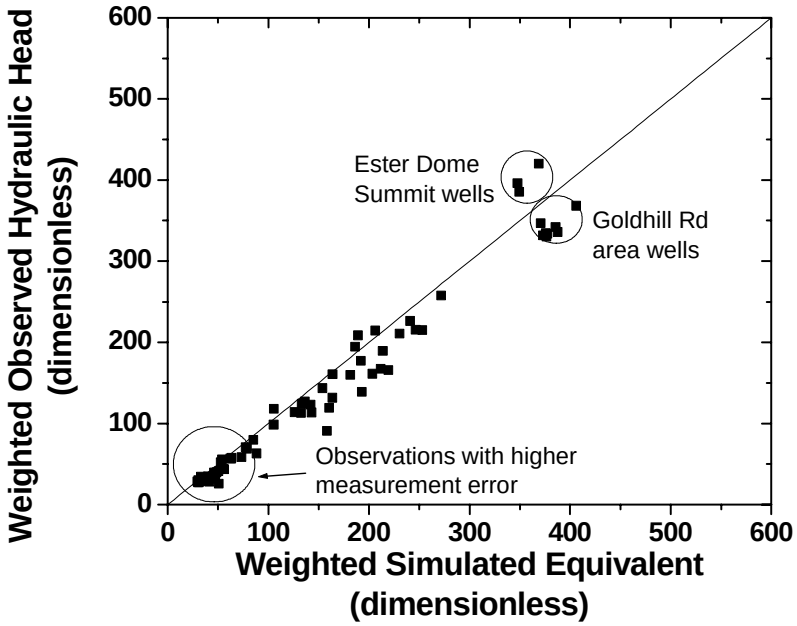

Figure 38. Weighted hydraulic head versus weighted simulated equivalent.

Figure 39 is a graph of the weighted residuals versus weighted simulated equivalent. Data points should be evenly distributed above and below the weighted residual zero axis, indicating random weighted residuals (Hill et al., 2000). This graph shows the majority of observations with a residual of plus or minus 40 meters. Most of the weighted residuals are negative indicating there may be a problem with the model. In the valley bottom parts of the aquifer, heads were predicted higher than they are observed. Adjustments to the hydraulic conductivity of the bedrock were made during the calibration procedure to fix this problem, however, the water levels at the top of Ester Dome were very sensitive to these changes. This may indicate a new hydraulic conductivity zone needs to be established at the higher elevations. Approximately 16 of the 71 observations have weighted residuals greater than +/-40 meters. Figure 40 shows the normal probability graph of the weighted residuals. Again, the weighed values should fall along a straight line. The majority of the values fall along a straight line, but the data does exhibit a degree of curvature indicating the data may not be normally distributed and there may be problems with the model. The correlation of the ordered weighted residuals and normal order statistics for observations was 0.95 while the critical value at the 5% confidence level is 0.968. Therefore, the hypothesis that the weighted residuals are normally distributed is rejected. This test failed either because there are not enough weighted residuals or the model is not accurate. Poor model fit can indicate problems with the model design and parameterization, data entry errors, and weighting errors (Hill, 1998). Figure 41 is a map showing the spatial distribution of the weighted residuals. The weighted residual for each observation is plotted with the symbols indicating the absolute value of the standard deviation.

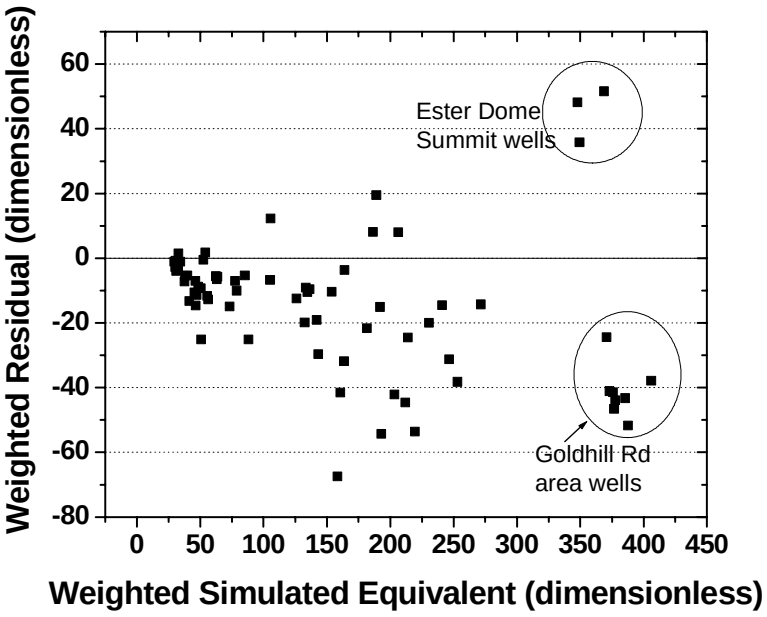

Figure 39. Weighted residual versus weighted simulated equivalent.

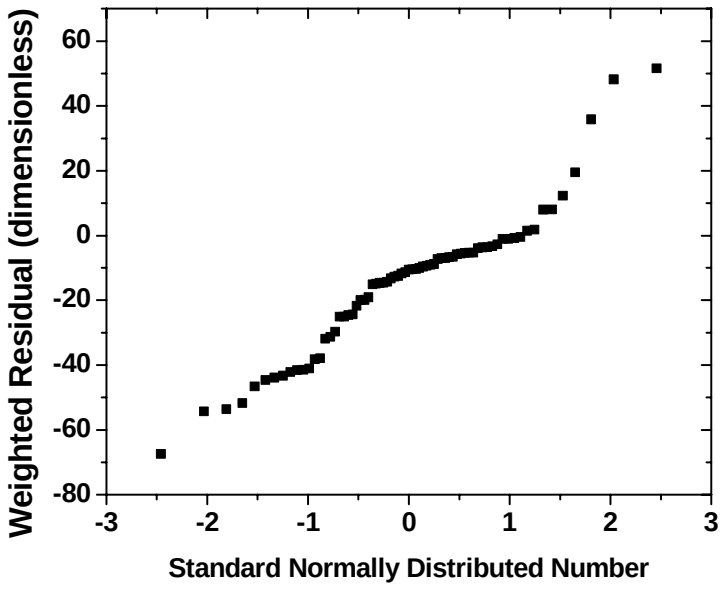

Figure 40. Weighted residual versus normally distributed number.

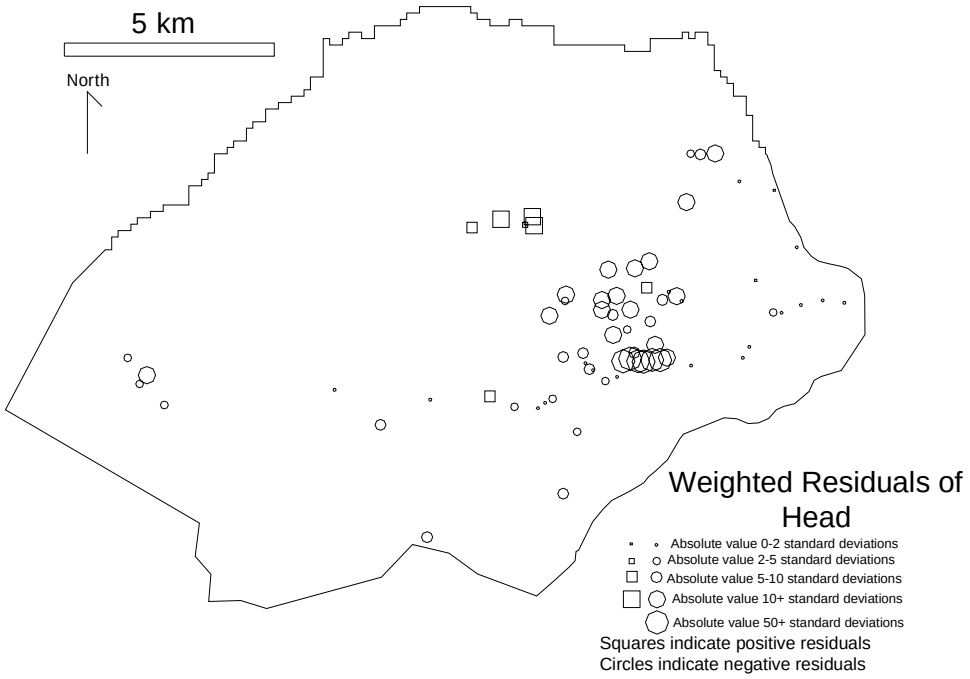

Figure 41. Spatial distribution of weighted residuals.

Sensitivity Analysis

The sensitivity analysis was conducted to examine the sensitivity of parameters and observations to changes in hydraulic head. It was also performed because sensitivities aid in indicating the success of any parameter-estimation techniques for future simulations. Sensitivities were calculated for all parameters at each grid cell. Figure 42 shows the composite scaled sensitivities. This figure indicates which parameters are the most and least sensitive and whether new parameters should be introduced. Insensitive parameters also indicate that future parameter estimation regressions may not converge or reach solution. For the Ester Dome ground-water model, the four parameters most sensitive to changes in water levels are:

- Hydraulic conductivity of bedrock (Bedrock)
- Hydraulic conductivity of the south gravel deposit (Qht_so)
- Recharge zone five (RCH_5)
- Recharge zone four (RCH_4)

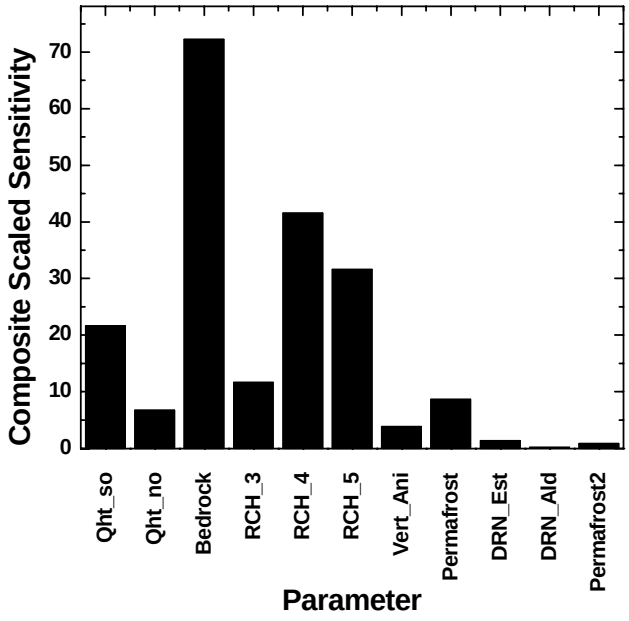

Figure 42. Composite Scaled Sensitivities

For future parameter estimation simulations, these parameters are more likely to converge due to the amount of observation information available. Parameters with low sensitivity such as the hydraulic conductivity of the northern gravel unit (Qht_no), vertical anisotropy (VERT_ANI), hydraulic conductivity of permafrost (Permafrost), and the drain conductance (DRN) may not be estimated successfully with nonlinear regression due to the limited observation information available. These parameters will need more observations for future parameter-estimation simulation runs to either converge or be accurate.

The dimensionless scaled sensitivity is examined for each of the parameters and observations. Figures 43a and 43b show the sensitivity and importance of an observation to the estimation of a parameter. Figure 43a shows the high sensitivity for the hydraulic conductivity of bedrock and recharge for all zones, except recharge zone one which has zero sensitivity because the starting parameter value was zero. Figure 43b shows the observations that would contribute the most to the estimation of a parameter.

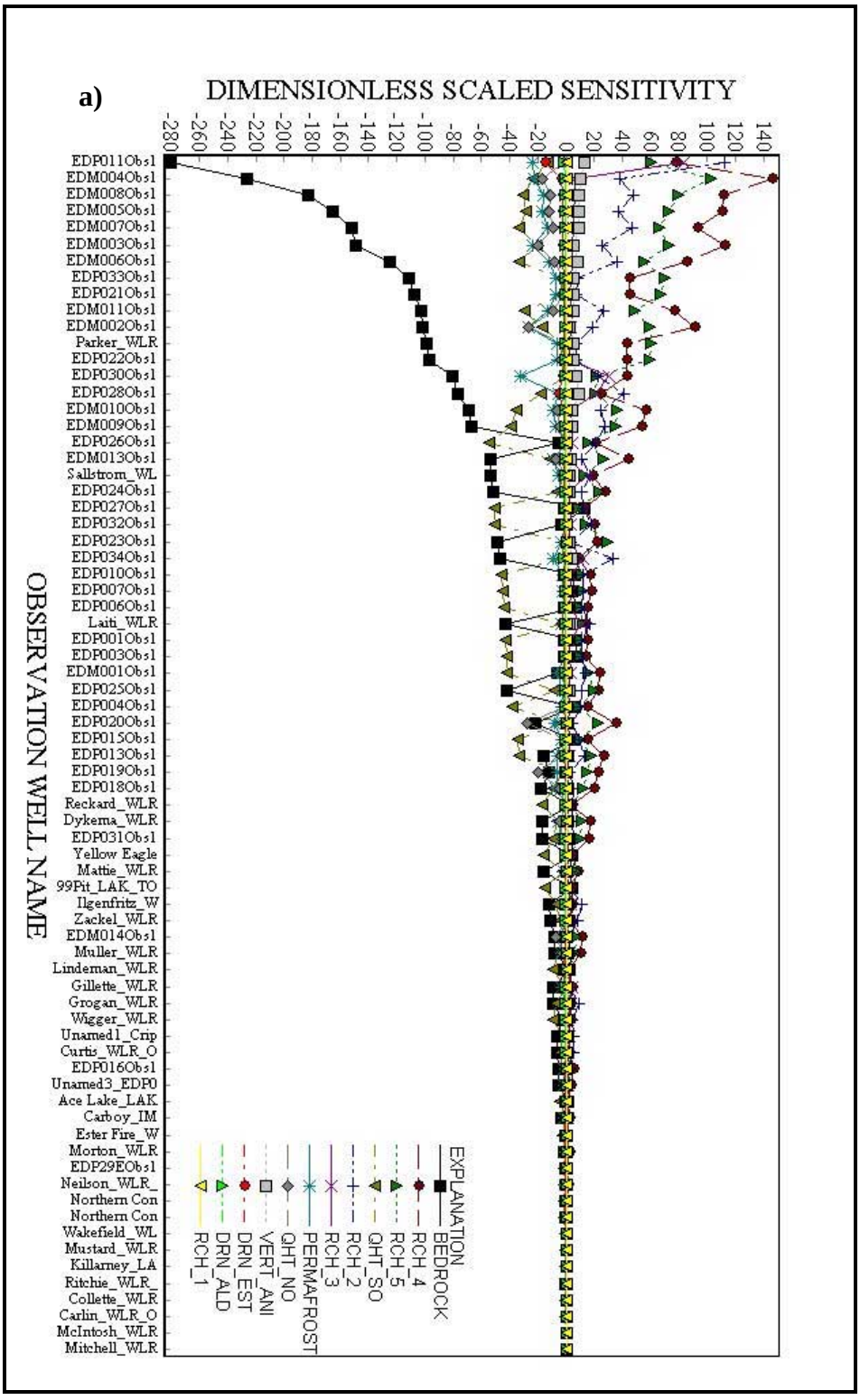

Figure 43. a) Dimensionless scaled sensitivities versus observation.

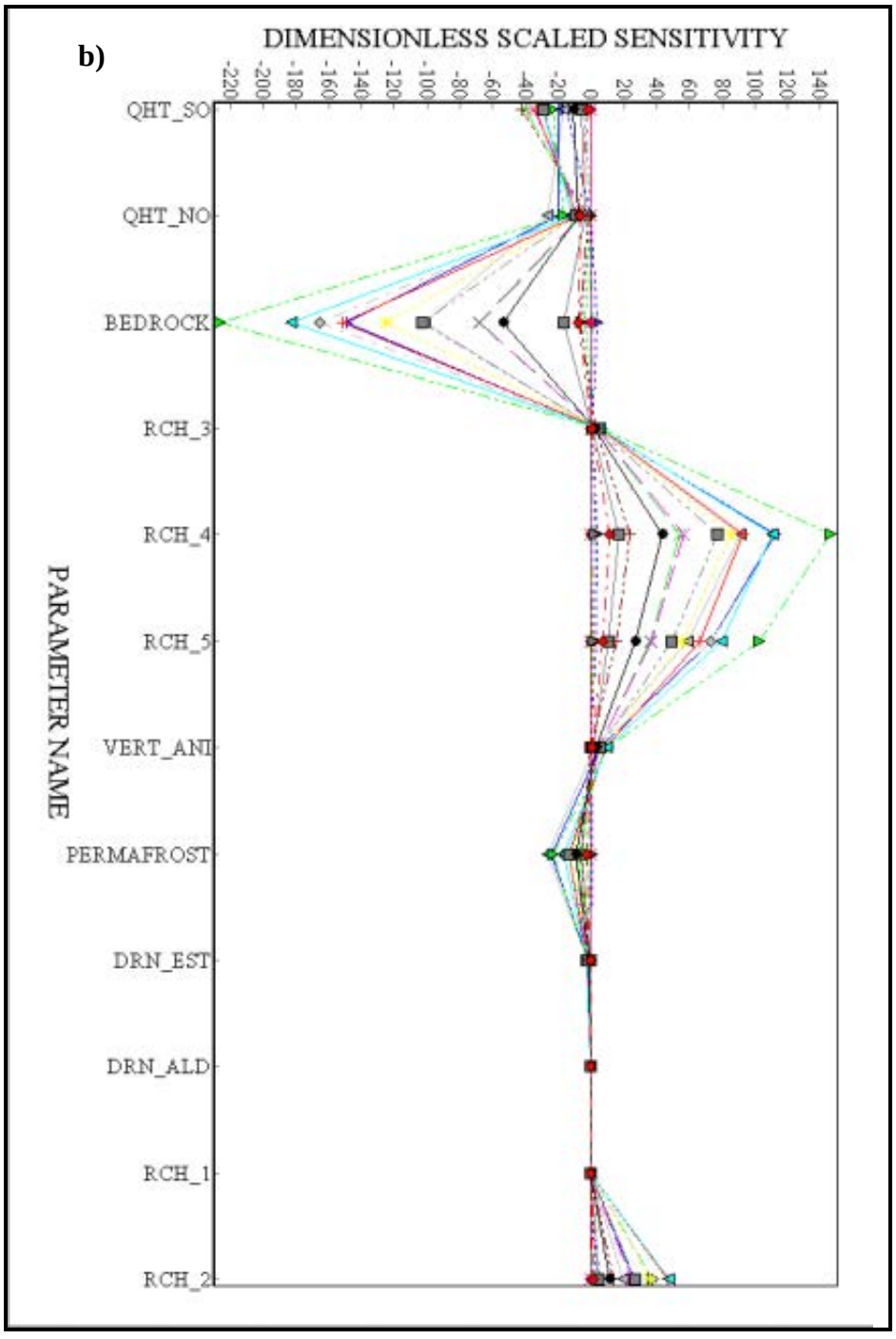

Figure 43. b) dimensionless scaled sensitivities versus parameter.

According to Hill et al. (2000),

> Parameters that have large composite scaled sensitivity and many large dimensionless scaled sensitivities will likely be better estimated than a parameter with a large composite scaled sensitivity and one large dimensionless scaled sensitivity because of the error in one observation is propagated directly into the estimate.

The hydraulic conductivity of bedrock and recharge zones four and five have large composite scaled sensitivity and several large dimensionless scaled sensitivities. This indicates that these parameters will be better estimated.

Figures 44-51 show the one-percent scaled sensitivities for the hydraulic conductivity of each unit and the recharge for each zone. These contour maps show the water-level change in meters to a one-percent increase in the defined value of hydraulic conductivity or recharge for each zone. High positive or high negative values indicate parameters that have greater sensitivities when the values are changed. Figure 44 shows the sensitivity of heads to hydraulic conductivity of permafrost in layer one. This sensitivity map shows the higher sensitivity in northwest portion of the field area. Unfortunately, there are no observations in this zone and it would be difficult to accurately calibrate this part of the model. Figure 45 shows the sensitivity of heads to hydraulic conductivity of the northern gravel zone in layer two and Figure 46 shows the sensitivity for the southern gravel zone. The gravel hydraulic conductivity sensitivity maps indicates the highest change in water levels in the Ester township area, and in the northeast corner of the model. Figure 47 shows the sensitivity of heads to hydraulic conductivity of the bedrock unit for layer one. Maps are similar for layers two, three, and four. All hydraulic conductivity sensitivities are negative, indicating a decrease in water levels with an increase in hydraulic conductivity. The highest changes in water levels with an increase in the bedrock hydraulic conductivity occur at the highest elevations on Ester Dome. A decrease of three meters in hydraulic head occurs in this location, indicating a high sensitivity to the bedrock hydraulic conductivity in this area of the model. Figures 48a, 48b, 48c, and 48d show the one-percent scaled sensitivity for the

vertical anisotropy in the four model layers. The most change occurred in layers 3 and 4 when the vertical anisotropy was increased from 1.0 by one percent.

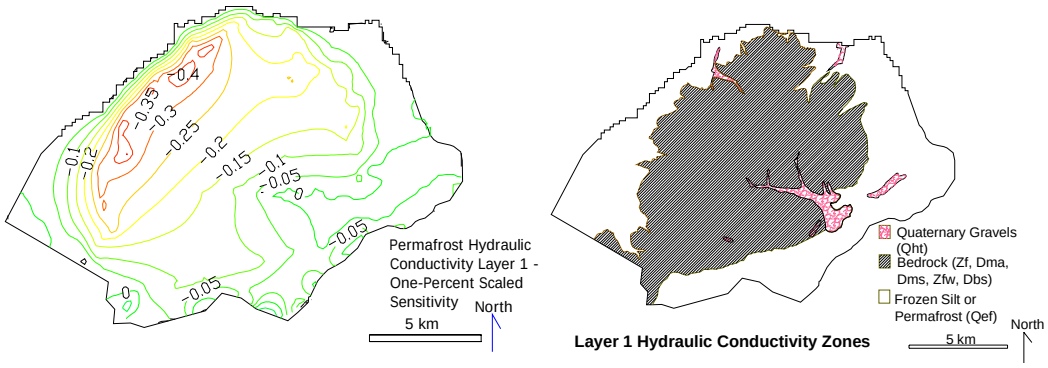

Figure 44. Permafrost hydraulic conductivity one-percent scaled sensitivity map (in meters) and hydraulic conductivity parameter map for layer one.

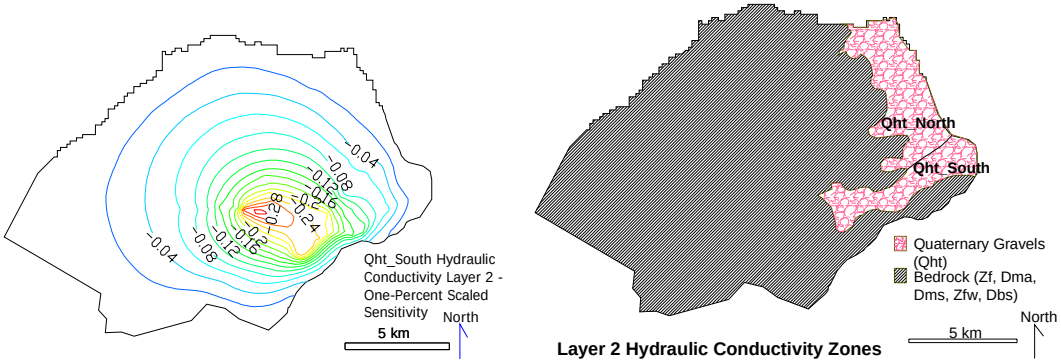

Figure 45. Gravel (south) hydraulic conductivity one-percent scaled sensitivity map for layer two (in meters) and hydraulic conductivity parameter map for layer two.

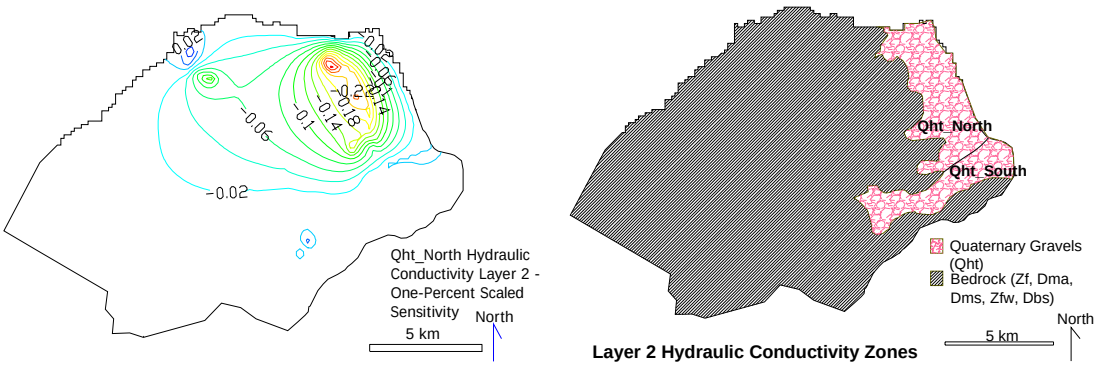

Figure 46. Gravel (north) hydraulic conductivity one-percent scaled sensitivity map for layer two (in meters) and hydraulic conductivity parameter map for layer two.

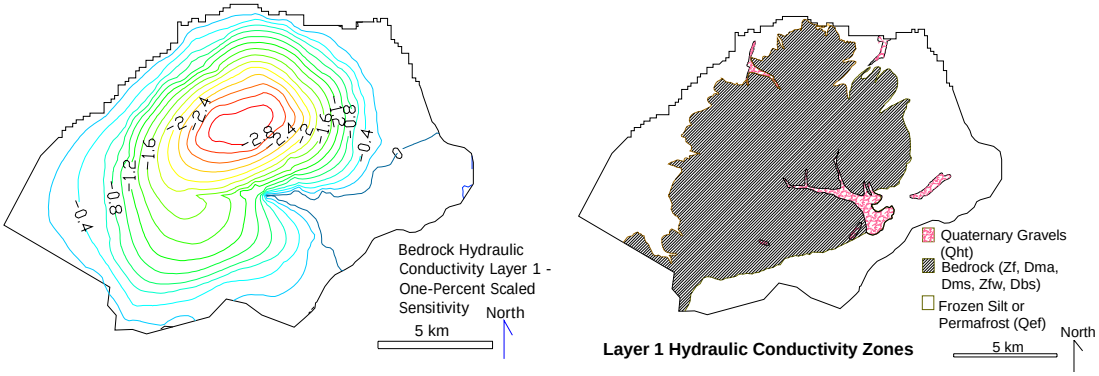

Figure 47. Bedrock hydraulic conductivity one-percent scaled sensitivity map (in meters) and hydraulic conductivity parameter map for layer one.

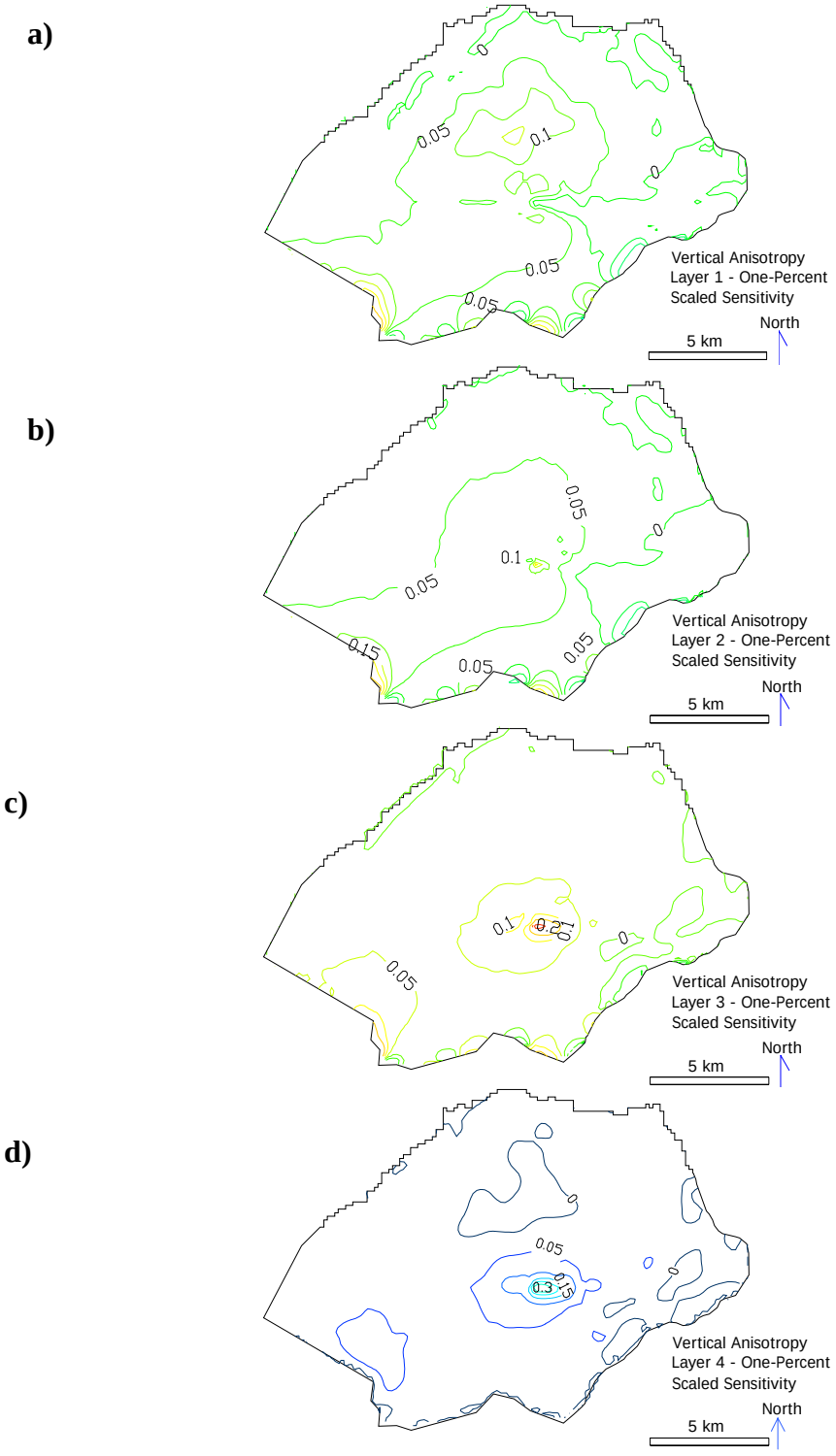

Figure 48. Vertical anisotropy one-percent scaled sensitivity map (in meters) for layers 1 through 4.

A one-percent scaled sensitivity map was not created for zone one because this zone was given no recharge, therefore values cannot be calculated. However, recharge zone two (Figure 49) is similar to zone one because it has a low recharge rate. This zone is primarily located on the north facing slopes in the south portion of the study area. Very little change in water levels occurs with a one-percent increase in the recharge. In recharge zone three (Figure 50), where the geology is mainly deposits of silt and the slope is south facing, the highest sensitivity occurs on the south-facing slope in the upstream end of the Alder Creek drainage. Unfortunately, this area is undeveloped and there are no monitoring wells. Recharge zone four (Figure 51), which was defined with a higher recharge rate and generally covers mid to high elevations, showed the most change in water levels with an increase in recharge at the higher elevations. This zone showed nearly three meters of increase in water levels with a one-percent increase in recharge from the initial value. Recharge zone 5 (Figure 52) shows a 1.8 m increase in water levels near the top of Ester Dome.

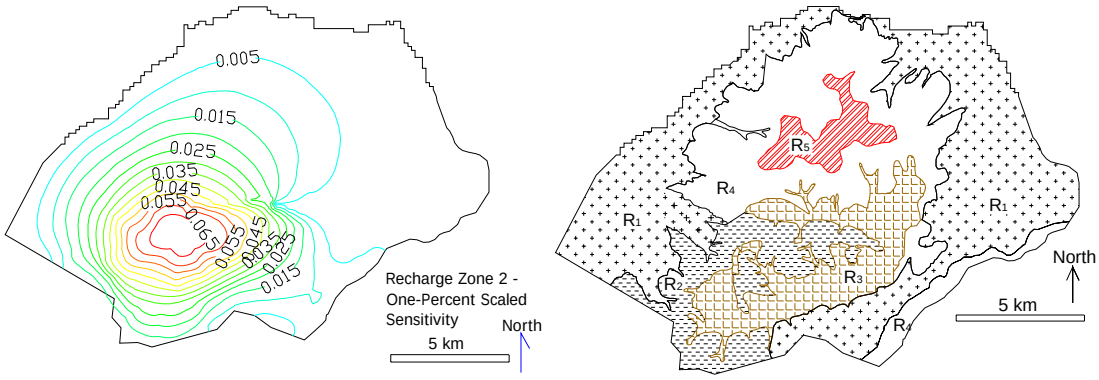

Figure 49. Recharge one-percent scaled sensitivity map for zone two (in meters) and recharge zone map.

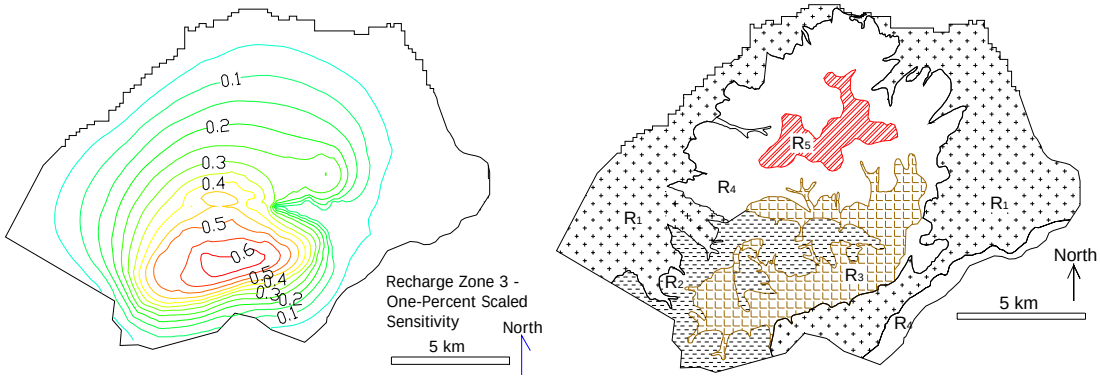

Figure 50. Recharge one-percent scaled sensitivity map for zone three (in meters) and recharge zone map.

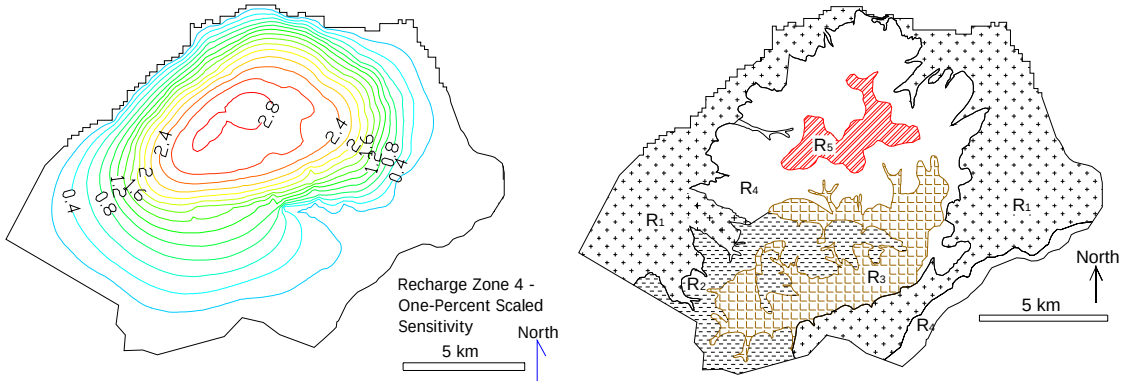

Figure 51. Recharge one-percent scaled sensitivity map for zone four (in meters) and recharge zone map.

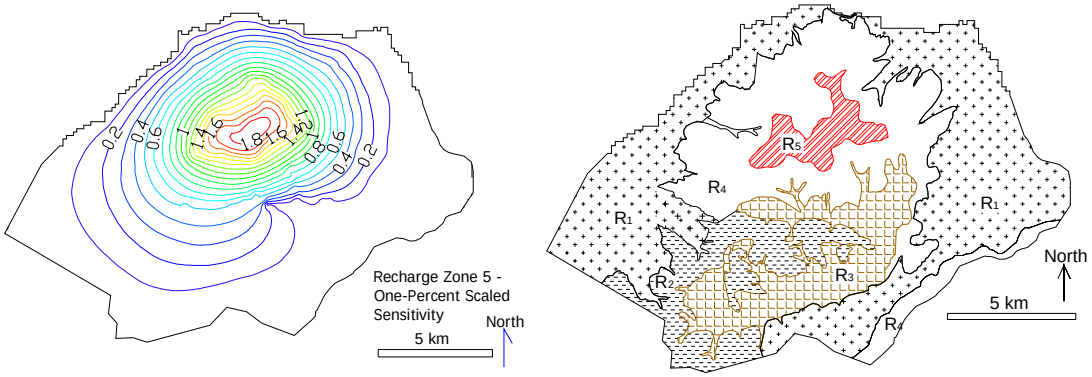

Figure 52. Recharge one-percent scaled sensitivity map for zone five (in meters) and recharge zone map.

High values of one-percent scaled sensitivity are areas of an increased change in head with the change in parameter and indicate where observations are most important for better model calibration. Figure 53a and 53b show a plot of the one-percent scaled sensitivity for each parameter and observation. These two plots indicate which observations would contribute most to the estimation of a give parameter.

a)

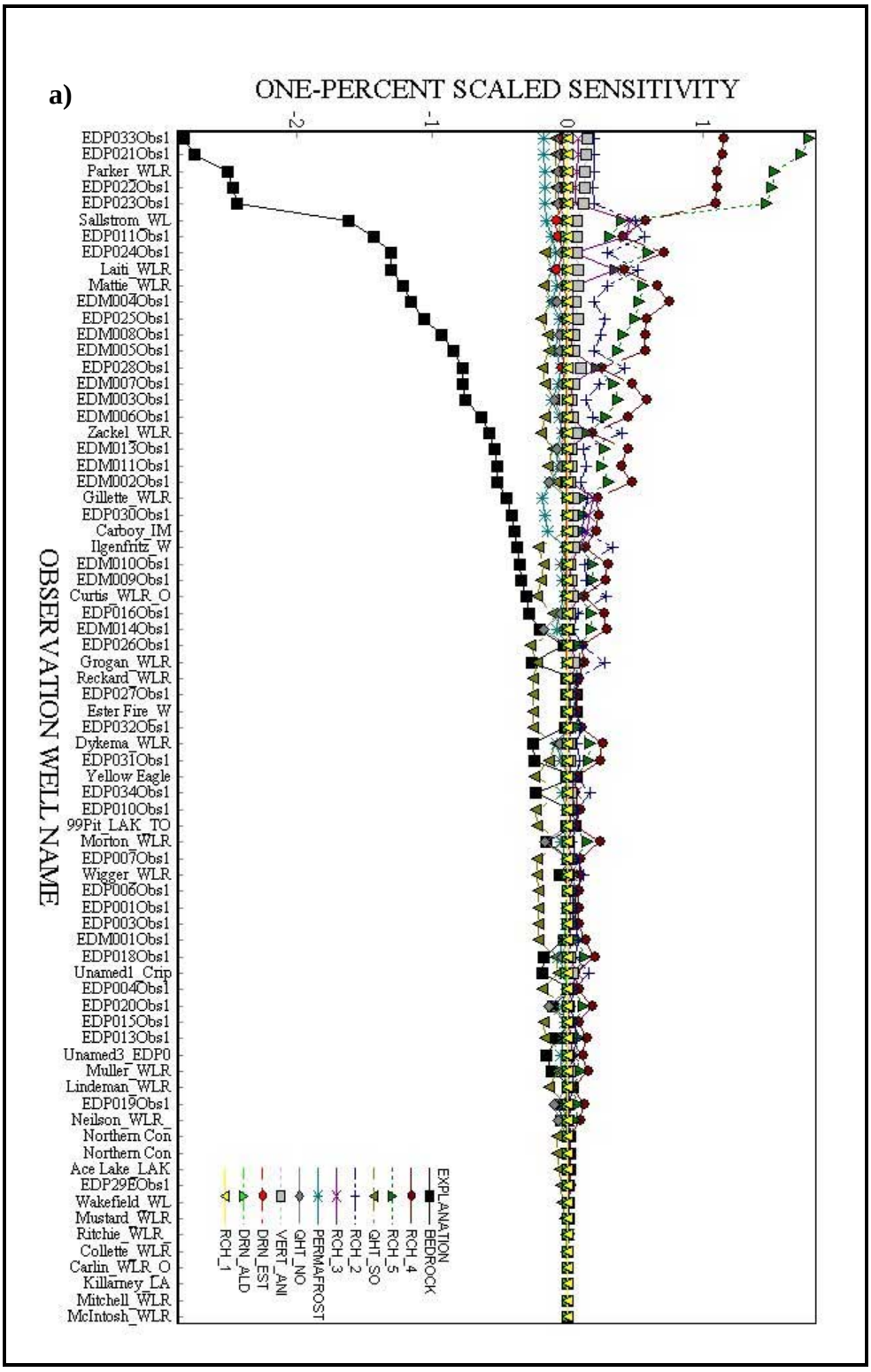
ONE-PERCENT SCALED SENSITIVITY
-2
-1
0
1
OBSERVATION WELL NAME
EDP033Obs1
EDP021Obs1
Parker_WLR
EDP022Obs1
EDP023Obs1
Sallstrom_WL
EDP011Obs1
EDP024Obs1
Laiti_WLR
Mattie_WLR
EDM004Obs1
EDP025Obs1
EDM008Obs1
EDM005Obs1
EDP028Obs1
EDM007Obs1
EDM003Obs1
EDM006Obs1
Zackel_WLR
EDM013Obs1
EDM011Obs1
EDM002Obs1
Gillette_WLR
EDP030Obs1
Carboy_IM
Ilgenfritz_W
EDM010Obs1
EDM009Obs1
Curtis_WLR_O
EDP016Obs1
EDM014Obs1
EDP026Obs1
Grogan_WLR
Reckard_WLR
EDP027Obs1
Ester Fire_W
EDP032Obs1
Dykema_WLR
EDP031Obs1
Yellow Eagle
EDP034Obs1
EDP010Obs1
99Pit_LAK_TO
Morton_WLR
EDP007Obs1
Wigger_WLR
EDP006Obs1
EDP001Obs1
EDP003Obs1
EDM001Obs1
EDP018Obs1
Unamed1_Crip
EDP004Obs1
EDP020Obs1
EDP015Obs1
EDP013Obs1
Unamed3_EDP0
Muller_WLR
Lindeman_WLR
EDP019Obs1
Neilson_WLR_
Northern Con
Northern Con
Ace Lake_LAK
EDP29EObs1
Wakefield_WL
Mustard_WLR
Ritchie_WLR_
Collette_WLR
Carlin_WLR_O
Killarney_LA
Mitchell_WLR
McIntosh_WLR
EXPLANATION
BEDROCK
RCH_4
RCH_5
QHT_SO
RCH_2
RCH_3
PERMAFROST
QHT_NO
VERT_ANI
DRN_EST
DRN_ALD
RCH_1

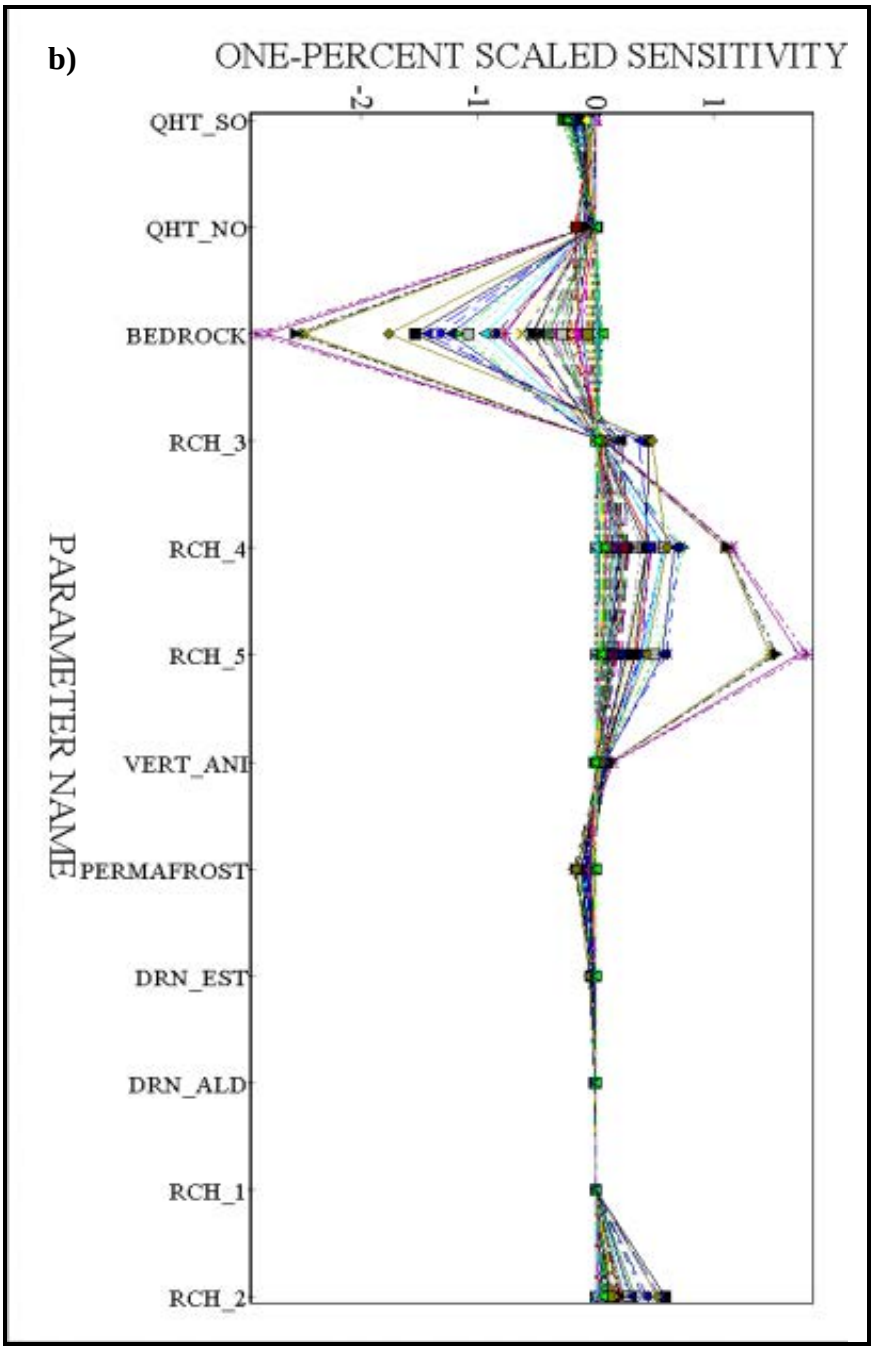

Figure 53. a) One-percent scaled sensitivity versus observation and b) one-percent scaled sensitivity versus parameter.

PARTICLE TRACKING

A particle-tracking program, MODPATH (Pollock, 1994), is a tool to further examine the ground-water flow processes in the ground-water flow model. MODPATH uses the results from a MODFLOW-2000 simulation to calculate travel times and flow paths through the aquifer. This program is used on the Ester Dome ground-water model to verify conceptual views of flow directions at Ester Dome. The input data required for this method are the information previously used by MODFLOW-2000, the simulated heads, the initial particle location, and the effective porosity. The porosity values for each Ester Dome geologic unit are shown in Table 7. Particles can be tracked in the forward direction to see where the particle would go from some location. They can also be tracked in a reverse direction, to see where the recharge area is for a certain location. MODPATH can also be used to calculate travel times.

Table 8. Effective porosity of geologic units for MODPATH simulation.

Geologic Unit	***Porosity***	***Reference***
Bedrock	0.15	Freeze and Cherry (1979)
Silt	0.3	Freeze and Cherry (1979)
Gravel	0.3	Freeze and Cherry (1979)

Particles were placed at the center of Ester Dome in each model layer for forward particle tracking. The results of the forward tracking for particles starting in layer two is shown in Figure 54. All particles that traveled east stayed in layer two except for one particle that discharged out a drain in layer one at Ester Creek. The particles that flowed to the west ended in layers three and four. It is likely that particles flowing toward the East Boundary are preferentially flowing toward the higher permeability gravel unit in layer two.

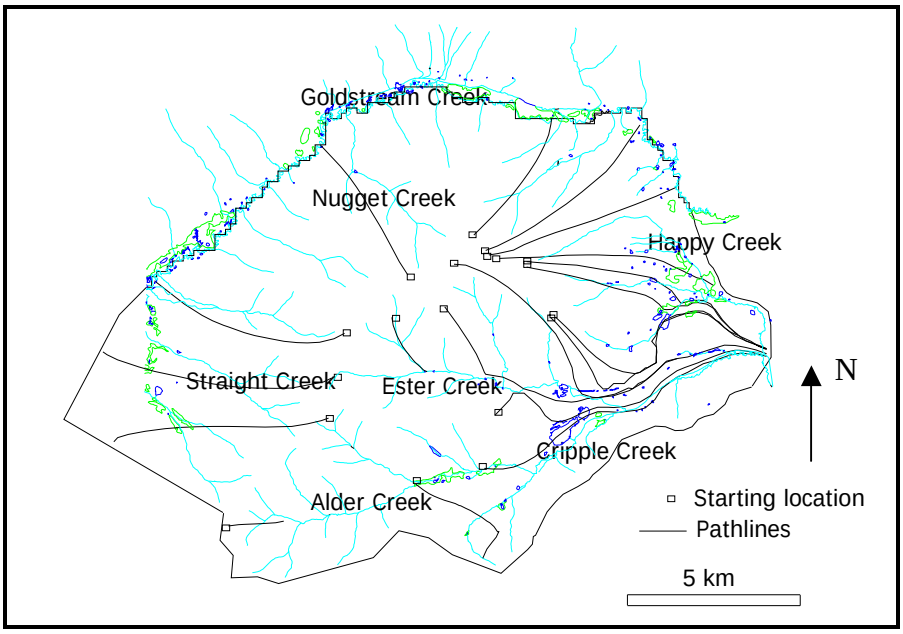

Figure 54. Forward particle-tracking results for particles placed in layer two.

Reverse particle tracking is a useful method of delineating capture zones. Figure 55 shows the results of the simulation for particles placed in model layer three. The figure shows the path lines of particles placed in valley bottom locations. The particle paths can be traced to their recharge areas, at the higher elevations in layer one.

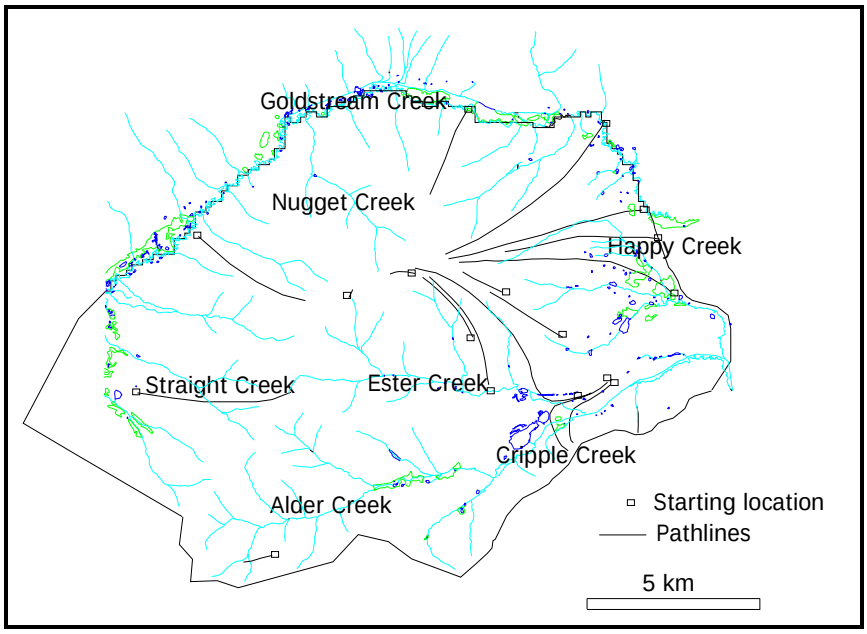

Figure 55. Reverse particle-tracking results for particles placed in layer three.

The other benefit of MODPATH particle tracking is the calculation of travel times. The results of the calculated travel times for particles in the forward run are shown in Table 8. For the Ester Dome ground-water flow model travel time uncertainties are largely due to uncertainties in the hydraulic conductivity of the geologic units. The travel times listed are much longer than expected, however there is no known available age dating of ground water to verify these numbers. A simple check of these calculations with Darcy's Law indicates that by increasing the bedrock hydraulic conductivity by one order of magnitude decreases the travel time by an order of magnitude. Bedrock hydraulic conductivity varies over several orders of magnitude, indicating these travel-time results are highly variable and greatly dependent on the hydraulic conductivity. Additionally, due to zonation and model simplification, the estimated value of the bedrock hydraulic conductivity is an average and does consider local heterogeneities. The bedrock aquifer at Ester Dome is fractured and there may be localized zones of intense fracturing, which was not considered in this simulation. Particles would travel faster through these higher transmissivity fracture zones resulting in lower travel times.

On the other hand, there could also be localized zones of low permeability gouge in certain areas of the fault zones, retarding flow.

Table 9. MODPATH calculated travel times for particles (forward tracking).

Travel Time Summary for all Particles (bedrock K=0.003)	
Minimum Travel Time (yr)	627
Maximum Travel Time (yr)	75,900
Average Travel Time (yr)	11,900
57% of the particles had travel times less than the average travel time	

MODEL LIMITATIONS AND CONCLUSIONS

The purpose of developing this model was to gain a better understanding of important geohydrologic processes in Interior Alaska upland aquifer systems. An additional intention of the study was to develop guidelines and techniques for working in upland aquifer systems. The development of the model required us to examine the spatial variations in recharge and hydraulic conductivity. It required us to examine the boundary conditions and identify where ground water is flowing in and out of the study area and what the vertical gradients are at the boundaries. Additionally, a residual and sensitivity analysis was performed to identify problems with the model configuration, parameter values, and the predictive capabilities.

A relatively large-scale ground-water flow simulation was applied to Ester Dome. The estimates of the aquifer properties may vary by orders of magnitude, depending on scale, due to heterogeneities in the aquifer. Additionally, small-scale features such as individual fractures are not considered in this type of model, but do affect the ground-water dynamics of the aquifer system and are important to consider in smaller-scale studies. The problem of a non-unique solution occurs in most forward ground-water flow models. There are a large number of parameter combinations that could lead to a single solution. We tried to constrain our recharge values in order to adjust the hydraulic conductivity during model calibration.

In certain modeled areas, particularly those with no observational data available, the model is less accurate. Areas include: 1) the northern half of Ester Dome (except at Goldstream Creek) where no observations of hydraulic head exist, 2) the western part of the study area, where simulated water levels were generally higher than observations, and 3) the top of Ester Dome, where simulated water levels are lower than observed water levels. It is not surprising that the simulated water levels were low at the top of Ester Dome, which is what we see at most ridges in the Fairbanks area. Establishing additional zones of bedrock hydraulic conductivity in future simulations, particularly for this area, would be useful to further examine the hydraulic conductivity of the fractured bedrock. Due to the geologic complexity and the number of unknowns involved in the model construction, the model would likely not make highly precise predictions for small-scale or detailed investigations until additional hydrogeologic information is available. This is reflected in the residual analysis, where the model predictions are less accurate for highly precise observations.

Despite the uncertainty of the ground-water flow model, the simulations actually were acceptable, given the constraints involved. Additionally, using a ground-water flow model to aid in the interpretation of the geohydrology of Ester Dome allowed us to better understand these hydrologic processes. In Alaska, we typically have very little data available to accurately describe geohydrologic processes. The development of this ground-water flow model requires that all hydrologic components and processes are addressed. Hydrogeologic units and potential aquifers were evaluated. We identified five zones of potential aquifer recharge. In the Ester Dome simulation, we examined the sensitivity of water levels to changes in the hydraulic conductivity and recharge. The particle-tracking techniques verify our conceptual view of ground-water flow paths and are a product useful to mining and development applications. Data shortcomings, such as the lack of stream flow measurements and water-level measurements on the north and western portions of Ester Dome, are identified in the ground-water flow modeling process. The modeling effort helped us organize and distribute available data on Ester Dome. Additionally, the Ester Dome ground-water flow model can be improved and

refined as new data becomes available. Certain regions of the model could be examined more closely. For example, we could add more hydrogeologic detail to the Ester Creek watershed and simulate ground-water flow in this watershed alone. This Ester Dome ground-water flow model, in the current stage, is a good starting point for future simulations. The Ester Dome ground-water flow model was a success because we now have a better understanding of geohydrologic processes important to Interior dome and ridge aquifer systems.

ACKNOWLEDGEMENTS

This project was supported by Alaska Science and Technology Foundation Grant #00-1-049. The project was co-funded by University of Alaska Fairbanks, GW Scientific, Alaska Department of Natural Resources, Fairbanks Gold Mining, Inc., Alaska Department of Fish and Game, Alaska Department of Environmental Resources, Alaska Department of Transportation and Public Facilities, Fairbanks North Star Borough, and Arctic Region Supercomputing Center. The residents and mining companies of Ester Dome who participated in this study were critically important to the success of this project. Through their cooperation we were able to extend the number and geographic distribution of our measurements far beyond what would have been possible without their support. Thanks to Richard Winston at the USGS for advice with ground-water modeling issues. We acknowledge the German National Research Center for Information Technology for use of the Algebraic Multigrid Solver (AMG) for MODFLOW-2000.

RECOMMENDATIONS AND PROJECT TRANSFERABILITY

The study of the important geohydrologic processes at Ester Dome leads us to conclusions regarding water-resource issues in the Fairbanks uplands. These upland-aquifer systems are very complex and certain information is necessary to complete a satisfactory hydrologic investigation. This section of the thesis provides general recommendations for further geohydrologic interpretations, guidelines for development projects in Interior uplands, and the transferability of this project to other Interior domes and ridges.

We found the ASTM standards were useful technical guidelines to follow during the Ester Dome study and they are recommended for any ground-water investigation. Guidelines include the following procedures:

- Conceptualization and Characterization of Ground-Water Systems (ASTM, 2003a)
- Site Characteristics for Environmental Purposes With Emphasis on Soil, Rock, the Vadose Zone and Ground Water (ASTM, 2003b)
- Design of Ground-Water Monitoring Systems in Karst and Fractured-Rock Aquifers (ASTM, 2003c)
- Minimum Set of Data Elements to Identify a Ground-Water Site (ASTM, 2003d)
- Documenting a Ground-Water Sampling Event (ASTM, 2003e)
- Presentation of Water-Level Information From Ground-Water Sites (ASTM, 2003f)
- Selecting a Ground-Water Modeling Code (ASTM, 2003g)
- Maintenance and Rehabilitation of Ground-Water Monitoring Wells (ASTM, 2003h)

There are many critical geohydrologic processes that play a role in the ground-water dynamics of Interior aquifer systems. Additional interpretive efforts are needed to better understand these processes and include:

- Hydraulic conductivity of fractured rock
- Recharge and infiltration processes through fractures
- Ground-water flow in fault zones
- Travel times, velocities, and ground-water ages

Future ground-water investigations in upland-bedrock aquifer systems should also include smaller scale studies to look more closely at these processes. Geophysical surveys could yield clues to the fracturing of the system and indicate the location of the water table. Geochemistry information and ground-water age dating techniques would be useful information to verify flow directions and constrain travel times. Further interpretations of these processes will greatly benefit Interior Alaska.

Residential and industrial development in Interior Alaska is increasing. Hydrologic investigations prior to development are necessary to determine baseline conditions and to better understand geohydrologic processes before development occurs. Some recommendations for developers include:

- Developing a conceptual model of the system
- Collection of ground-water levels and geochemistry (or collect historical ground-water levels), if available
- Examination of basic subsurface lithology, with an estimate of permafrost distribution
- Identify contributing aquifer recharge and aquifer discharge areas near the site (i.e., where does the ground water originate and where does it flow in relation to the site location?)
- Reporting all collected data to the appropriate government agency for archival purposes

A conceptual model is a description of the processes taking place in the system. An inexpensive means to begin the configuration of a conceptual model is the collection of historical geohydrologic data if available. This could include geologic well log records or previous investigative reports. Water-level information is needed to accurately describe ground-water flow processes. If monitoring wells cannot be installed, current

ground-water levels can be collected from private water-supply wells. Surface-water features yield clues to the ground-water flow system and can often be identified on topographic maps. Geologic maps are useful for identifying hydrogeologic units, mapping potential aquifers, and inferring hydraulic conductivities of these units. We stress the importance of estimating the permafrost distribution to determine whether the aquifer is unconfined or confined and if recharge can reach the subpermafrost aquifer system. All data that is collected such as geologic well logs, water levels, and geochemistry information need to be archived in a government database for future use. Costs will be reduced if a database of information is available for future development projects.

One of the goals of this project was to identify the transferability of this project to other Interior upland-dome and ridge aquifer systems. This project, along with other research sites in Interior Alaska such as the Caribou Poker Creek Research Watershed (CPCRW) provide useful geohydrologic information transferable to other watersheds, domes, and ridges. The Ester Dome investigation and ground-water flow model yields useful geohydrologic information and serves as a tool to describe important hydrologic processes that occur on Interior domes. The process of constructing the model, identifying data input parameters, and evaluating the results is transferable. A simple model can often give valuable information about the aquifer hydraulic conductivity, recharge processes, and the effects of pumping. Construction of a model requires one to examine the geology of the system and identify important hydrologic processes, which control the ground-water flow of a system. The model also ascertains data collection needs. The ground-water flow model for the Ester Dome aquifer system predicts the water levels for each cell based on the input parameters. The subsequent sensitivity analysis indicates which parameters and observations were the most sensitive. Although the water-level predictions are not transferable from the Ester Dome aquifer system to another upland aquifer system, the process of constructing a model *is* transferable.

The construction of the boundary conditions for the Ester Dome model is likely to be similar for other Interior-dome systems. Model boundaries are likely to be

discharging water into streams, therefore, boundary conditions such as constant head or mixed (constant head with leakage) should be used. Drains or streams should be used where water leaves the model through spring-fed streams. Additionally, the zonation of recharge areas is applicable to other domes or ridges. At Ester Dome, winter precipitation increases while the silt and permafrost thickness tends to decrease with increasing elevation leading to a non-uniform recharge distribution. It is highly likely that other Interior upland aquifer systems exhibit a non-uniform recharge distribution.

The sensitivity analysis quantifies the sensitivity of a change in hydraulic head to a given parameter or observation. This Ester Dome sensitivity analysis examines which parameters and observations can most accurately describe the system and the accuracy of the estimated value. The estimated value of the Ester Dome aquifer parameter and the sensitivity of the parameter to changes in heads will be useful information when examining other interior aquifer systems with similar aquifer parameters.

Even though historical and current data may not exist on all upland domes and ridges, there may be a similar setting where data exists. For example, if one were looking for data of seasonal fluctuations on ground-water levels on Birch Hill, but there were no records available, data collected from the Ester Dome study may be useful if the geologic setting is similar. Although the geology at Birch Hill may be slightly different than at Ester Dome, we do know that at Birch Hill, upland geohydrologic processes control the ground-water flow system. We showed that at Ester Dome ridge tops, the seasonal fluctuations are more pronounced and well yields are low. In valley bottoms, we find thick deposits of loess and permafrost is often present as a confining unit. It is likely that similar processes occur at other Interior upland dome and ridge aquifer systems.

LITERATURE CITED

Aeromap US Inc., 1999. Ester Dome/Fairbanks Aerial Photography for May 19, 1999. Aeromap, Merrill Field Drive, Anchorage, Alaska.

Alaska Department of Natural Resources, Land Records Information Section, 1990. Rivers, 1:2,000,000. URL:ftp://wwwdev.dnr.state.ak.us/asgdc/adnr/rvr2mil.e00.gz. ADNR, LRIS, Anchorage, Alaska.

American Society for Testing and Materials, 2003a. Standard Guide for Conceptualization and Characterization of Ground-Water Systems, Standard D5979-96 (2002), vol. 04.09: West Conshohocken.

American Society for Testing and Materials, 2003b. Standard Guide for Site Characteristics for Environmental Purposes With Emphasis on Soil, Rock, the Vadose Zone and Ground Water, Standard D5730-98, vol. 04.09: West Conshohocken.

American Society for Testing and Materials, 2003c. Standard Guide for Design of Ground-Water Monitoring Systems in Karst and Fractured-Rock Aquifers, Standard D5717-95e1, vol. 04.09: West Conshohocken.

American Society for Testing and Materials, 2003d. Standard Guide for Practice of Minimum Set of Data Elements to Identify a Ground-Water Site, Standard D5254-92 (1998), vol. 04.09: West Conshohocken.

American Society for Testing and Materials, 2003e. Standard Guide for Documenting a Ground-Water Sampling Event, Standard D6089-97e1, vol. 04.09: West Conshohocken.

American Society for Testing and Materials, 2003f. Standard Guide for Presentation of Water-Level Information From Ground-Water Sites, Standard D6000-96e1, vol. 04.09: West Conshohocken.

American Society for Testing and Materials, 2003g. Standard Guide for Selecting a Ground-Water Modeling Code, Standard D6170-97e1, vol. 04.09: West Conshohocken.

American Society for Testing and Materials, 2003h. Standard Guide for Maintenance and Rehabilitation of Ground-Water Monitoring Wells, Standard D5978-96e1, vol. 04.09: West Conshohocken.

Anderson, G.S., 1970. Hydrologic reconnaissance of the Tanana Basin, central Alaska, U.S. Geological Survey Hydrologic Investigations Atlas HA-319, 4 sheets.

Anderson, M. P. and Woessner, W. W., 1992. *Applied Groundwater Modeling*. Academic Press, San Diego. CA, 381 p.

Barenblatt, G.E., Zheltov, I.P., and Kochina, I.N., 1960. Basic concepts in the theory of homogeneous liquids in fissured rocks. *Journal of Applied Mathematics and Mechanics*. Engl. Trans., **24** (5), pp. 1286-303.

Bear, J., 1993. Modeling Flow and Contaminant Transport in Fractured Rocks, Chap. 1 *in* Flow and Contaminant Transport in Fractured Rocks, Bear, J., Tsang C.F., and G. de Marsily (eds.). Academic Press, San Diego, CA, pp. 1-37.

Bradbury, K.R., Muldoon, M.A., Zaporozec, A., and Levy, J., 1991. Delineation of Wellhead Protection Areas in Fractured Rocks. Technical Guidance Document, U.S. Environmental Protection Agency, Office of Ground Water and Drinking Water, Washington, DC, EPA 570/9-91-009, 144 p.

Caine, J.S., 2000. The brittle structures and ground-water hydrogeology of the Turkey Creek watershed, Colorado Rocky Mountain Front Range, Geological Society of America, Rocky Mountain Section, 52nd annual meeting, Abstracts with Programs - Geological Society of America, **32** (5), p. 4.

Cameron, C. E., 2000. Fault-hosed AU mineralization, Ester Dome, Alaska, MS Thesis. University of Alaska Fairbanks, Fairbanks, 115 p.

Cederstrom, D.J., 1963. Water resources of the Fairbanks area, Alaska. U.S. Geological Survey Water-Supply Paper 1590, 84 p.

Collins, C.M., Haugen, R.K. and Kreig, R.A., 1988. Natural ground temperatures in upland bedrock terrain, interior Alaska, *in* Proceedings, Fifth International Conference on Permafrost, Vol. 1. Trondheim, Norway, pp. 56-60.

Dashevsky, S.S., Hunter, E.N., Lukens, J.H., and Rush, P.J., 1993. Ester Dome Joint Venture 1992 Report of Activities: American Copper and Nickel Company, Inc., and Inco Exploration and Technical Services, Inc., unpublished company report, 43 p.

Design Science and Engineering, 2000. Miscellaneous ground-water data prepared for Ryan Lode Mines, Inc., 1993-1999, variously paged.

Domenico, P. A., and F. W. Schwartz, 1998. *Physical and Chemical Hydrogeology*, 2nd ed., John Wiley and Sons, New York, NY, 506 p.

Farmer, G.L., Goldfarb, R.J., Lilly, M.R., Bolton, B., Meier, A.L., and Sanzolone, R., 2000. The chemical characteristics of ground water near Fairbanks, Alaska, *in* Geological

Studies in Alaska by the U.S. Geological Survey 1998, Kelley, K.D., and Gough, L.P., (eds.). U.S. Geological Survey Professional Paper 1615, p. 167-178.

Farris, A.M., 1996. Numerical Modeling of Contaminant Transport in Discontinuous Permafrost: Ft. Wainwright, Alaska, MS Thesis. University of Alaska, Fairbanks, 109 p.

Fathauer, T., 2001. Miscellaneous ground-water data 1984-2002, variously paged.

Faunt, C. C., D'Agnese, F. A., and Hill, M. C., 1999. Hydrogeologic-framework and ground-water flow models of the Death Valley region, Nevada and California, Geological Society of America, 1999 annual meeting, Abstracts with Programs - Geological Society of America, **31** (7), p. 86.

Fetter, C. W., 1994. *Applied Hydrogeology*, (3rd edition). New York, Macmillan, 691 p.

Forbes, R.B., 1982. Bedrock geology and petrology of the Fairbanks Mining District, Alaska. Alaska Division of Geological and Geophysical Surveys Open File Report 169, 69 p.

Foster, H.L., Keith, T.E.C., and Menzie, W.D., 1994. Geology of the Yukon-Tanana area of east-central Alaska *in* The Geology of Alaska: The Geology of North America, Volume G-1, Plafker, G., and Berg, H.C. (eds.). Geol. Soc. Amer. DNAG Series, pp. 205-240.

Freeze, R.A. and Cherry, J.A., 1979. *Groundwater*. Prentice-Hall Inc., Englewood Cliffs, N.J., 604 p.

Gieck, R., 1986. A Water Resource Evaluation of Two Subarctic Watersheds. MS Thesis. University of Alaska Fairbanks, Fairbanks, 90 p.

Gieck, R.E. and Kane, D.L., 1986. Hydrology of two subarctic watersheds *in* Kane, D.L., (ed.), Cold Regions Hydrology Symposium, American Water Resources Association, Proceedings, pp. 283-291.

Glass, R.L., Lilly, M.R., and Meyer, D.F., 1996. Ground-water levels in an alluvial plain between the Tanana and Chena Rivers near Fairbanks, Alaska 1986-1993. U.S. Geological Survey Water Resources Investigations Report 96-4060, 93 p.

Goldfarb, R.J., Farmer, G.L., Cieutat, B.A., and Meier, A.L., 1999. Major element, trace element, and strontium isotope systematics of natural waters in the Fairbanks Mining District- Constraints from local geology: *in* Geological Studies in Alaska by the U.S. Geological Survey, 1997, Kelly, K.D., (ed). U.S. Geologic Survey Professional Paper 1614, pp. 139-150.

Gringarten, A.C., 1982. Flow-test evaluation of fractured reservoirs, *in* Recent Trends in Hydrogeology, T.N. Narasimhan (ed.). Geol. Soc. Am. Special Paper 189, pp. 237-63.

Hall, M., 1985. Structural geology of the Fairbanks Mining District, MS Thesis. University of Alaska, Fairbanks, 68 p.

Harbaugh, A. W., Banta, E.R., Hill, M.C. and McDonald, M.G., 2000. MODFLOW-2000, The U.S. Geological Survey Modular Ground-Water Model-User Guide to Modularization Concepts and the Ground-Water Flow Process. U.S. Geological Survey Open-File Report 00-92, 121 p.

Haugen, R.K., 1982. Climate of remote areas in north-central Alaska 1975-1979 summary. CRREL Rep. 82-35. Hanover, NH: U.S. Army Cold Regions Research and Engineering Laboratory. 110 p.

Haugen, R.K., Slaughter, C.W., Howe, K.E., and Dingman, S.L., 1982. Hydrology and climatology of the Caribou-Poker Creeks Research Watershed, Alaska. CRREL Rep. 82-26. Hanover, NH: U.S. Army Cold Regions Research and Engineering Laboratory. 42 p.

Hawkins, D.B., Forbes, R.B., Hok, C.I., and Dinkel, D., 1982. Arsenic in the Water, Soil, Bedrock, and Plants of the Ester Dome area of Alaska. IWR-103, University of Alaska, Fairbanks, 82 p.

Heath, R.C., 1983. Basic Ground-water Hydrology, U.S. Geological Survey Water-Supply Paper 2220. Washington, DC, 84 p.

Hill, M. C., 1998. Methods and Guidelines for Effective Model Calibration. U.S. Geological Survey Water-Resources Investigation 98-4005, 97 p.

Hill, M. C., Banta, E.R., Harbaugh, A.W., and Anderman E.R., 2000. User Guide to the Observation, Sensitivity, and Parameter-Estimation Processes and Three Post-Processing Programs. U.S. Geological Survey Open-File Report 00-184, 209 p.

Hinzman, L.D., Wegner, M., and Lilly, M.R., 2000. Hydrologic Investigations of Groundwater and Surface-Water Interactions in Subarctic Alaska. *Nordic Hydrology*, **31**(41/5), pp. 339-356.

Hok, C.I., 1986. Evaluation of Linear Feature Mapping as a Groundwater Prospecting Technique in the Metamorphic Terrane of Fairbanks, MS Thesis. University of Alaska, Fairbanks, 238 p.

Hsieh, P.A., Shapiro, A.M., and Tiedeman, C.R., 1999. Computer simulation of fluid flow in fractured rocks at the Mirror Lake FSE well field, *in* U.S. Geological Survey Toxic Substances Hydrology Program--Proceedings of the Technical Meeting,

Charleston, South Carolina, March 8-12, 1999--Volume 3 of 3--Subsurface Contamination from Point Sources, Morganwalp, D.W., and Buxton, H.T., (eds). U.S. Geological Survey Water-Resources Investigations Report 99-4018C, pp. 777-781.

Intermap Technologies, 2000. Demo Star3i Digital Elevation Model for the Fairbanks Area.

Kane, D. L. and Slaughter, C.W., 1973. Recharge of a Central Alaska Lake by Subpermafrost Groundwater *in* Permafrost: The North American Contribution to the Second International Conference, Washington DC, US, National Academy of Sciences, pp 452-462.

Kane, D.L., Fox, J.D., Seifert, R.D. and Taylor, G.S., 1978. Snowmelt infiltration and movement in frozen soils *in* Proceedings of the 3rd International Conference on Permafrost, National Research Council of Canada, Ottawa, pp. 201-206.

Kane, D. L., 1980. Snowmelt Infiltration into Seasonally Frozen Soils. *Cold Regions Science and Technology*, **3**, pp. 153-161.

Kane, D. L., 1981a. Physical Mechanics of Aufeis Growth. *Canadian Journal of Civil Engineering*, **8**, pp. 186-195.

Kane, D. L., 1981b. Groundwater Recharge in Cold Regions. *The Northern Engineer*, **13**, pp. 28-33.

Kane, D.L. and Stein, J., 1983a. Field evidence of groundwater recharge in interior Alaska *in* Proceedings of Permafrost: 4th International Conference. National Academy Press, Washington, D.C., pp. 572-577.

Kane, D. L., and Stein, J., 1983b. Water Movement into Seasonally Frozen Soils. *Water Resources Research*, **19**, pp. 1547-1557.

Long, J.C.S., Remer, J.S., Wilson, C.R. and Witherspoon, P.A., 1982. Porous media equivalents for networks of discontinuous fractures. *Water Resources Research*, **18**(3), pp. 645-58.

McDonald, M.G., and Harbaugh, A.W., 1988. A modular three-dimensional finite-difference ground-water flow model. U.S. Geological Survey Techniques of Water-Resources Investigations, book 6, chap. A1, 586 p.

Morris, D.A. and Johnson, A.I., 1967. Summary of hydrologic and physical properties of rock and soil materials as analyzed by the hydrologic laboratory of the U.S. Geological Survey, U.S. Geological Survey Water-Supply Paper, 1839-D.

Mueller, S.H., 2002. A Geochemical Characterization of Groundwater Near Fairbanks, Alaska, with Emphasis on Arsenic Hydrogeochemistry, MS Thesis. University of Colorado, Boulder, 109 p.

McCrum, M. A., 1985. A Chemical Mass Balance of the Ester Creek and Happy Creek Watersheds on Ester Dome, Alaska, MS Thesis. University of Alaska, Fairbanks, 101 p.

Nakanishi, A.S., and Lilly, M.R., 1998. Estimate of aquifer properties by numerically simulating ground-water/surface-water interactions in cross section at Fort Wainwright, Alaska. U.S. Geological Survey Water-Resources Investigations Report 98-4088, 35 p.

National Weather Service, 2002. Climate statistics for Fairbanks International Airport, 1904-2002, Fairbanks, Alaska.

Natural Resources Conservations Service, USDA, 2002. Climate statistics for Fairbanks, Alaska, 2000-2002, URL: http://ambcs.org/, Fairbanks, Alaska.

Nelson, G.L., 1978. Hydrologic information for land-use planning, Fairbanks vicinity, Alaska. U.S. Geological Survey Open-File Report, 78-959, 47 p.

Newberry, R.J., 2001. University of Alaska Fairbanks Department of Geology and Geophysics. Personal communication with Rainer Newberry.

Newberry, R.J., Bundtzen, T.K., Clautice, K.H., Combellick, R.A., Douglas, T., Laird, G.M., Liss, S.A., Pinney, D.S., Reifenstuhl, R.R., and Solie, D.N., 1996. Preliminary geologic map of the Fairbanks Mining District, Alaska. Alaska Division of Geological and Geophysical Surveys, Public Data File 96-16, 17 p.

Pewé, T.L., 1958. Geology of the Fairbanks (D-2) Quadrangle, Alaska. Department of the Interior, U.S. Geological Survey.

Pewé, T.L. and Bell, J.W., 1975a. Maps showing distribution of permafrost in the following Fairbanks quadrangles, Alaska:
D-2 NW U.S. Geological Survey Miscellaneous Field Studies Map MF-668-A
D-2 SE U.S. Geological Survey Miscellaneous Field Studies Map MF-669-A
D-2 NE U.S. Geological Survey Miscellaneous Field Studies Map MF-670-A
D-2 SW U.S. Geological Survey Miscellaneous Field Studies Map MF-671-A

Pewé, T.L., Bell, J.W., Forbes, R.B., and Weber, F.R., 1975b. Geologic map of the Fairbanks D-2 NW quadrangle, Alaska, U.S. Geological Survey Miscellaneous Investigations Series Map I-907, scale 1:24000, 1 sheet.

Pewé, T.L., Bell, J.W., Forbes, R.B., and Weber, F.R., 1976. Geologic map of the Fairbanks D-2 SW quadrangle, Alaska, U.S. Geological Survey Miscellaneous Investigations Series Map I-829-A, scale 1:24000, 1 sheet.

Poeter, E.P., and Hill, M.C., 1997. Inverse models: a necessary next step in groundwater modeling, *Ground Water*, **35**(2), pp. 250-260.

Pollock, D.W., 1994. User's guide for MODPATH/MODPATH-PLOT, version 3: A particle tracking post processing package for MODFLOW, the U.S. Geological Survey finite-difference ground-water flow model. U.S. Geological Survey Open-File Report 94-464, 249 p.

Robinson, M.S., Smith, T.E., and Metz, P.A., 1990. Bedrock Geology of the Fairbanks Mining District: Fairbanks, Alaska Division of Geological and Geophysical Surveys Professional Report 100, 2 sheets, scale 1:63,360.

Rogers, J.A., McCoy, D.T., Nerup, M., Yuengling, K., Bean, K., Cameron, C., Graham, G., Frantz, P., and Athey, J., 1998. Placer Dome-Silverado lease 1998 Annual Report for Ester Dome: Unpublished company report, 68 p.

Rovansek, R.J., Kane, D.L., and Hinzman, L.D., 1993. Improving estimates of snowpack water equivalent using double sampling, *in* Proceedings of the 61st Western Snow Conference, Quebec, Canada, pp. 157-163.

Shapiro, A.M., 1993. The influence of heterogeneity in estimates of regional hydraulic properties in fractured crystalline rock, in Banks, S., and Banks, D., (eds.): Memoirs of the 24th Congress, International Association of Hydrogeologists, Hydrogeology of Hard Rocks, Oslo, Norway, June 28-July 2, 1993, p. 125-136.

Shapiro, A. M., and Hsieh, P.A., 1993. Overview of research on use of hydrologic, geophysical, and geochemical methods to characterize flow and chemical transport in fractured rock at the Mirror Lake Site, New Hampshire. USGS Toxic Substances Hydrology Program: Proceedings of the Technical Meeting, Colorado Springs, CO, USGS.

Singhal, B. B. S., and Gupta, R.P., 1999. *Applied Hydrogeology of Fractured Rocks*. Dordrecht, Kluwer Academic.

Slaughter, C.W., and Kane, D.L., 1979. Hydrologic role of shallow organic soils in cold climates, *in* Proceedings of 1979 Canadian hydrology symposium: cold climate hydrology. National Research Council of Canada, Ottawa, Ontario, pp. 380-389.

Smith, D.W. and Casper, L.A., 1974. Groundwater quality effects on domestic water utilization. IWR-48, University of Alaska Fairbanks, 139 p.

Streltsova-Adams, T.D., 1978. Well hydraulics in heterogeneous aquifer formations, in Advances in *Hydroscience* (ed. V.T. Chow), Vol. 11, Academic Press, New York, pp. 357-423.

Sun, N-Z, 1994. Inverse Problems in Groundwater Modeling. Kluwer Academic Publishers, Netherlands, 364 p.

Tiedeman, C.R., Goode, D.J., and Hsieh, P.A., 1997. Numerical simulation of ground-water flow through glacial deposits and crystalline bedrock in the Mirror Lake area, Grafton County, New Hampshire: U.S. Geological Survey Professional Paper 1572, 50 p.

Trabant, D., 2001. Miscellaneous groundwater data, 1977-2001, variously paged.

U.S. Geological Survey, 2001. National Water Information System (NWISWeb) data available on the World Wide Web, Miscellaneous groundwater data 1979-2001, accessed 2001, at URL http://waterdata.usgs.gov/nwis/gwsi.

Verplanck, P.L., Mueller, S.H., Youcha, E., Goldfarb, R.J., Sanzolone, R., McCleskey, R. B., Roller, M., Briggs, P.H., Adams, M., and Nordstrom, D.K., 2003. Chemical Analyses of Ground and Surface Waters, Ester Dome, Alaska, 2000-2001. U.S. Geological Survey Open-File Report - in press.

Viereck, L. A., K. Van Cleve, and C.T. Dyrness. 1986. Forest ecosystem distribution in the taiga environment *in* K. Van Cleve, F. S. Chapin III, P. W. Flanagan, L. A. Viereck and C. T. Dyrness, eds, Forest ecosystems in the Alaskan taiga: a synthesis of structure and function. Springer-Verlag, New York, pp. 22-43.

Vohden, J., 2000. A technical review of the September 1999 groundwater disturbance near Ester, Alaska. Alaska Division of Geological and Geophysical Surveys, Preliminary Investigative Report 2000-3, 68 p.

Vohden, J., 2003. Alaska Department of Natural Resources. Email written communication with Jim Vohden.

Walther, M., 1987a. A drawdown model for groundwater appropriations in the Fairbanks Uplands, unpublished MS report, University of Alaska, Fairbanks, 83 p.

Walther, M., 1987b. Report of Pumping Test (Aquifer Test) for Grant Mine, Ester Dome near Fairbanks, Alaska. Alaska Department of Natural Resources, Fairbanks, 8 p.

Weber, E.F., 1986. A stochastic model and risk analysis of Arsenic, well depth, and well yield in the Fairbanks Area, MS Thesis, University of Alaska, Fairbanks, 196 p.

Wegner, M.A., 1997. Transient groundwater and surface-water interactions at Fort Wainwright, Alaska. MS Thesis, University of Alaska, Fairbanks. 75 p.

Wilson, F.H., and Hawkins, D.B., 1978. Arsenic in the streams, stream sediments, and ground water, Fairbanks Area, Alaska. *Environmental Geology*, **2**(4), pp. 195-202.

Winston, R. B., 2000. Graphical User Interface for MODFLOW, Version 4. U.S. Geological Survey Open-File Report 00-315, 27 p.

Yeh W.W.G., 1986. Review of parameter identification in procedures in groundwater hydrology – The inverse problem, *Water Resources Research*, **22**(2), pp. 95-108.

Yoshikawa, K., 2001. University of Alaska Fairbanks Water and Environemental Research Center. Personal Communication with Kenji Yoshikawa.

Yoshikawa, K., Hinzman, L. D., and Gogineni, P., 2002. Ground temperature and permafrost mapping using an equivalent latitude/elevation model. *Jour. Glaciology and Geocryology*, **24**(5), pp. 526-531.

APPENDIX A: WELL INFORMATION

Site ID	UTM Easting Zone 6 (m) NAD27	UTM Northing Zone 6 (m) NAD27	Land Altitude TOC (m) NAVD29	+/- Error (m)	Well Depth (m)	Geologic Unit	Hydrogeologic Unit	Survey Crew
EDM001	453320.32	7191860.91	216.08	2.00	48.77	Dbs	Bedrock	FGMI
EDM002	453679.52	7194053.02	250.19	2.00	85.34	Dbs	Bedrock	FGMI
EDM003	453352.74	7193858.53	279.30	2.00	91.44	Zf	Bedrock	FGMI
EDM004	452715.15	7193826.48	394.07	2.00	103.63	Zf	Bedrock	FGMI
EDM005	452893.36	7193212.21	337.96	2.00	97.54	Zf	Bedrock	FGMI
EDM006	452849.44	7192744.57	303.28	2.00	98.45	Dbs	Bedrock	FGMI
EDM007	452598.22	7192843.32	263.33	2.00	32.00	Zf	Bedrock	FGMI
EDM008	452620.47	7193148.10	283.88	2.00	48.77	Zf	Bedrock	FGMI
EDM009	452832.86	7192267.01	283.45	2.00	111.25	Dbs	Bedrock	FGMI
EDM010	453173.93	7192410.57	282.62	2.00	111.25	Dbs	Bedrock	FGMI
EDM011	453280.70	7192865.06	302.69	2.00	99.06	Dbs	Bedrock	FGMI
EDM013	453624.52	7193399.89	341.27	2.00	103.63	Dbs	Bedrock	FGMI
EDM014	454601.86	7195377.47	238.73	2.00	111.25	Zf	Bedrock	UAF
EDP001	453626.18	7191692.95	198.71	2.00	73.15	Dbs	Bedrock	UAF/DNR
EDP002			187.94	2.00	45.72	Dbs/Qht	Gravel	UAF
EDP003	453740.70	7191711.57	200.89	2.00		Dbs/Qht	Gravel	UAF/DNR
EDP004	453947.61	7191717.25	199.11	2.00		Dbs/Qht	Gravel	UAF
EDP005			195.95	2.00		Dbs/Qht	Gravel	
EDP006	453533.03	7191686.39	198.49	2.00	54.86	Dbs/Qht	Gravel	UAF/DNR
EDP007	453182.92	7191690.69	201.27	2.00		Dbs/Qht	Gravel	UAF/DNR
EDP008	453432.79	7191670.35	199.00	2.00		Dbs/Qht	Gravel	UAF
EDP009			192.95	2.00	35.36	Dbs/Qht	Gravel	
EDP010	453045.89	7191630.59	193.98	2.00	54.86	Dbs/Qht	Gravel	UAF/DNR
EDP011	447360.41	7190082.00	429.19	2.00		Zf	Bedrock	UAF
EDP013	453801.69	7192087.18	236.76	2.00	93.57	Dbs	Bedrock	UAF
EDP014	449899.23	7185198.67	215.76	2.00		Zf	Bedrock	UAF
EDP015	454064.56	7191759.67	201.64	2.00		Dbs/Qht	Gravel	UAF/DNR
EDP016	454011.88	7193104.39	264.83	2.00	83.82	Dbs	Bedrock	UAF
EDP018	454323.39	7193185.42	238.39	2.00	64.01	Dbs	Bedrock	UAF
EDP019	455263.51	7196624.10	206.38	2.00	59.74	Zf	Bedrock	UAF
EDP020	454947.86	7196533.88	212.12	2.00	80.77	Zf	Bedrock	UAF
EDP021	450184.61	7195031.66	661.82	2.00	67.06	Zfw	Bedrock	UAF
EDP022	450891.57	7195011.54	655.84	2.00	77.42	Zf	Bedrock	UAF
EDP023	450912.78	7194909.14	636.30	2.00	54.86	Zf	Bedrock	UAF
EDP024	451708.71	7193205.82	386.12	2.00	87.17	Dms	Bedrock	UAF
EDP025	451311.63	7192741.88	342.34	2.00	27.43	Dms	Bedrock	UAF
EDP026	451643.95	7191719.24	214.91	2.00	25.30	Dbs	Bedrock	UAF
EDP027	452271.36	7191463.72	181.82	2.00	61.57	Dbs	Bedrock	UAF

EDP028	449897.79	7190782.04	405.98	2.00	115.82	Zf	Bedrock	UAF
EDP029	456622.58	7192810.15	196.53	2.00		Dbs/Qht	Gravel	UAF
EDP030	441755.92	7191297.49	184.82	2.00	65.53	Zf	Bedrock	UAF
EDP031	453750.30	7192593.50	245.67	2.00		Dbs	Bedrock	UAF
EDP032	452114.62	7191798.84	226.26	2.00	61.87	Dbs	Bedrock	UAF
EDP033			640.00	2.00	39.01	Zfw	Bedrock	USGS topo
EDP034	448406.75	7187443.32	416.82	2.00	121.92	Zf	Bedrock	UAF
EDP_BIA	448728.47	7201735.48	256.32	5.00	89.00	Zf	Bedrock	USGS topo
EDP_CARB	441613.64	7191092.72	193.44	5.00		Dbs	Bedrock	USGS topo
EDP_CARL	458331.42	7193029.34	143.00	5.00	39.62	Qht	Gravel	USGS topo
EDP_COL_WLR	457832.62	7193084.19	157.21	5.00	77.72	Dbs	Bedrock	USGS topo
EDP_CUR	451188.76	7190637.05	271.00	5.00	109.12	Dbs	Bedrock	USGS topo
EDP_DAV	7193281.73	7193281.73	213.35	5.00	145.61	Zf	Bedrock	USGS topo
EDP_DEL_WLR	457155.17	7193093.88	184.74	5.00	67.06	Zf	Bedrock	USGS topo
EDP_DYK	454163.75	71933414.92	244.00	5.00	64.01	Zf	Bedrock	USGS topo
EDP_EsterFire2	452271.00	7191463.00	182.00	5.00	60.96	Zf	Bedrock	USGS topo
EDP_GILL_WLR	449295.35	7185298.33	215.46	5.00	55.17	Dma	Bedrock	USGS topo
EDP_GILLET	442181.71	7190585.75	195.00	5.00	80.77	Qht	Gravel	USGS topo
EDP_GROG_WLR	459310.00	7190716.00	258.13	5.00	109.12	Dms	Bedrock	USGS topo
EDP_ILLG_WLR	451045.80	7190483.69	287.23	5.00	115.82	Zf	Bedrock	USGS topo
EDP_LAI_WLR	448534.23	7190757.79	388.33	5.00	48.77	Zf	Bedrock	USGS topo
EDP_LIND_WLR	454702.87	7191451.47	185.80	5.00	38.71	Dma	Bedrock	USGS topo
EDP_MAT	451628.86	7193039.48	352.94	5.00	79.25	Qht	Gravel	USGS topo
EDP_MCI_WLR	453443.89	7200051.48	176.28	5.00	48.77	Dms	Bedrock	USGS topo
EDP_MEY_WLR	448911.59	7186880.55	274.61	5.00	103.63	Zf	Bedrock	USGS topo
EDP_MIHM	453897.54	7200567.59	233.26	5.00	86.87	Zf	Bedrock	USGS topo
EDP_MITC	455405.23	7198926.79	167.91	5.00	10.67	Zf	Bedrock	USGS topo
EDP_MORT_WLR	454679.25	7196598.70	220.76	5.00	52.12	Zf	Bedrock	USGS topo
EDP_MUL_WLR	454434.33	7193085.34	213.92	5.00	48.77	Qht	Gravel	USGS topo
EDP_MUS_WLR	457283.30	719298.45	175.36	5.00	48.77	Dbs	Bedrock	USGS topo
EDP_NEIL	455821.74	7195926.51	179.44	5.00	70.10	Qht	Gravel	USGS topo
EDP_NEU_WLR	449179.12	7185491.28	230.66	5.00	53.64	Dbs	Bedrock	USGS topo
EDP_NORTH1_WLR	455932.50	7191725.26	160.81	5.00	15.24	Zf	Bedrock	USGS topo
EDP_NORTH2_WLR	456088.27	7191992.23	152.79	5.00	17.07	Qht	Gravel	USGS topo
EDP_PAR_WLR	450737.70	7194900.00	623.00	5.00	44.20	Qht	Gravel	USGS topo
EDP_PHIL	457519.35	7195659.03	208.73	5.00	65.53	Zf	Bedrock	USGS topo
EDP_RECK	452175.00	7191614.00	200.00	5.00	44.20	Dbs	Bedrock	USGS topo
EDP_RITC	456660.89	7195710.17	200.00	5.00	72.54	Dbs	Bedrock	USGS topo
EDP_SALS	446222.38	7190949.22	465.00	5.00	73.15	Dbs	Bedrock	USGS topo
EDP_WADE	453872.83	7200660.86	233.26	5.00	96.93	Zf	Bedrock	USGS topo
EDP_WAKECONST_WLR	456851.39	7192815.72	174.02	5.00	54.86	Zf	Bedrock	USGS topo
EDP_WIG_WLR	451988.53	7189940.84	194.36	5.00	65.23	Qht	Gravel	USGS topo
EDP_ZAC_WLR	450478.40	7190571.53	334.16	5.00	149.35	Zf	Bedrock	USGS topo

APPENDIX B: SNOW SURVEY DATA, MARCH 2001

ID	Location	UTM Easting Zone 6 (m) NAD27	UTM Northing Zone 6 (m) NAD27	Land Altitude (m) NAVD29	Vegetation	Slope	Measurement Date	SWE (cm)	SWE (in)
1	Goldstream Dome Spur	7200255.10	447995.76	145.01	Spr/Asp/Bir	flat/northside	3/12/2001 14:10	7.30	2.87
2	EDP027	7191386.30	452172.27	181.82	None	flat/southside	3/12/2001 15:30	7.40	2.91
3	Goldstream Martin	7198563.90	442997.80	208.35	Spr/Asp/Bir	flat/northside	3/12/2001 13:14	7.40	2.91
4	EDP030	7191286.28	441713.35	184.82	Aspen/Birch	flat/westside	3/13/2001 10:40	8.60	3.39
5	Schloesser/ Ester Dome Rd	7197071.42	454333.04	229.71	Spr/Asp/Bir	flat/eastside	3/12/2001 14:52	11.20	4.41
6	EDM003	7193858.53	453352.74	279.30	None	east	3/14/2001 16:23	7.10	2.80
7	Ester Dome Rd mid	7196513.23	453185.33	318.86	Aspen/Birch	south	3/13/2001 14:03	7.90	3.11
8	Krogstie Ln	7190621.89	450139.15	370.47	Aspen/Birch	south	3/13/2001 9:52	8.10	3.19
9	Saphire/ Amethyst	7192983.55	451457.44	371.96	Aspen/Birch	south	3/13/2001 11:54	7.10	2.80
10	Old Nenana Hwy/ Parks	7185760.73	443247.78	464.57	Aspen/Birch	west	3/13/2001 11:16	7.30	2.87
11	Henderson/ Ester Dome Rd	7195602.77	451635.46	511.31	Spruce	southeast	3/13/2001 12:31	9.50	3.74
12	Ester Dome Rd east of Nordstrasse	7195082.13	451444.21	575.40	Spruce	south	3/13/2001 13:33	10.50	4.13
13	Top of Ester Dome Rd	7195046.48	449690.41	666.36	None	flat/top	3/13/2001 13:01	9.70	3.82
14	West side Ester Dome	7192573.30	446773.27	494.60	Spruce	west	3/23/2001 9:29	10.04	3.95
15	Ester Creek	7192286.25	447600.79	392.87	Aspen/Birch	south	3/23/2001 10:21	8.20	3.23
16	North face Ester Dome	7196232.23	449699.79	585.93	Spruce	north	3/23/2001 11:21	11.16	4.39
17	North side Ester Dome	7196513.12	448475.79	348.33	Willow	north	3/23/2001 11:52	9.53	3.75

APPENDIX C: SIMULATED HEAD DISTRIBUTION LAYERS 2-4

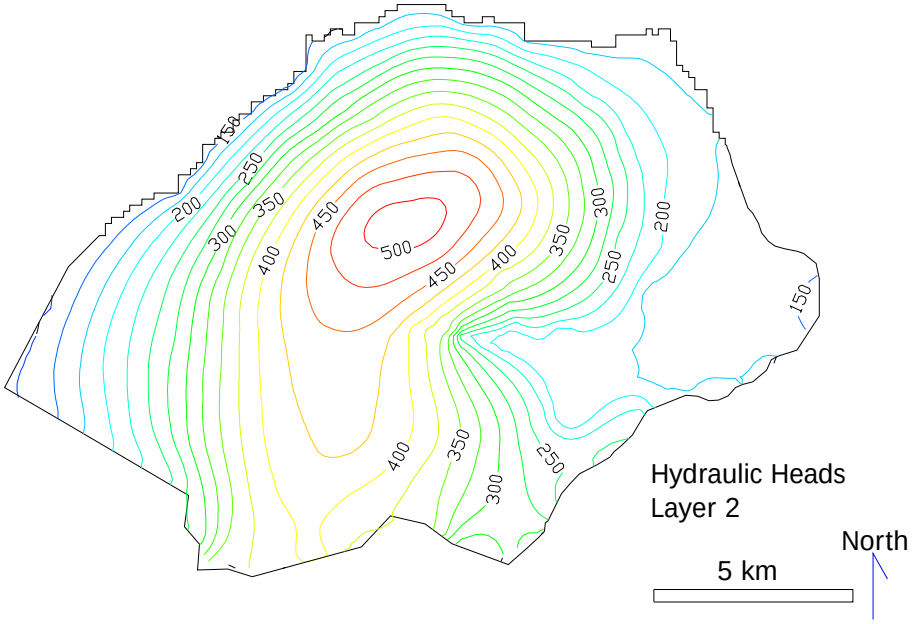

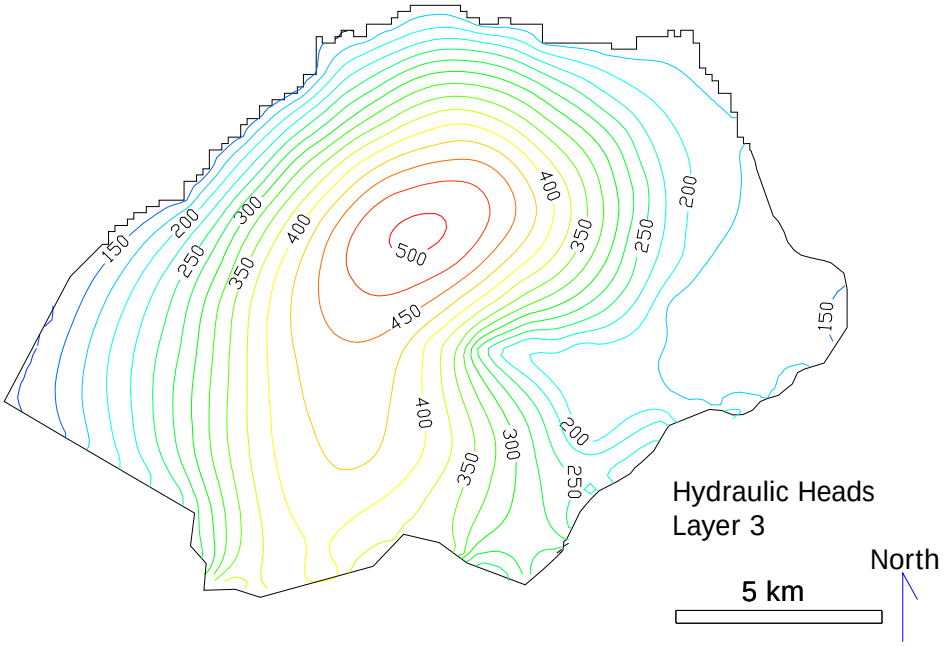

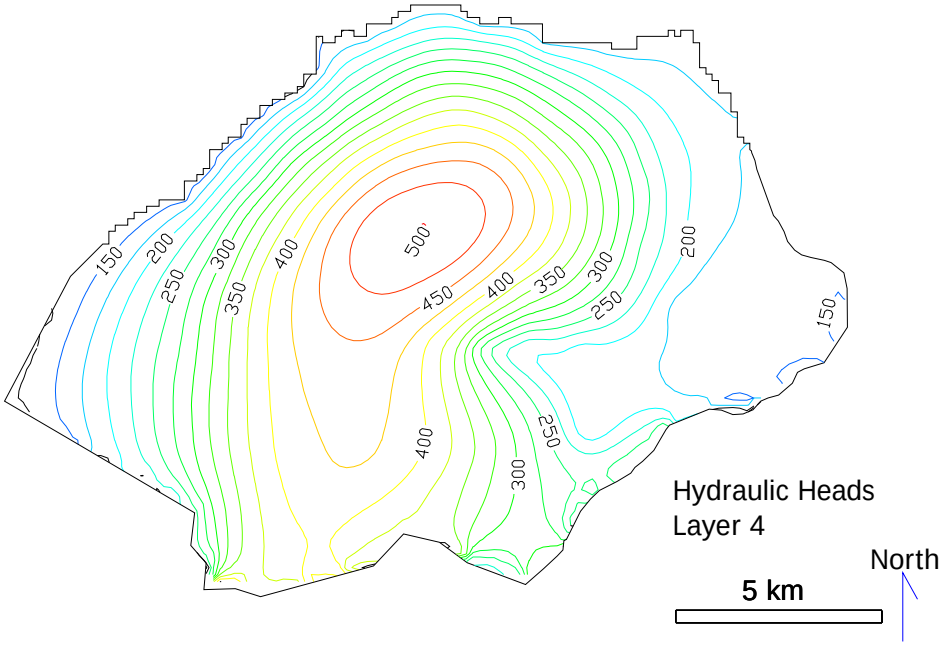
150
200
250
300
350
400
500
450
400
350
300
250
200
150
400
300
250
Hydraulic Heads
Layer 4
North
5 km